FRIEDA RIVER

Frieda River Limited
Sepik Development Project
Environmental Impact Statement

Appendix 9 – Desktop Assessment of Commercial Forestry and Agroforestry within the Sepik Development Project Infrastructure Corridor

SDP-6-G-00-01-T-003-020

coffey
A TETRA TECH COMPANY

University of Nottingham
UK | CHINA | MALAYSIA

Desktop assessment of commercial forestry and agroforestry within the Sepik Development Project infrastructure corridor

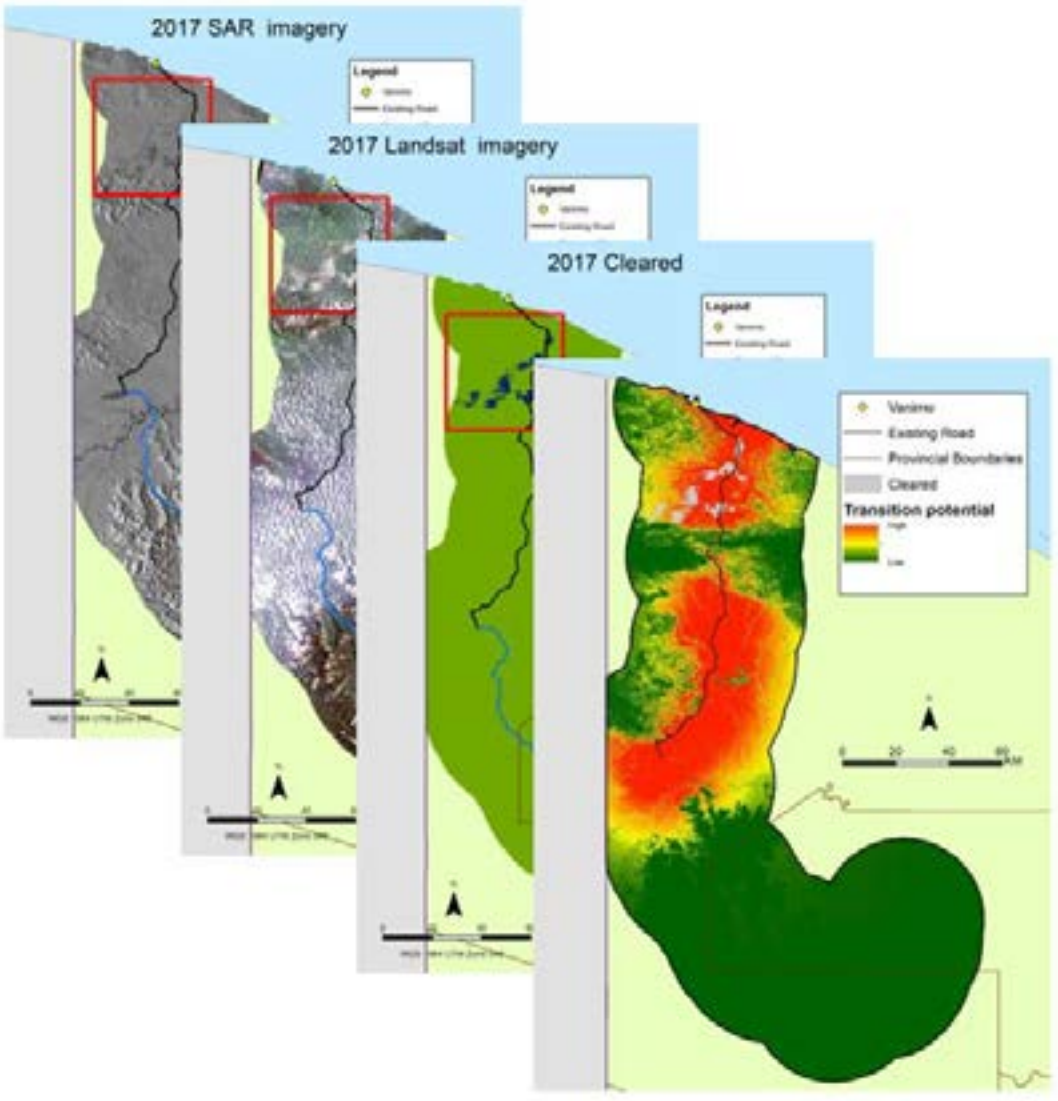

Dr Alex M. Lechner, Dr John Hunter and Khanh Ngo Duc

14 September 2018

Desktop assessment of commercial forestry and agroforestry within the Sepik Development Project infrastructure corridor

Prepared for Frieda River Limited (FRL)

Report by: Dr Alex M. Lechner, Dr John Hunter and Khanh Ngo Duc

School of Environmental and Geographical Sciences

University of Nottingham Malaysia Campus

Jalan Broga

43500 Semenyih

Selangor Darul Ehsan

Malaysia

E: Alex.Lechner@nottingham.edu.my

P: +60 (0)3 8725 3613

M: +60 (0)10 906 9167

Acknowledgements

We wish to acknowledge the help and feedback from the Coffey team of Heath Synnott, Michael Sale and Kristen Hall, and Professor Simon Saulei from the Papua New Guinea Forest Research Institute. In addition, Michelle Ang, Darrel Tiang and Zoe Lum from University of Nottingham Malaysia campus provided invaluable assistance with the spatial analysis.

University of Nottingham
UK | CHINA | MALAYSIA

Contents

Desktop assessment of commercial forestry and agroforestry within the Sepik Development Project infrastructure corridor 1
Acknowledgements 2
1.0 Introduction 7
1.1. Background 7
1.2. Summary of objectives 8
1.3. Study Area 9
2.0 High-level assessment of the existing commercial forestry and agroforestry industries in the region 10
2.1. Overview 10
2.2. Regional summary 12
3.0 Remote sensing and GIS analysis of forest change 18
3.1. Summary 18
3.2. Mapping objectives 18
3.3. Data selection 19
3.4. Methods 21
3.5. Results - Remote sensing mapping of broad-scale clearance 24
3.6. Results - GIS mapping of logging 35
3.7. Results – Rates of change 38
3.8. Final summary 38
4.0 Land capability, land change modelling and assessment of the impacts of the proposed road 40
4.1. Background 40
4.2. Methods 41
4.3. Results 44
4.4. Summary 53
5.0 Conclusions and limitations 56
References 57
Appendix 61
5.1. Appendix A - Support material for Section 2 61
5.2. Appendix B: Land Change Modeler MLP Model Results for transition between forest and cleared 83
5.3. Appendix C: Land Change Modeler MLP Model Results for transition between forest and cleared sensitivity analysis with distance to Vanimo 87
5.4. Appendix D: Land Change Modeler MLP Model Results for transition between forest and logging 91

5.5. Appendix E: Land Change Modeler MLP Model Results for transition between forest and logging sensitivity analysis with distance to Vanimo 95

Figures

Figure 1: Study area with existing and proposed road buffered by 30 km. The analysis was performed within the buffered area. 7

Figure 2: Scanned Forest Resource Map of the West Sepik Province (PNGFA, 2016) with existing (yellow) and planned roads (red) overlaid along with 30 km buffer zone. 14

Figure 3: Known and proposed logging concessions within the Sandaun and East Sepik Provinces (taken from Rogers (2011)) with existing (yellow) and planned roads (red) overlaid along with 30 km buffer zone. 15

Figure 4: SABLs (in white) identified by the Forest Observatory (http://forest.pngsdf.com). 17

Figure 5: Comparison of Landsat 8 and Sentinel 1 SAR imagery. 19

Figure 6: CLASLite - automated system for converting satellite imagery from its original (raw) format, through calibration, pre-processing, atmospheric correction, and cloud masking steps, Monte Carlo Spectral Mixture Analysis http://claslite.ciw.edu/en/about/software.html. 21

Figure 7: Workflow – from pre-processing to classification and accuracy assessment. 22

Figure 8: Example of locations with minor roads which can be used to identify selective logging areas. This analysis was confounded by streams, which appear very similar to roads, and cloud cover.....24

Figure 9: Cleared areas for 2011. Note we could not identify any broadscale clearing for 2011. Landsat archival imagery pre-2011 also supports this conclusion. 25

Figure 10: Landsat mosaic for 2011 focusing on areas where clearing occurs in later years.....26

Figure 11: Broad-scale clearance identified in 2014 using Landsat imagery. 27

Figure 12: Landsat mosaic for 2014 focusing on the areas of extensive clearing. 28

Figure 13: SAR mosaic for 2014 focusing on the areas of extensive clearing. 29

Figure 14: Broad-scale clearing identified in 2017 using Landsat imagery. 30

Figure 15: Landsat mosaic for 2017 focusing on the areas of extensive clearing. 31

Figure 16: SAR mosaic for 2017 focusing on the areas of extensive clearing. 32

Figure 17: Assessment of total area of cleared area as of 2017.....33

Figure 18: Frequency of cleared pixels at a range of distances from the existing road. 34

Figure 19: Logged area derived from PNG observatory data in 2002.....35

Figure 20: Logged area derived from PNG observatory data in 2015.....36

Figure 21: Frequency of logged pixels at a range of distances from the existing road.....37

Figure 22: Comparison between extent derived from a qualitative assessment of the SAR and Landsat 2014 and 2017 remote sensing data and the 2015 PNG observatory data. Note that the qualitative assessment was only conducted south of Bewani mountain range identified approximately by the purple line. 37

Figure 23: Change in area for logged and cleared land covers over time. 38

Figure 24: Variables tested for assessing land cover change 41

Figure 25: Two soil maps for PNG with contrasting distributions: a) CSIRO 1965 and b) Bleeker 1983. 44

Figure 26: Transition probabilities for clearing. a) final model and b) sensitivity analysis scenario with distance to Vanimo included as a driver 45

Figure 27: Transition probabilities for logging. a) final model and b) sensitivity analysis scenario with distance to Vanimo included as a driver 47

Figure 28: Existing suitability maps for the region. Left: Forest Resources map of West Sepik Province. Right: CSIRO Land Research Series No 31 1972. These diagrams illustrate how different models and maps provide vastly different spatial representations of suitability for forestry. 48

Figure 29: Hard projections for land clearing. a) existing road and b) proposed road. 49

Figure 30: Soft projections for logging. a) existing road and b) proposed road. 50

Figure 31: Hard projections for logging. a) existing road only and b) proposed road. 51

Figure 32: Soft projections for logging. a) existing road and b) proposed road. 52

Figure 33: Combined logging and cleared projected land cover change scenarios for both with and without the proposed road. 53

Figure 34: Annual forest change in forest area cleared/and or degraded in commercially accessible forest and overall forest area (Diagram from Shearman et al., (2009)). 55

Tables

Table 1: Available information on Forest production areas traversed by the existing and proposed roads. Note this does not include all areas as many did not have available information. Also note Amanab Block 7 does not overlap the existing or proposed road but it is within a very short distance from the road (PNGFA, 2016). 16

Table 2: Potential volume of timber from major forest types within the Idam Siawi Integrated Agro-forestry development project area (Tangoy Vivafounder Holdings Limited, 2017)..... 16

Table 3: Harvest area and volumes within the 2011 Frieda River dam proposal area (Towney, 2011). 17

Table 4: Imagery data used in the analysis for 2011, 2014 and 2017 20

Table 5: PNG Forest observatory for classification of logged area 21

Table 6: Confusion matrix 34

Table 7: Total area logged area based on extracted PNG observatory data 37

Table 8: Land cover change statistics for logged and cleared areas. 38

Table 9: Variables tested in land change model 42

Table 10: Parameterisation of the multi-layer perceptron (MLP) neural network 43

Table 11: Land change modelling scenarios and input variables and sensitivity analysis. *Note that distance from previous land conversion (i.e. cleared or logged) compared 43

Table 12: Final forest to clearing transition probability model and assessment of forcing a single independent variable constant on accuracy, skill and assessment of influence 45

Table 13: Final Logging transition probability model and assessment of forcing a single independent variable constant on accuracy, skill and assessment of influence. 46

Table 14: Sensitivity of Model to forcing a single independent variable to be constant and influence on transition probabilities i.e. impact on Accuracy and Skill measures on overall model performance. A large drop in Accuracy or Skill measures indicate that not including a variable will negatively affect the accuracy of the model.....54

1.0 Introduction

1.1. Background

The Sepik Development Project is a series of interdependent projects underpinned by the Frieda River Copper-Gold Project (FRCGP) in northwest Papua New Guinea (PNG). The four key components of the Sepik Development Project are:

- Frieda River Copper-Gold Project (FRCGP).
- Frieda River Hydroelectric Project (FRHEP).
- Sepik Infrastructure Project (SIP).
- Sepik Power Grid Project (SPGP).

As part of the SIP, a 325-km-long infrastructure corridor will be developed between the FRCGP mine site and the Vanimo Ocean Port, located on the north coast of mainland Papua New Guinea. It will comprise an unsealed 7.5 m wide dual-lane road suitable for all cargoes (according to the proposal), a concentrate pipeline (FRCGP) and a power transmission line (SPGP). The road alignment includes 237 km of existing road and 192 km of proposed road (according to the spatial data) (Figure 1). The mine will be accessed via the existing road from Vanimo to Green River and then a new road via Hotmin to site. The road will be public from Vanimo to Hotmin and private from Hotmin to the site.

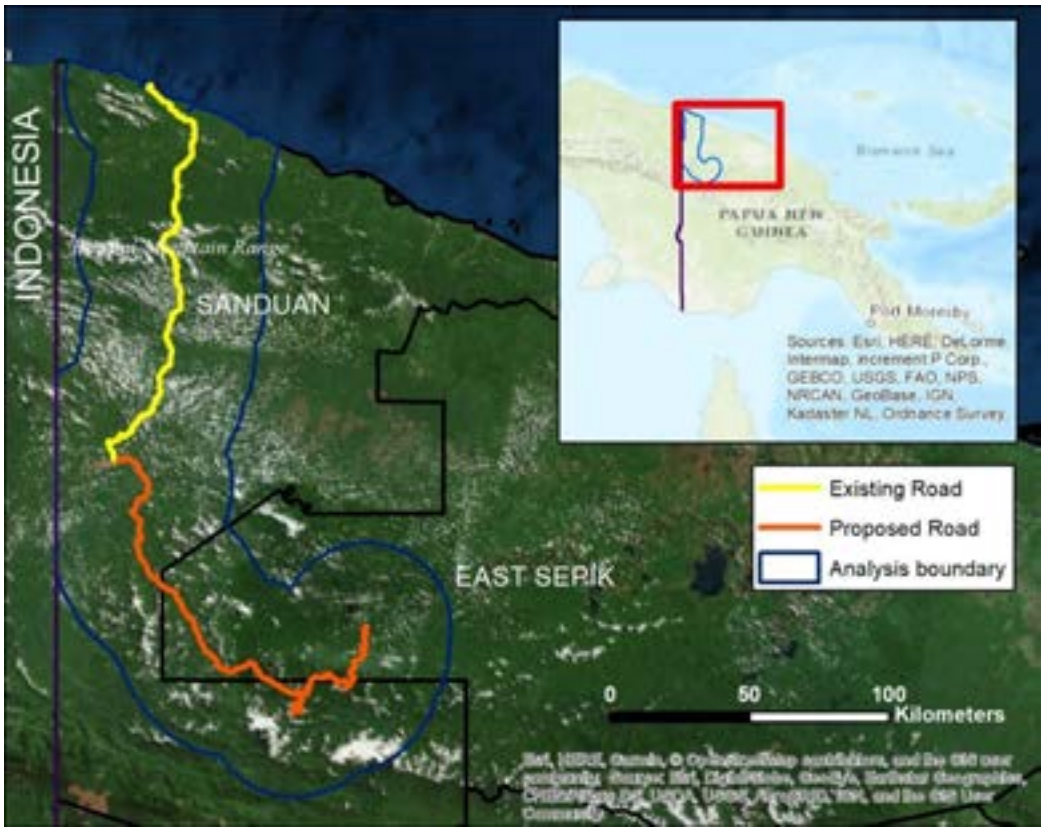

Figure 1: Study area with existing and proposed road buffered by 30 km. The analysis was performed within the buffered area.

A consideration for the project proponents and regulators is the potential secondary environmental impacts associated with the creation of the road corridor. In addition to the loss of forest cover associated with the clearance for the road footprint, the creation of a road can increase habitat loss and fragmentation by providing access to areas for forestry and agroforestry (Laurance et al., 2015, 2014). These impacts potentially could be reduced and/or made explicit at the project planning stage through the application of leading practice spatially explicit modelling (Cane et al., 2015; Lechner et al., 2017b, 2017a). The objective of this study was to assess the secondary impacts of the proposed road which could result in the facilitation of forestry and agroforestry.

This report utilises remote sensing to provide a current estimate of broad-scale clearing of forest, and existing spatial data to characterise logging with spatially explicit land cover change modelling to characterise the suitability of the forest within the road corridor for future agroforestry and forestry and how the proposed road extension may further contribute to these activities. In addition, we include a broad review of the commercial forestry and agroforestry in the region.

1.2. Summary of objectives

The project has three desktop-based work components:

1. Review of the commercial forestry and agroforestry in the region
2. Remote sensing and GIS mapping of the spatial extent of forestry and agroforestry.
3. a. Modelling and assessment of land capability to characterise potential future forestry and/or agroforestry.
   b. Assessment of the impact of the road corridor on future land use change due to forestry and/or agroforestry.

1.2.1. Work component 1: Review of the commercial forestry and agroforestry industries in the region

Utilising information from the grey and academic literature we provided a high-level assessment of existing commercial forestry and agroforestry industries in the region. In addition, we used GIS analysis to characterise the total amount of commercially viable timber resources.

1.2.2. Work component 2: Remote sensing and GIS mapping of the spatial extent of forestry and agroforestry

This work component involved two phases: data selection and data classification.

In the first phase we identified the appropriate remote sensing data based on: cloud cover, length of available images, resolution and quality, number of images required to cover the study site and availability of ground truth. In the tropics one of the greatest limitations for remote sensing is cloud cover making multi-spectral remote sensing difficult.

Multi-spectral sensors such as Landsat, Sentinel and MODIS which provide free long-term datasets (except for Sentinel) are the best for long-term forest monitoring. However, these can be problematic to use in the tropics due to cloud cover and thus cloud penetrating Synthetic Aperture Radar (SAR) is a useful alternative.

In the next phase a landcover classification algorithm was applied to classify land cover after appropriate pre-processing. Then using imagery from multiple dates, current and historical land use was mapped.

1.2.3. Work component 3a: Modelling and assessment of land capability to characterise potential future forestry and/or agroforestry.

A land change model was used to inform an assessment of potential future agroforestry land based on a range of variables

1.2.4. Work component 3b: Assessment of the impact of the road corridor on future land use change due to forestry and/or agroforestry.

Using the rate of forest/land use change, a comparison of projected land cover change with and without the road corridor extension was conducted.

1.3. Study Area

In order to ensure that the assessment was focused on local-scale drivers of land change and to reduce computational and practical limitations associated with conducting the assessment we buffered around the existing and proposed road at 30 km (i.e. for a total width of 60 km).

This width was selected as:

- the majority of the forest change is found within 30 km.
- widths greater than 30 km would have taken the study area outside of PNG.
- extending the buffer size further would have included areas of land cover change that are closer to other existing large roads and thereby confounding the analysis.
- mapping larger areas would have increased the complexity of the classification method (requiring a massive mosaic of multiple satellited image) yet provide no useful extra information for understanding the link between the road corridor and land cover change.

2.0 High-level assessment of the existing commercial forestry and agroforestry industries in the region

2.1. Overview

Approximately 10% of the global land area is covered by tropical forests of which the third largest contiguous area occurs within the island of New Guinea (Brooks et al., 2006; Testolin et al., 2016). The nation of Papua New Guinea (PNG) contains approximately half of this tropical forest which is considered to be some of the most diverse ecologically distinct forested ecosystems known (Brooks et al., 2006; Myers et al., 2000). The rainforests provide food and building materials locally, provide a backup resource when crops fail or natural disasters occur and are important for the export economy of PNG (Shearman and Bryan, 2011). These forests also provide important ecosystems services protecting watersheds, acting as filtration areas, providing coastal protection and protecting soils and their fertility (Shearman and Bryan, 2011). Currently 200 commercial species are targeted for logging enterprises of which only a few have the highest market values (Rogers, 2011).

Between 2-7% of global deforestation and carbon emissions have been attributed to the modification of primary and secondary forest in PNG (Bryan et al., 2010). Primary tropical rainforests around the world have been increasingly targeted by the selective logging industry and approximately 20% of such forests are allocated to selective logging operations (Shearman et al., 2012). Within PNG, once primary forests have been utilised by selective logging they may be left to regenerate and be relogged at a later date or be converted to alternative forms of use such as plantations, crops or pastures. In PNG and other nations selective logging and its associated access tracks have allowed once inaccessible areas to be exploited by colonisation and human usage such as hunting, mining and logging both legal and illegal (Koh and Wilcove, 2009; Laurance et al., 2009; McAlpine and Quigley, 1998; Shearman et al., 2012). Human pressure on the margins of forests is increasing significantly in PNG which has a very high population growth rate (2.009-2.85%/yr; currently 2.034) (ITS Global, 2006; Laurance et al., 2012; https://data.worldbank.org/indicator/SP.POP.GROW?locations=PG 2017). Such utilisation of forests can be substantial. For example, annual firewood use in PNG, primarily by villagers, is estimated to be three times higher than log exports by volume and usually undertaken in areas most intensively modified by selective logging (Filer et al., 2009). Subsistence farming such as slash and burn agriculture is believed to be the second largest converted or forest (land cover) after selective logging (Shearman et al., 2009).

Various measures have been used to quantify the utilisation of primary forests leading to disagreement based on definitions, terminology, methodologies used and subsequent meanings of mapped units (Filer et al., 2009; McAlpine and Quigley, 1998; Shearman et al., 2009). In spite of these differences there is consensus that between 1972 and 2002 selective logging activities had the most significant impact in terms of land area utilised. Over this time period most of these changes occurred within island provinces and lowland accessible areas on the mainland (Shearman and Bryan, 2011; Shearman et al., 2009). Other changes have occurred through palm

oil conversion which has seen a steadier rise than logging exports (Filer, 2010). Mining is considered to have affected approximately 0.2% of forested areas (Shearman et al., 2009) though this may be an underestimate (Filer, 2010).

Selective logging is currently one of the more important contributors to the PNG economy and thus ensuring the sustainability of silviculture practices has been an important focus of natural research management in the country (Filer et al., 2009; ITS Global, 2006; Laurance, 2011; Shearman et al., 2012). Evidence indicates that logging has largely occurred in the more productive forests with the highest densities of merchantable timbers (McAlpine and Quigley, 1998; Shearman and Bryan, 2011). These forest are generally lowland forests with lower rainfall areas and are also the most likely to be converted to other usages due to accessibility and proximity to habitation and ports (McAlpine and Quigley, 1998; Shearman and Bryan, 2011). Lowland forests comprise 65% of PNG's forest estate with 42% of PNG's forest estate considered to be inaccessible to forestry operations (Shearman and Bryan, 2011). Inaccessibility has generally been characterised as areas with over 30 degrees as the dominant slope, over 2400 m altitude, land in polygonal karst landscapes, areas inundated over 80% of the area permanently or near permanently and coastal areas containing mangroves (McAlpine and Quigley, 1998).

Selective logging operations within PNG have been criticised because of various, damage caused to soils, by increasing the vulnerability of forests to fire, changes to biodiversity and forest composition and conversion to agriculture (Marsden and Pilgrim, 2003; Nepstad et al., 1999; Rogers, 2010; Testolin et al., 2016). Two of the most sustained issues involve collateral damage involving damage to surrounding trees from felling and removal and cycles of secondary logging (Katsigris et al., 2004; Laurance, 2011; Rogers, 2010; Shearman et al., 2012). Tropical forest merchantable timber resources are low due to the diversity of tropical forest tree species at any stand. Primary forests often only contain a basal area of 2-5 m^2 per hectare of usable timber as many species have properties which make them less suitable for timber such as small size, are unknown to the market or are slow to grow (Da Silva et al., 2002; Shearman et al., 2012).

The silvicultural practices used to selectively extract these timbers up to the early 2000s often caused significant secondary damage particularly through skidding of timbers to access points for removal to offsite processing areas (Jackson et al., 2002; Rogers, 2010). The damage of residual stems can cause the mortality of other species for up to 10 years after a logging event impacting 30-70% of the remaining stand (Rogers, 2010). To combat this issue reduced impact logging (RIL) has been promoted along with portable sawmill logging. Reduced impact logging is defined as well planned, controlled harvesting by trained workers to minimise impacts (Rogers, 2010). Portable sawmills have been found to reduce skidding impacts as timbers are processed on site. Rogers (2010) found that although reductions in skidding were apparent the overall lowering of impact of portable mills was largely due to the smaller scale of operations with larger scale portable sawmill operations causing similar subsidiary impacts as conventional logging.

Return logging cycles have been called into question for their potential lack of sustainability (Katsigris et al., 2004; Laurance et al., 2012; Rogers, 2010; Shearman et al., 2012). New logging concessions officially only allow one fortieth of the loggable area to be logged in any one year (Filer, 2010). However, return logging cycles in many concessions have historically been half the

return rate i.e. 20 years (Katsigris et al., 2004). Recovery of large merchantable timbers may take more than the 40-year cycle (Shearman et al., 2012) and whether commercial timbers regenerate well in the post logging environment is not fully resolved (Rogers 2010). The yields of second and third round logging areas are known to be much lower due to lack of larger stems and the damage caused in the first logging event (Filer 2010). Generally, logs from subsequent logging rounds are more suitable for pulp and low grade uses as larger logs are not present (Shearman et al., 2012). Overall conventional commercial harvesting within PNG is of selective logging of select commercial tress of good stature and diameter (Towney, 2011).

Such silvicultural practices have led to a steady decline in the loggable areas available to forestry that contain merchantable timbers for export. Logging companies increasingly require entry into primary forest areas and areas with a lower density of resources in less accessible locales (Shearman et al. 2012). The economics of the forestry industry has been of importance to PNG and has contributed 6% of tax receipts and 5% of government revenue between 1999 and 2002 and added to local economies and infrastructure (ITS Global 2006). Currently renegotiation of logging concessions to reduce the rate of removal are being sought by the PNG Government (PNGFA, 2016). In addition, as a primary resource, the industry is vulnerable to the vagaries of markets. Export log income peaked in 1994 but declined during 1996-2002 during the Asian economic downturn (Filer et al. 2009). The industry is vulnerable to changes in government regulation, unresolved property rights and corruption (Filer et al. 2009; Laurance 2011; Laurence & Laurance 2012).

It was estimated that as of 1998 some 70% of the land area of PNG was primary forest (McAlpine & Quigley 1998) with estimates that at least 80,000 km^2 of potential production forest remaining in 2010 (Filer 2010). Although a number of estimates have been made using various remote sensing products much of these focus on imagery dating only to as late as 2002. Impacts over the last 15 or more years since these assessments requires a new round of analyses and interpretations, which are beyond the scope of this study.

2.2. Regional summary

Currently little direct information exists to enable a thorough and targeted discussion of the potential logging resources found along the existing and current roads that may be impacted. The most recently available information for parts of the study area is from 1992, 1994 and 1999. However, under the National Forest Inventory (NFI) program both East and West Sepik Province is being assessed and may be available in the future. More recent resources provide anecdotal information that may assist in understanding the current potential resources found along the development road. However, these ‘grey’ resources are highly limited and do not provide a consistent understanding or methodology across the entire potential impact area and often use different terminology for forest types making comparison difficult. In particular much of the area affected by the proposed new road has no currently available data. Using generally available up to date resources the following information has been extracted.

The existing road passes through six forest production areas in West Sepik which include Vanimo Block 6, Vanimo Block 1-5, Amanab Block 5, Amanab Block 3-4, and Amanab Block 1 & 2. Amanab Block 7 is also of interest as the road is within a very short distance of the existing road

(~1.5 Km) (Figure 2). The proposed road starts within a small southern section of Amanab Block 1-2 before entering areas of Idam Siawi and areas not included within assessments of the West Sepik Province (Figure 2). Of these designated timber production areas dissected by the existing and proposed roads the Vanimo timber area was acquired by the state and is currently allocated to industrial wood production which is currently operational (PNGFA, 2016). Within this forest production area Vanimo Forest Products takes 65,000 m3 annually in sawn timber (PNGFA, 2016). Within the Idam Siawi area 139 species of trees were recorded that had verifiable stock volume (Tangoy Vivafounder Holdings Limited, 2017). The largest stock volume is attributable to Kwila accounting for approximately 13% of all stock volume (Tangoy Vivafounder Holdings Limited, 2017). A summary of the potential commercial loggable areas and some estimates of sustainable volume are given in

Table 1 and Table 2. Data pertaining to survey of timber resources from surveys conducted species are given in Appendix A. Within the Sandaun Province (Figure 2) 22 logging concessions existed in 2004 which had been logged, were being logged or were in proposals to be logged comprising 67% of the land area of that province (Rogers, 2011).

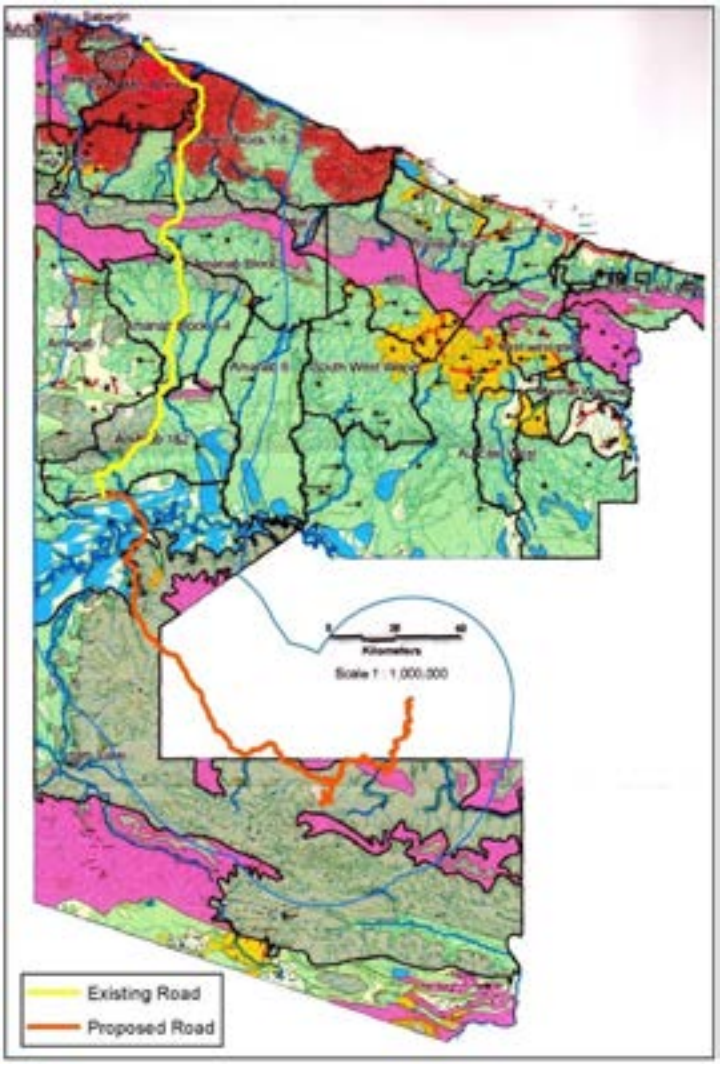

Figure 2: Scanned Forest Resource Map of the West Sepik Province (PNGFA, 2016) with existing (yellow) and planned roads (red) overlaid along with 30 km buffer zone.

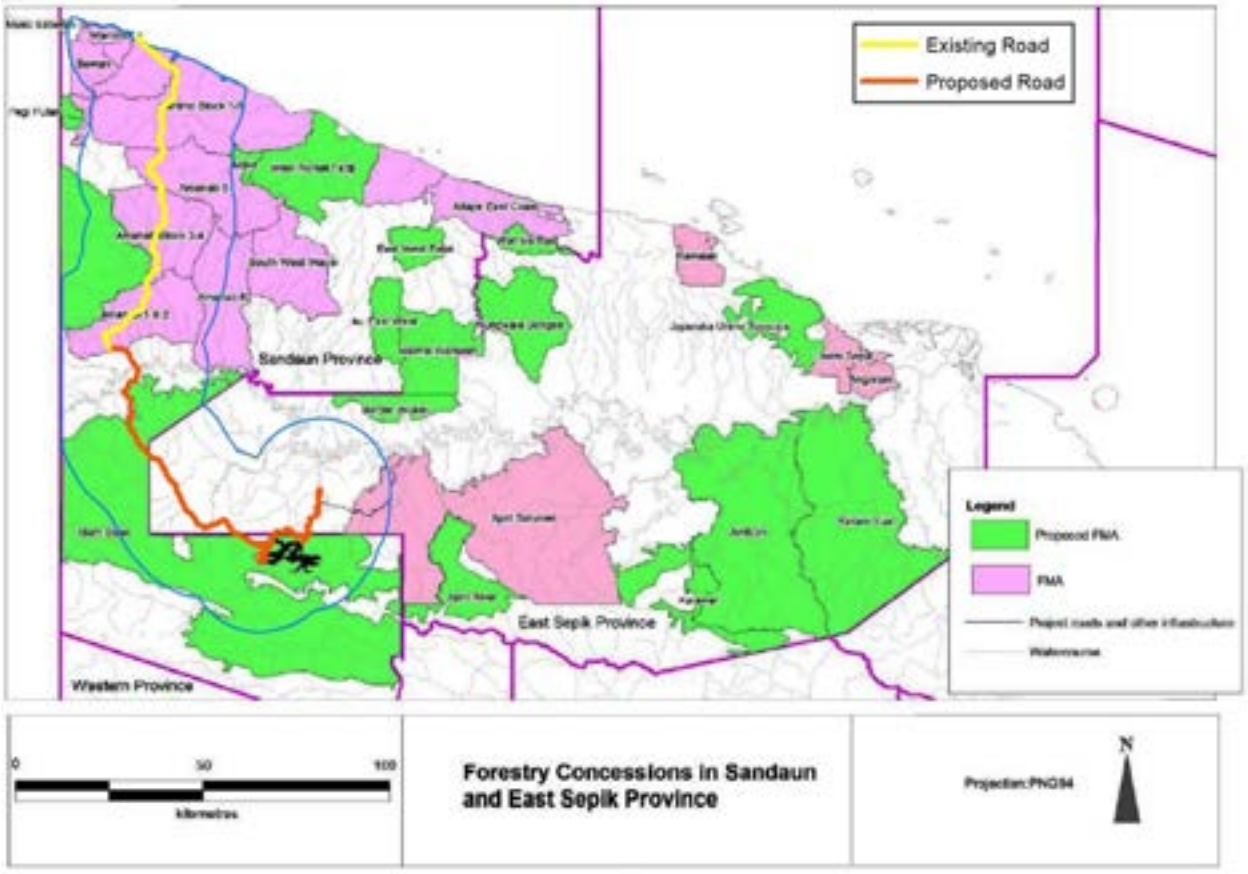

Figure 3: Known and proposed logging concessions within the Sandaun and East Sepik Provinces (taken from Rogers (2011)) with existing (yellow) and planned roads (red) overlaid along with 30 km buffer zone.

Table 1: Available information on Forest production areas traversed by the existing and proposed roads. Note this does not include all areas as many did not have available information. Also note Amanab Block 7 does not overlap the existing or proposed road but it is within a very short distance from the road (PNGFA, 2016).

Area	Forest Potential (Ha)	Total Area (Ha)	Sustainable cut (m^3/annum)	Proposed (P) or Existing (E)
1. Allocated Area				
Vanimo	195,189	291,827		E
2. Unallocated Area				
Amanab Block 3-4	113,204	119,909	48,000 (inclusive of Blks 1-4)	E
3. Outside of Timber Rights Purchase Areas				
Amanab Block 1-2	77,011	92,524	See above	E
Idam Siawi	730,820	781,501	459,000	P
Frieda River	No data	No data		P
4. Reserve Forest Proposed Inclusion				
Amanab Block 5	126,963	135,008	258,000 (inclusive of blocks 5, 6 & 7)	E
Amanab Block 7*	138,370	186,715	See above	E

Table 2: Potential volume of timber from major forest types within the Idam Siawi Integrated Agro-forestry development project area (Tangoy Vivafounder Holdings Limited, 2017).

Type	Area	Stock Volume
Low altitude highlands	7000 ha	1,580,000 m^3
Sparse Forests	10,000 ha	860,000 m^3
Swamp Forest	10,000 ha	970,000 m^3
Total area loggable forest	141,000 ha	35,000,000 m^3

Within the proposed mining area, areas considered for inundation for power generation were assessed for commercial log/biomass removal prior to a dam build under a previous project

design proposed by Xstrata (Towney, 2011). The potential inundation of the river involved 6,433 ha of which 5, 616 ha is natural forest. Due to the low volume per hectare, the lower-quality species encountered, and the poor form of the larger trees in the Frieda River Catchment harvesting was considered to be unlikely to generate interest from contractors (Rogers, 2011; Townley, 2011; Table 3).

Table 3: Harvest area and volumes within the 2011 Frieda River dam proposal area (Towney, 2011).

Total Export Volume (m^3)			
Forest Types	**Area (ha)**	**<50 cm dbh**	**>50 cm dbh**
Terrace Forest	1 352.2	16 269.6	21 430.3
Hill Forest	3 132.5	28 319.5	25 227.4
Low /Medium Canopy Forest	1 130.9	1 804.3	0.0
Total	5 615.6	46 393.4	46 657.7

The final potential sources of land clearing in the region is the Special Purpose Agricultural Business Leases (SABL) and the Idam-Siawi Integrated Agro-forestry development. Within the study area the Forest Observatory web mapping service shows the presence of these in the region but mostly in the northern already cleared areas and towards the edge of the study area (Figure 4). However, no publicly available information on this exists to our knowledge. Another potential source of land clearing for agricultural development in the region is from the 126,800 ha Idam-Siawi Integrated Agro-forestry development near Green River (Tangoy Vivafounder Holdings Limited, 2017) which a recent news report suggests will go ahead (Tarawa, 2018). However, according to the same report the landowners have spent over 26 years trying to develop this project (Tarawa, 2018).

Figure 4: SABLs (in white) identified by the Forest Observatory (http://forest.pngsdf.com).

3.0 Remote sensing and GIS analysis of forest change

3.1. Summary

In the first phase we identified the appropriate remote sensing data based on: cloud cover, length of available images, resolution and quality, number of images required to cover the study site and availability of ground truth data. In the tropics one of the greatest limitations for remote sensing is cloud cover making multi-spectral remote sensing difficult.

Multi-spectral sensors such as Landsat, Sentinel and MODIS which provide free long-term datasets (except for Sentinel) are the best for long-term forest monitoring. However, a preliminary assessment of Landsat imagery showed that identifying cloud free imagery for the study area will be problematic[1]. Synthetic Aperture Radar (SAR), is a potential alternative for such an analysis as it is unaffected by cloud cover. However, such analyses typically do not produce results of similar quality to multispectral remote sensing. Thus, the first phase involved experimentation around which sensor or combination of sensors can be used for the study region.

In the next phase a landcover classification algorithm was applied to the data to classify land cover (i.e. nature vs disturbed forest) after appropriate pre-processing. Pre-processing of the data were conducted to remove atmospheric effects (in the case of multi-spectral data) and/or noise in the case of SAR. The land cover classification was based on known land cover locations (ground truth locations) which were identified using freely available data.

We used imagery from three dates to assess current and historical land use in order to assess the rate of land use change. We assessed historical changes from 1984, which is the date of the first publicly available Landsat imagery (though archival Landsat data can be obtained before that). We aimed to select an image as close to January 2018 as possible to represent current landcover. However, the image dates were dependent on the available imagery.

While the primary focus of this analysis was to utilise remote sensing data to characterise all land cover change, due to the inadequacies of this data and lack of ground truth, we used existing GIS analysis and qualitative analysis to characterise changes in land cover due to logging which were not captured with the remote sensing assessment.

3.2. Mapping objectives

The objective of this component of the project was to map and assess coarse-scale forest cover change surrounding the existing and proposed road. This includes:

1. **Agroforestry broadscale clearance** (i.e. clearing or conversion of native forest commonly to oil palm) - conducted with remote sensing classifiers.
2. **Logged areas -** mapped using a combination of existing data and photointerpretation.

[1] Google Earth Timelapse assessment of available imagery for the region https://earthengine.google.com/timelapse/#v=-4.12406,141.90084,8.941,latLng&t=1.20. Note areas in the image with high distortion are where the data were resampled to remove clouds. These images are useful for visualisation, but inappropriate for quantitative analysis.

3.3. Data selection

We assessed the utility of all freely available remote sensing data including optical multispectral MODIS, Landsat and Sentinel 2 and Synthetic Aperture Radar (SAR) Sentinel 1. For the study site it was extremely difficult to find cloud free imagery thus we used a combination of Landsat and Synthetic Aperture Radar (SAR) Sentinel 1 imagery (Figure 5,Table 4).

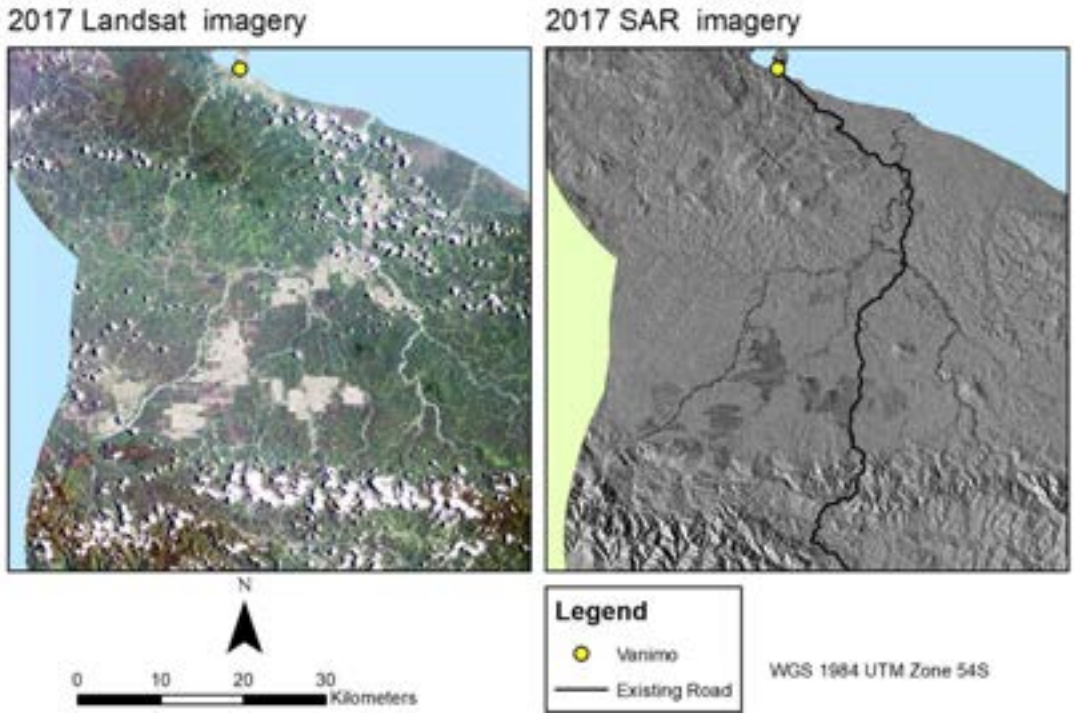

Figure 5: Comparison of Landsat 8 and Sentinel 1 SAR imagery.

We assessed forest change at 3 timesteps: 2011; 2014 and 2017. These timesteps were chosen based on available cloud free imagery for the entire study area. 2011 represents the most recent time period with available data across the entire study area in which all the land cover was predominantly natural, undisturbed or selectively logged (not including Vanimo). A qualitative assessment of available imagery pre-2011 also showed that there is no evidence of clearing pre-2011, suggesting that all the land cover present in 2011 represent primary forest or forest that has not undergone major disturbance such as land clearing, and therefore provides an effective baseline. However, there are areas that visually appear to be impacted by selectively logging (discussed below).

For the 3 timesteps we created land cover mosaics composed of two Landsat scenes or two SAR scenes (Table 4). Landsat has 45 years of historical records, dating back to 1972 (Young et al., 2017). However, Sentinel 1 SAR has only imagery from 2014 onwards. Thus, there was no available SAR imagery for the 2011 timestep. A total of 12 Landsat and Sentinel-1 scenes were processed for this project.

Table 4: Imagery data used in the analysis for 2011, 2014 and 2017

Imagery dataset	Product ID	Acquisition date
Landsat 7	LE07_L1TP_100062_20110106_20161210_01_T1	Jan 06 2011
	LE07_L1TP_100063_20110106_20161210_01_T1	Jan 06 2011
	LE07_L1TP_100063_20140215_20161117_01_T1	Feb 15 2014
	LE07_L1TP_100063_20140215_20161117_01_T1	Feb 15 2014
Landsat 8	LC08_L1TP_100062_20170319_20170328_01_T1	19 Mar 2017
	LC08_L1TP_100063_20170319_20170328_01_T1	19 Mar 2017
Sentinel-1 (SAR)	S1A_IW_GRDH_1SSV_20141023T085458_20141023T085523_002954_0035BA_9566	23 Oct 2014
	S1A_IW_GRDH_1SSV_20141023T085523_20141023T085548_002954_0035BA_163F	23 Oct 2014
	S1A_IW_GRDH_1SSV_20141023T085548_20141023T085614_002954_0035BA_9194	23 Oct 2014
	S1A_IW_GRDH_1SDV_20171218T085513_20171218T085538_019754_02197C_1A72	18 Dec 2017
	S1A_IW_GRDH_1SDV_20171218T085538_20171218T085603_019754_02197C_4E0A	18 Dec 2017
	S1A_IW_GRDH_1SDV_20171218T085603_20171218T085628_019754_02197C_BC1E	Dec 2017

The study mapped wide scale clearance associated with agroforestry using remote sensing data, however, due to the nature of the satellite imagery and the lack of field data it was impossible to map changes in forest quality/degradation that may have been associated with logging which didn't involve broad-scale clearing or utilisation of forests for traditional land use practices which do not result in coarse scale clearance. For example, the clearance of a single tree will not be captured by Landsat's 30 m pixel size using automated classifiers. Thus, logging was analysed qualitatively using a combination of satellite data sources, guided by on ground information supporting the existence of these activities and existing data from the PNG forest observatory (http://forest.pngsdf.com/) but only for 2002 and 2015.

Data from the PNG Forest observatory (Bryan and Shearman, 2015) were used to identify logged areas and also to provide an independent validation of our remote sensing mapping for our specific study area (Table 5). As the spatial data was not available, we screen shot images from the PNG Forest observatory mapping portal and then used an unsupervised ISODATA classifier to identify the logged areas. This method resulted in a lower resolution map of logged areas than the original PNG observatory data.

The PNG observatory data were mapped using methods outlined in Shearman et al. (2008) based on visual interpretation of recent logging-related deforestation and degradation such as logging roads, skid rack and canopy gaps.

Table 5: PNG Forest observatory for classification of logged area

Imagery dataset	Description	Acquisition date
The PNG Forest Observatory	"The PNG Forest Observatory is an interactive website showing the vegetation map of PNG in 2014, as well as maps of the area of forest cleared and logged over the period 2002-2014." http://forest.pngsdf.com/	Range of dates in order to characterise land cover for two timesteps: 2002 to 2015

3.4. Methods

For broadscale clearance associated with agroforestry we utilised CLASlite (Asner, 2009), a system for mapping forest cover change (Figure 6). It includes calibration, pre-processing, atmospheric correction, and cloud masking steps. The classification algorithm uses Monte Carlo Spectral Mixture Analysis, and expert classification. We also tested the utility of Sentinel-1 SAR imagery pre-processed and then classified using Support Vector Machinery, however, we found it did not provide as good land cover mapping results as Landsat and CLASlite. But, due to cloud cover which affects optical remote sensing there were data gaps in the Landsat data which the SAR imagery could be used to qualitatively address the data gaps. To summarise, we selected the Landsat imagery to ensure there were no cloud cover in the areas where we identified land cover change. We were able to validate the Landsat cloud cover "no data" areas with the Sentinel-1 SAR which can penetrate clouds to confirm no land cover change.

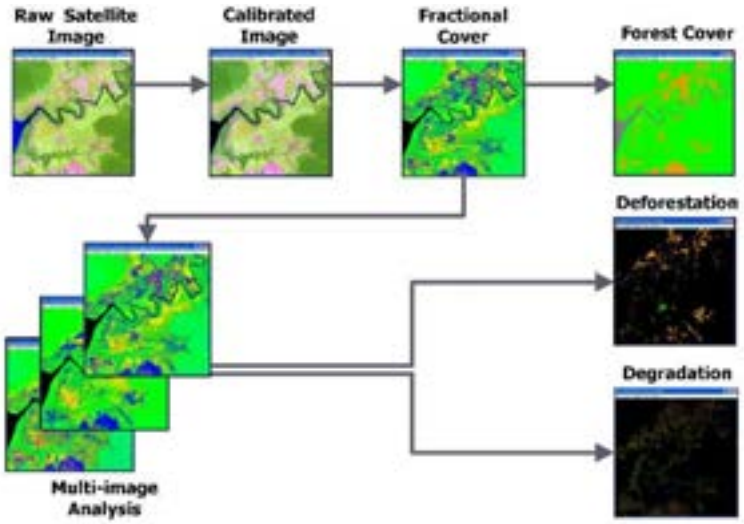

Figure 6: CLASLite - automated system for converting satellite imagery from its original (raw) format, through calibration, pre-processing, atmospheric correction, and cloud masking steps, Monte Carlo Spectral Mixture Analysis http://claslite.ciw.edu/en/about/software.html**.**

Figure 7 describes the workflow for pre-processing analysing, classifying and assessing the accuracy of the remote sensing data products.

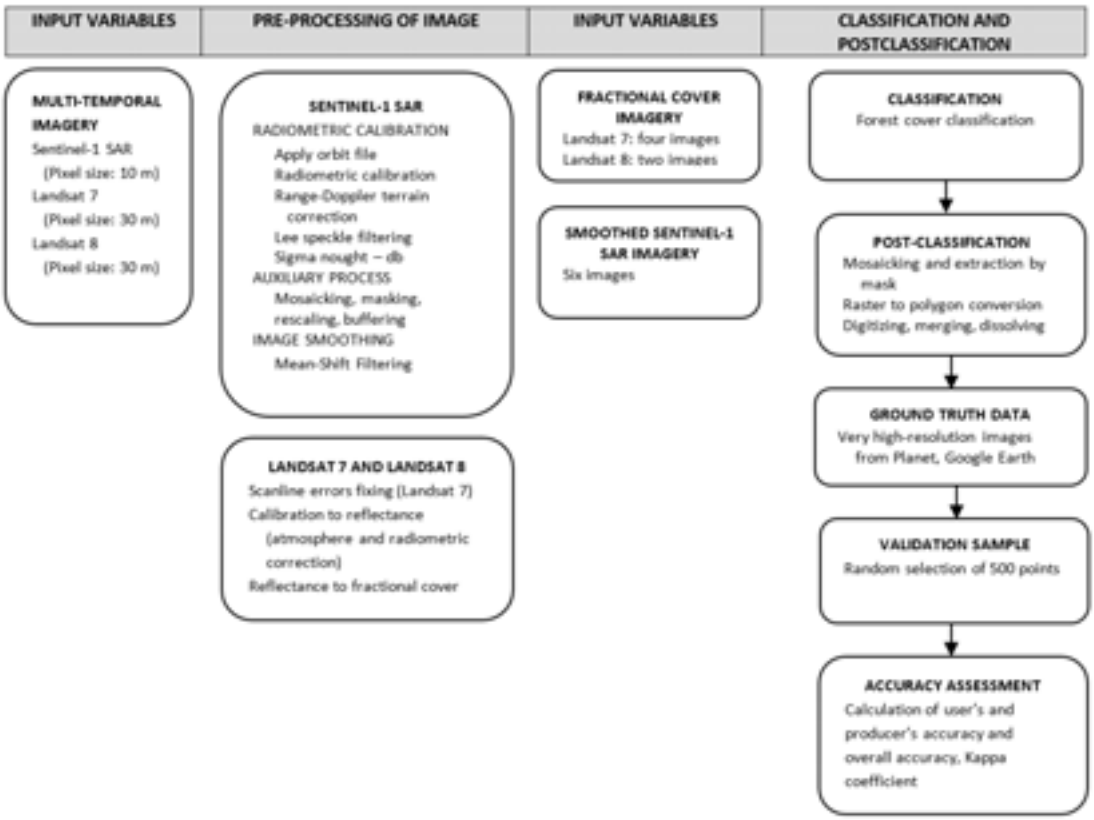

Figure 7: Workflow – from pre-processing to classification and accuracy assessment.

As described above the remote sensing assessment was unable to accurately detect selective logging and small-scale land clearance (i.e. traditional farming) and for this analysis we used a combination of readily available data from the PNG observatory data and a qualitative assessment.

3.4.1. Data pre-processing

The Sentinel-1A images were radiometrically-calibrated, terrain-corrected, and speckle-filtered using the SNAP 5.0 Sentinel Application Platform toolbox (available at http://step.esa.int/main/toolboxes/snap/). The radiometric calibration was conducted to convert pixel values of VH and VV amplitude into sigma naught (σ0) values which correctly represent the radar backscatter from the earth surface.

The calibrated multi-temporal images were then geometrically corrected using the Range-Doppler Terrain Correction algorithm with the 3 sec Shuttle Radar Topography Mission (SRTM) elevation model. After applying geometric correction, the images were resampled to a 10 meters spatial resolution and re-projected.

SAR images are affected by inherent speckle which results from random constructive and destructive interference of the return waves by elementary scatterers reducing image segmentation and classification accuracy (Lee et al., 1999). In this study, we applied a 5x5 adaptive Lee filter to reduce speckle based on the methods described in Lee et al. (Lee et al., 1999), who demonstrated such approaches are important for preserving polarimetric properties,

improve image quality, and dramatically boost classification performance. We used 5x5 kernel size filter as it has been found to be suitable in many recent studies (Haas and Ban, 2017; Son et al., 2017). These SAR images were then converted to decibel unit.

SAR image smoothing was performed with a spatial-range mean-shift filter which is a filtering technique which preserves edge and textures (Wang and Han 2010; Jarabo-Amores et al. 2011; Lang et al. 2014). The mean-shift filter was conducted with the Orfeo Toolbox (available at https://www.orfeo-toolbox.org/). The following parameters were empirically determined and found to produce the best results for preserving land cover features: spatial radius 5 and range radius 15. Mode convergence threshold and maximum number of iteration were kept at the default value of 0.1 and 100 respectively.

For Landsat 7 we utilized ArcGIS Landsat Toolbox to fix scanline error issues before performing image calibration. Then, CLASlite software was used for image calibration and pre-processing including atmospheric and radiometric correction. A total of six Landsat 7 and Landsat 8 images were calibrated to produce fractional cover images.

3.4.2. Classification cleared areas

Classification

The CLASlite software platform was used to perform forest cover classification. The thresholds for S (bare substrate cover fraction) and PV (photosynthetic vegetation cover fraction) were set to 20 and 80 respectively to generate forest cover classification.

Post-classification

Forest cover classified images were mosaiced and extracted within 30 km buffer from existing and proposed roads and then converted to polygons. Furthermore, cleared areas on smoothed SAR images were digitized as polygons. Converted forest cover polygons and digitized polygons were dissolved and merged to produce final forest cover classification map. Erroneous polygons were removed classified as cleared (i.e. rivers) were removed.

Accuracy assessment

A randomly spatial distributed set of 500 validation points was produced to test accuracy. The validation points were informed by high resolution Google EarthTM, Planet and the ArcGIS base map. Accuracy was measured and described using an error matrix, Kappa and producer and user accuracy. The error matrices and overall accuracy reports were generated from ArcMap 10.4.1.

3.4.3. Classification of logging

The CLASlite algorithm was not able to identify areas of selective logging that were identified by the consultants through discussions with people working on the ground. To address this we utilised data from the PNG forest observatory. However, the most recent data available was only 2015 and thus logging was characterised for different time steps.

We also conducted a coarse scale qualitative classification using manual image interpretation. We assumed based on discussions with the consultant that where multiple trails/roads are visible they provide indicators of the existence of selective logging (Figure 8).

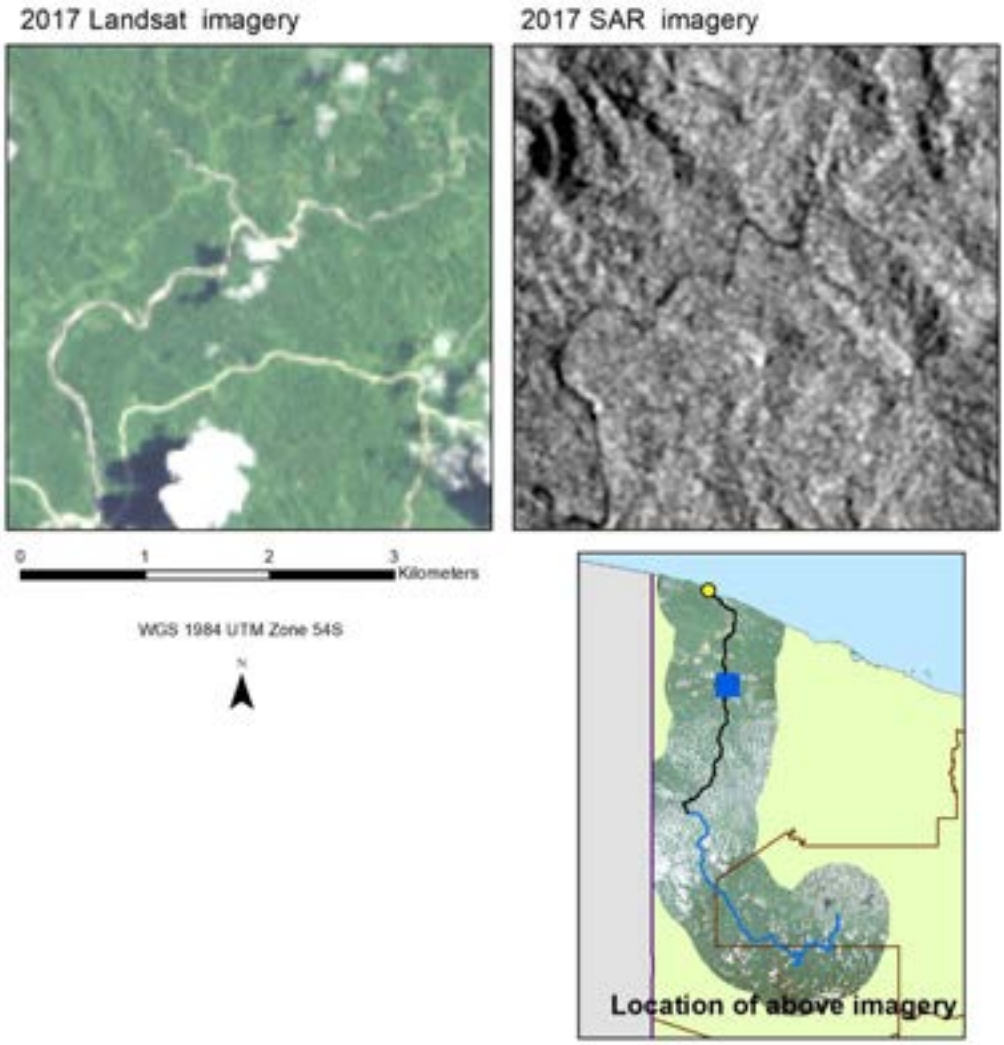

Figure 8: Example of locations with minor roads which can be used to identify selective logging areas. This analysis was confounded by streams, which appear very similar to roads, and cloud cover

3.5. Results - Remote sensing mapping of broad-scale clearance

In the following section we provide maps of broad-scale clearance for 2011, 2014 and 2017 along with the remote sensing data used in this assessment.

3.5.1. Broad-scale clearance assessment for 2011

For 2011 both qualitatively and using CLASlite we did not identify any broad-scale clearance within the study area (Figure 9, Figure 10). Before 2011 the Landsat archival imagery pre-2011 indicates there was no broad-scale clearance based on an assessment using image interpretation. Note that there is no SAR imagery for 2011. Also note that fine-scale clearance most likely occurred and was qualitatively observed.

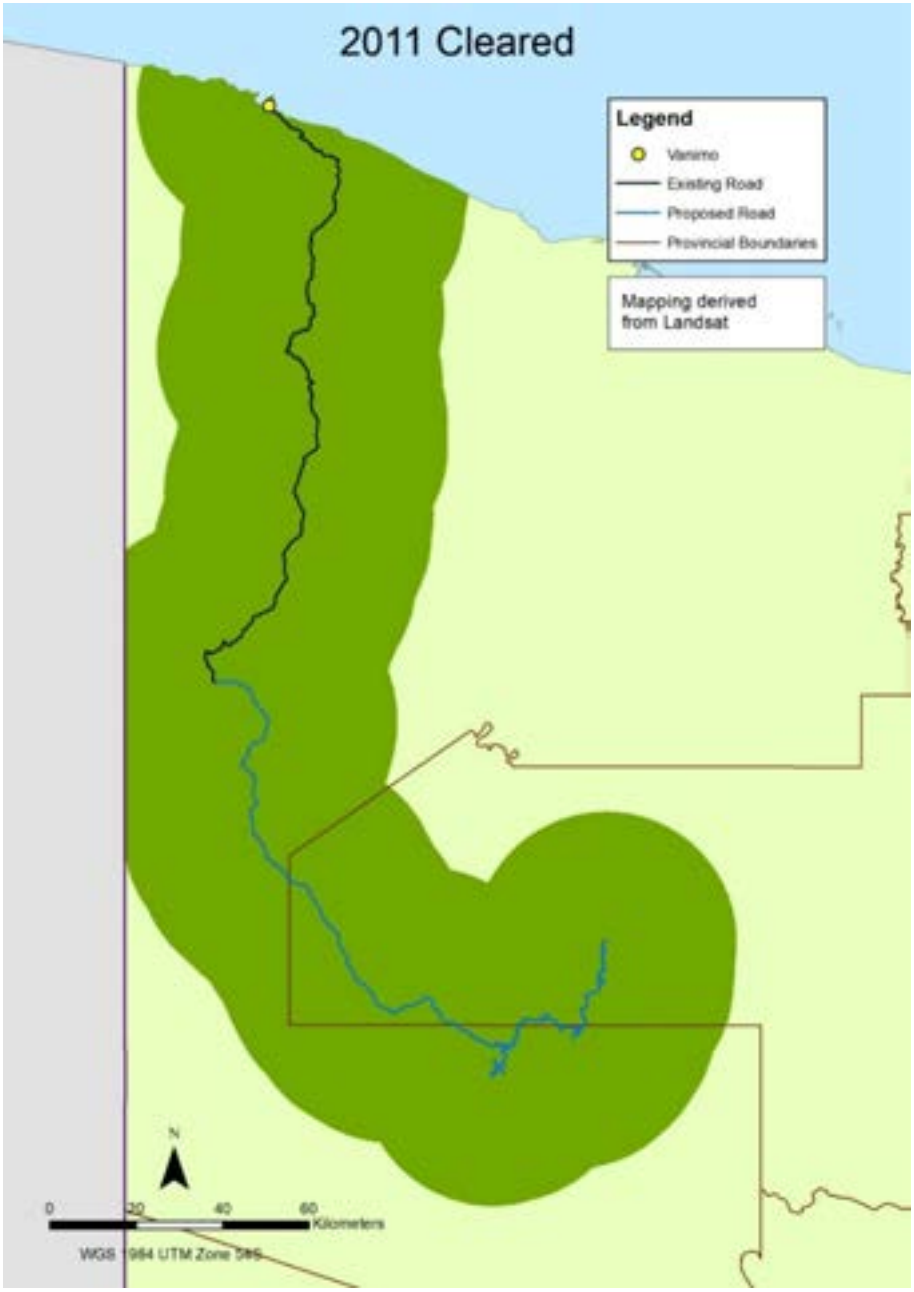

Figure 9: Cleared areas for 2011. Note we could not identify any broadscale clearing for 2011. Landsat archival imagery pre-2011 also supports this conclusion.

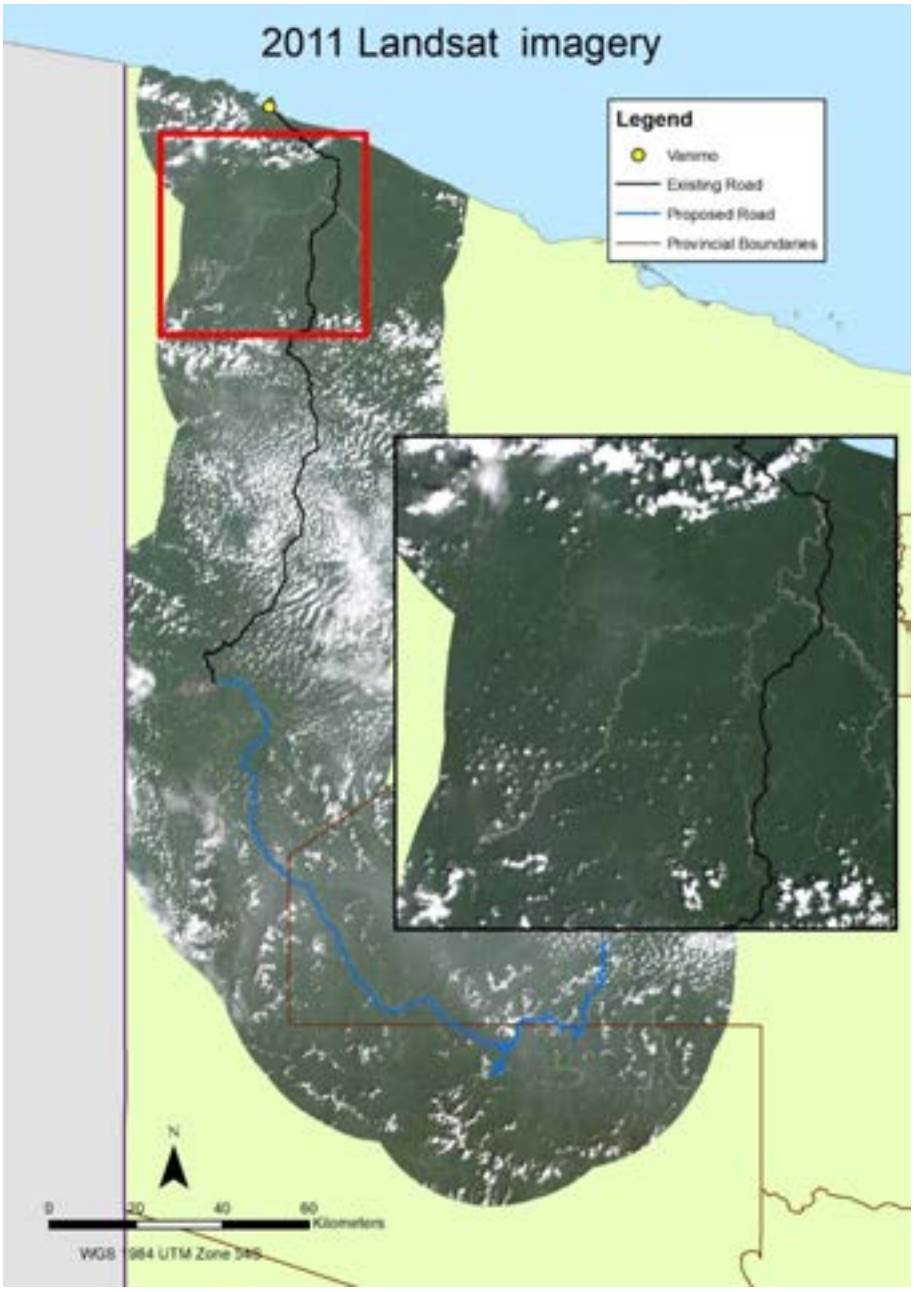

Figure 10: Landsat mosaic for 2011 focusing on areas where clearing occurs in later years.

3.5.2. Broad-scale clearance assessment for 2014

From around 2014 onwards, broadscale clearance, along with the creation of a road network, was observed in the northern part of the study area near Vanimo (Figure 11). The mapping was conducted using the Landsat imagery (Figure 12) and in areas with cloud cover assessed with the cloud penetrating SAR imagery (Figure 13). The exact year, between 2011 and 2014, when the clearance began was hard to determine due to the lack of cloud free imagery available. Note that the majority of cleared areas were near the road.

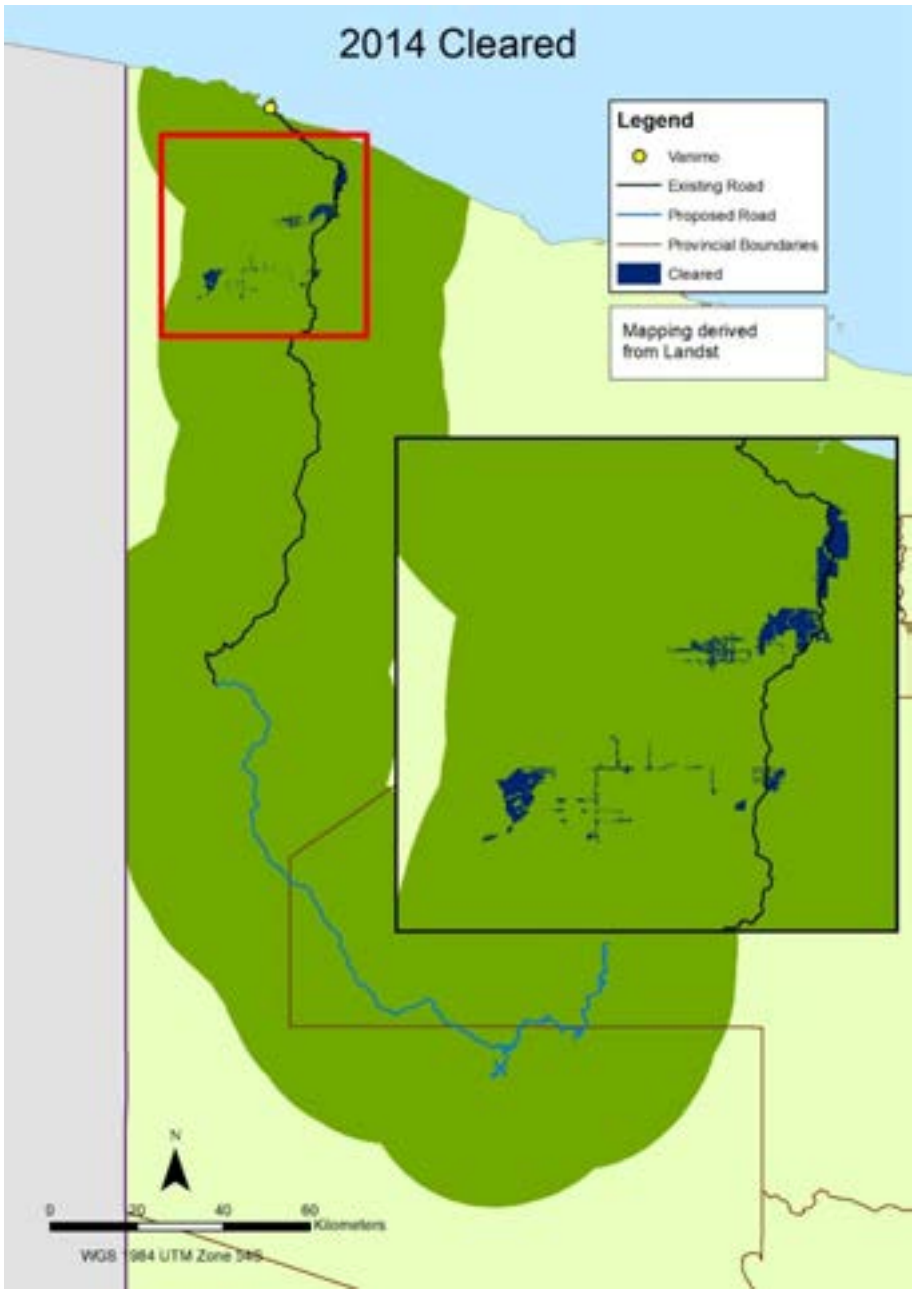

Figure 11: Broad-scale clearance identified in 2014 using Landsat imagery.

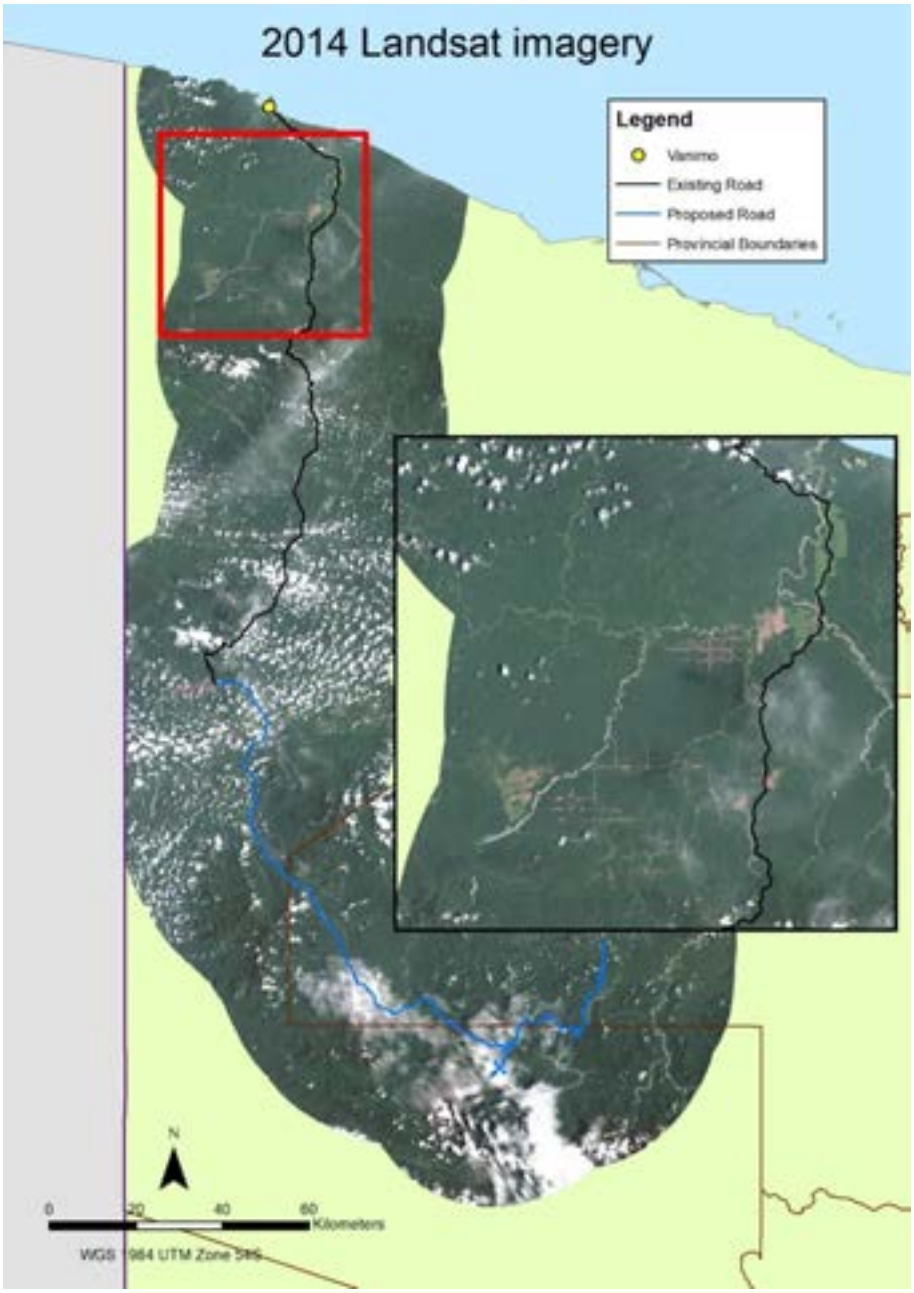

Figure 12: Landsat mosaic for 2014 focusing on the areas of extensive clearing.

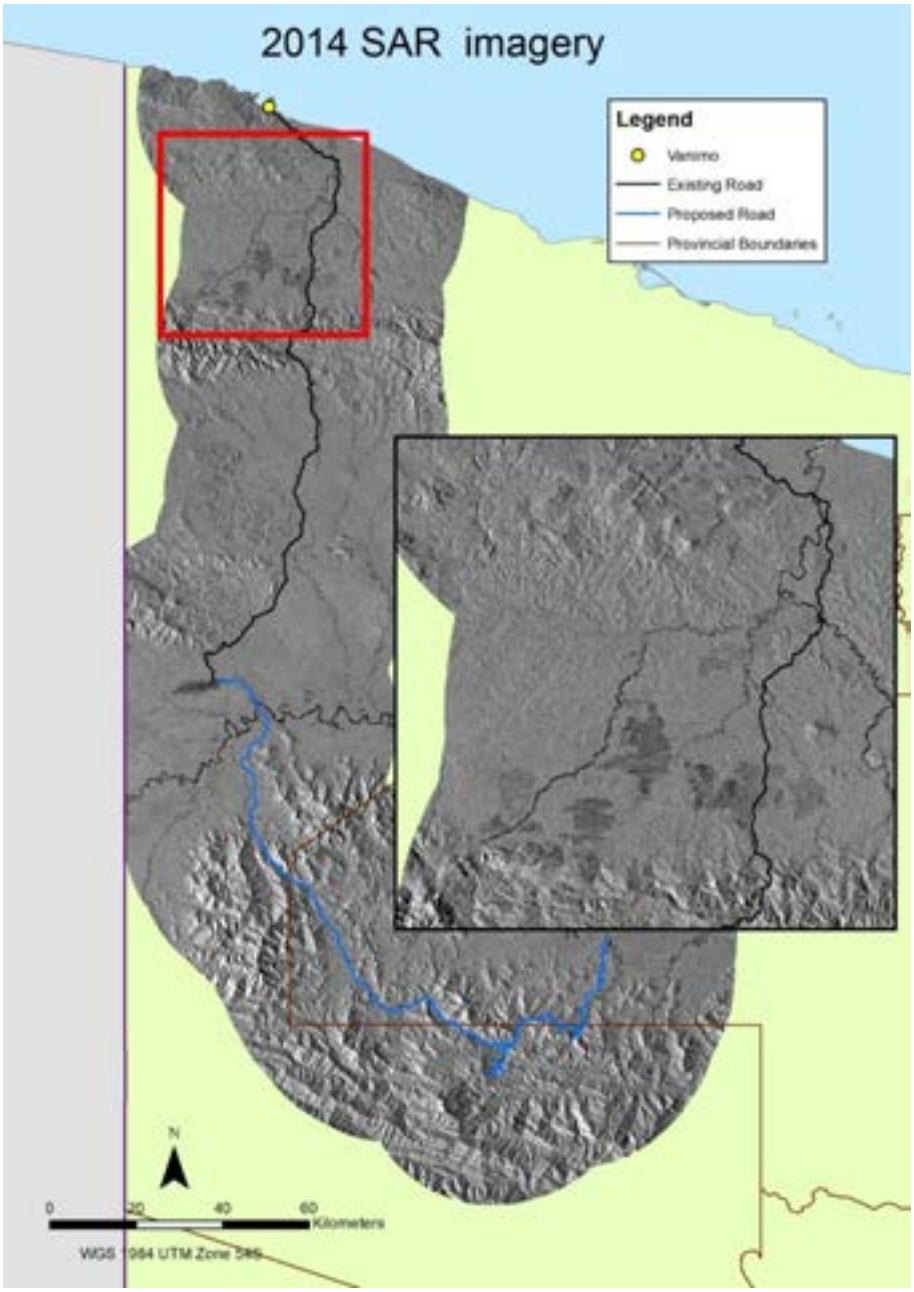

Figure 13: SAR mosaic for 2014 focusing on the areas of extensive clearing.

3.5.3. Broad-scale clearance assessment for 2017

For the latest available and cloud free mosaic for the study area in 2017 it appeared as though the clearance had expanded further Figure 14, Figure 15, and Figure 16).

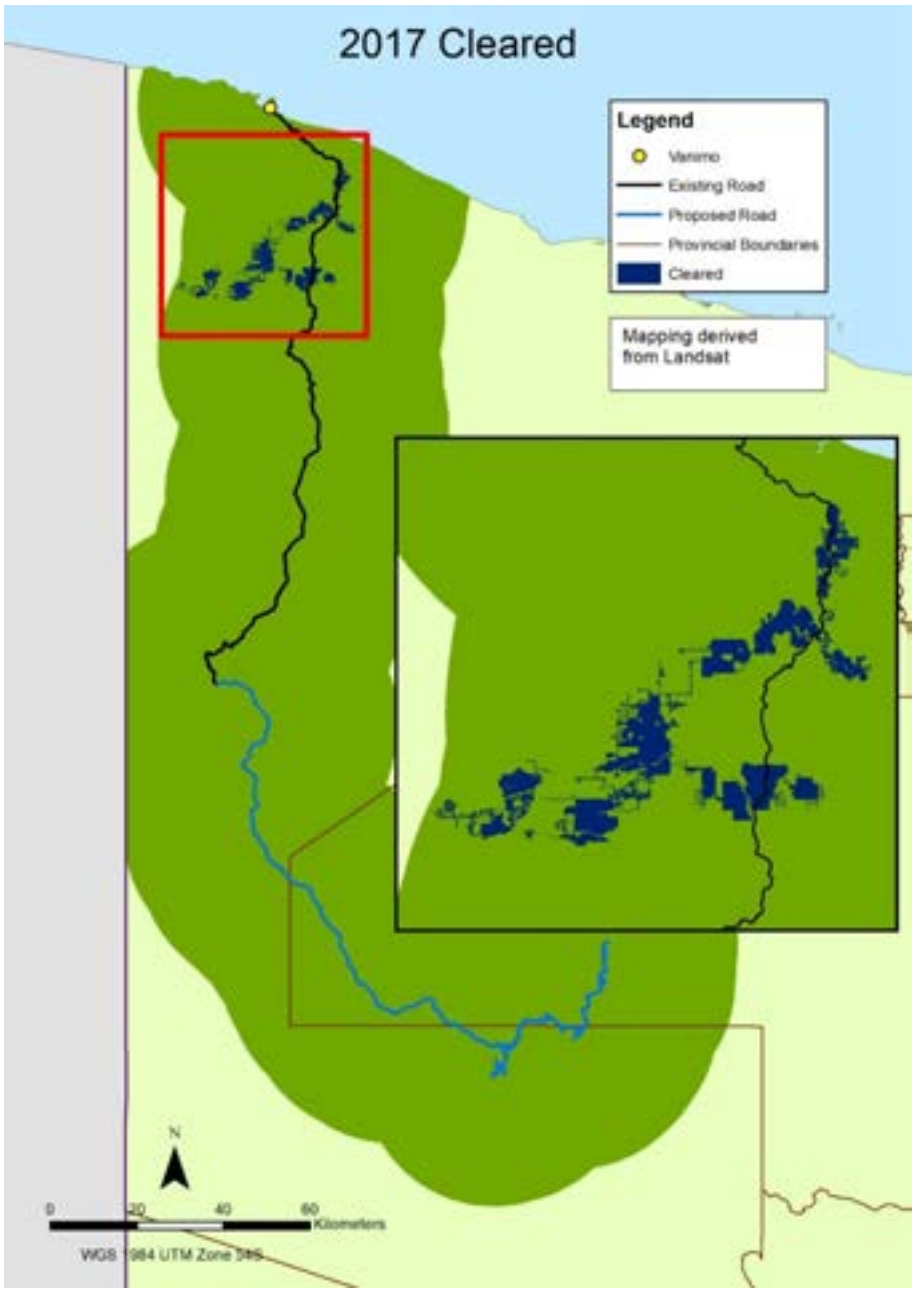

Figure 14: Broad-scale clearing identified in 2017 using Landsat imagery.

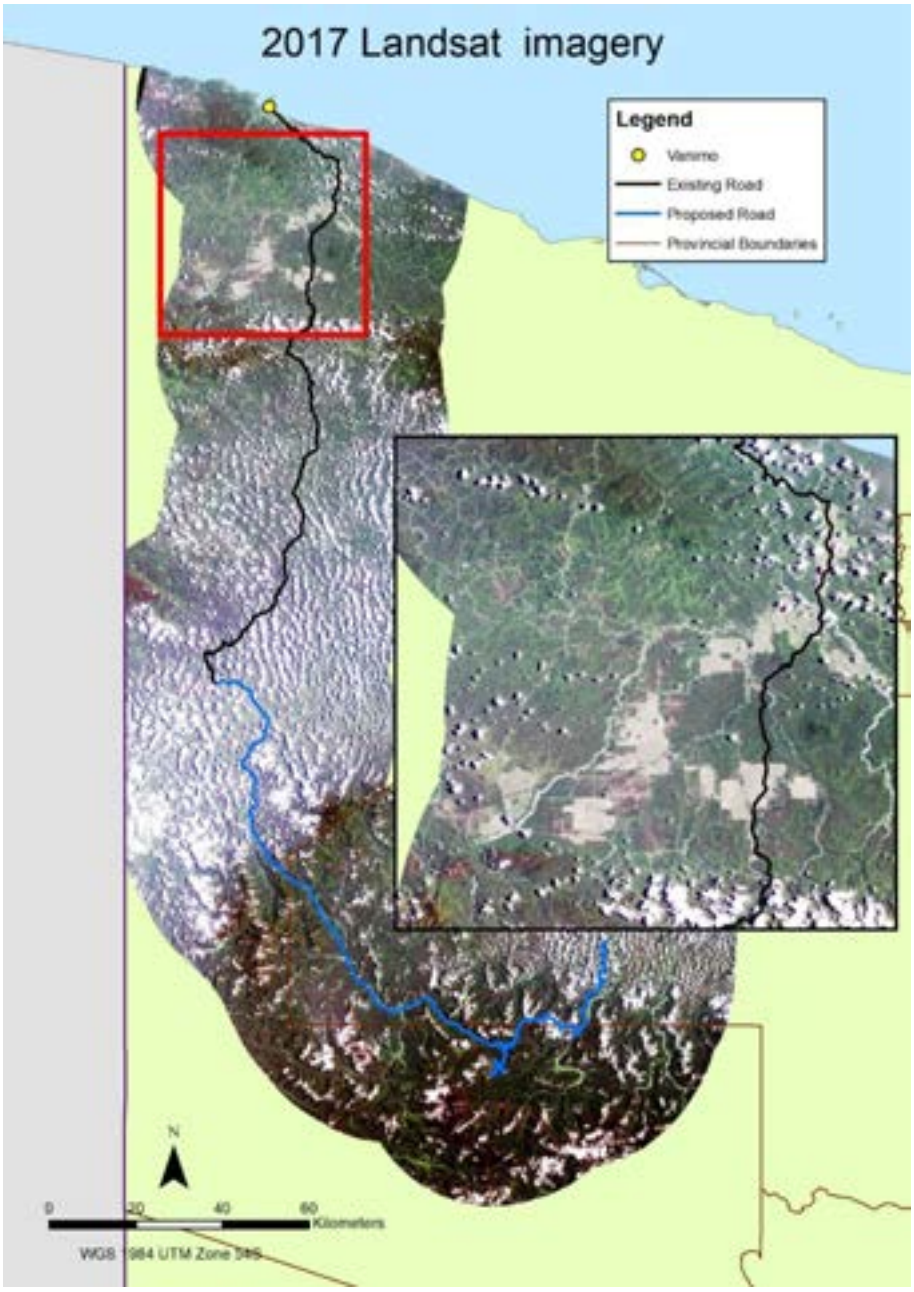

Figure 15: Landsat mosaic for 2017 focusing on the areas of extensive clearing.

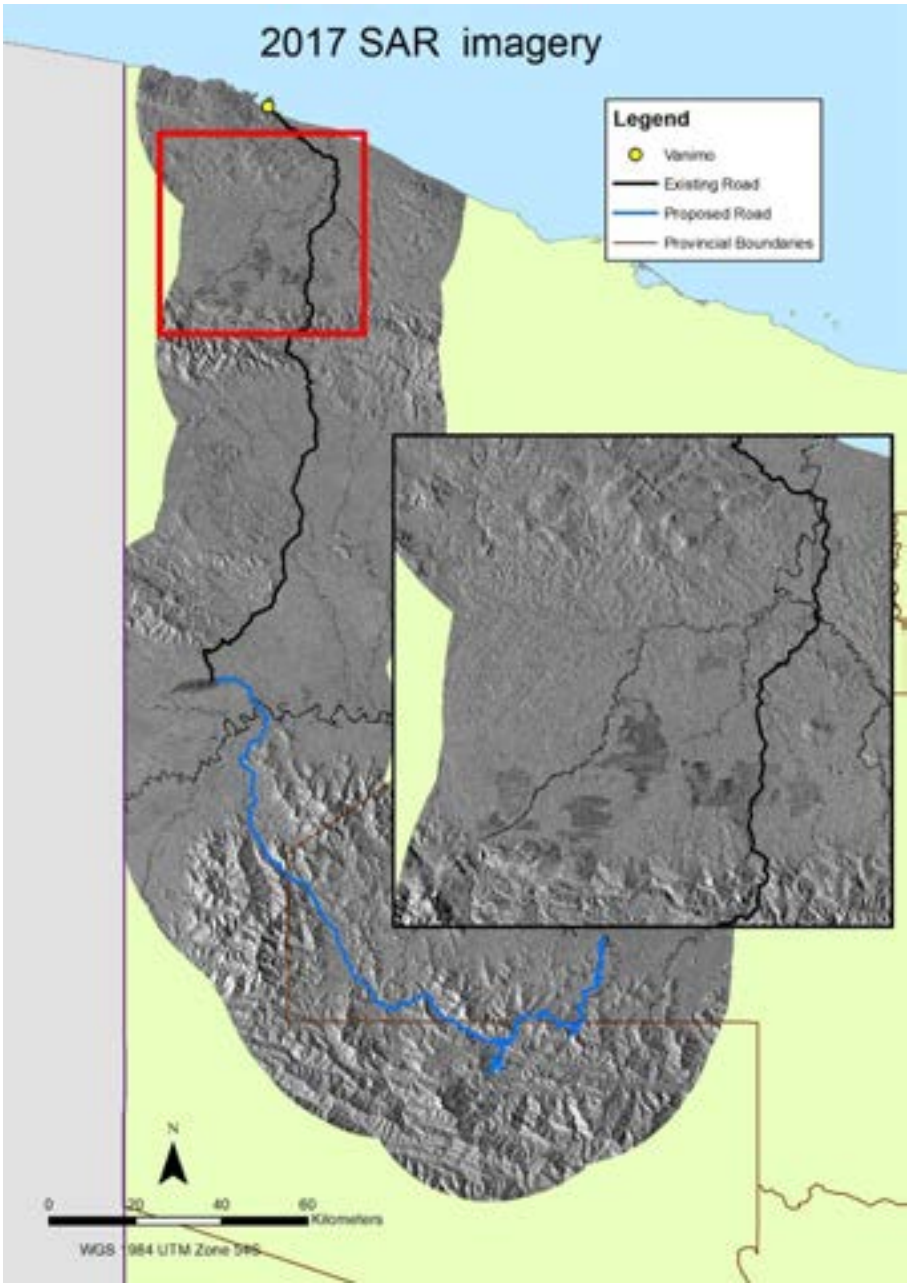

Figure 16: SAR mosaic for 2017 focusing on the areas of extensive clearing.

3.5.4. Broad-scale clearance assessment for change between 2011 to 2017

The final assessment combined the area for 2011 and 2017 to characterise the total area cleared since 2011 to 2017. While the remote sensing assessment did appear to show areas which returned to forest from 2014 to 2017, we assumed that this was mainly the result of misclassification or perhaps thick ground cover growing back in cleared areas. Thus, the total cleared area for 2017 was considered any pixel identified as cleared in either 2014 or 2017 (Figure 17).

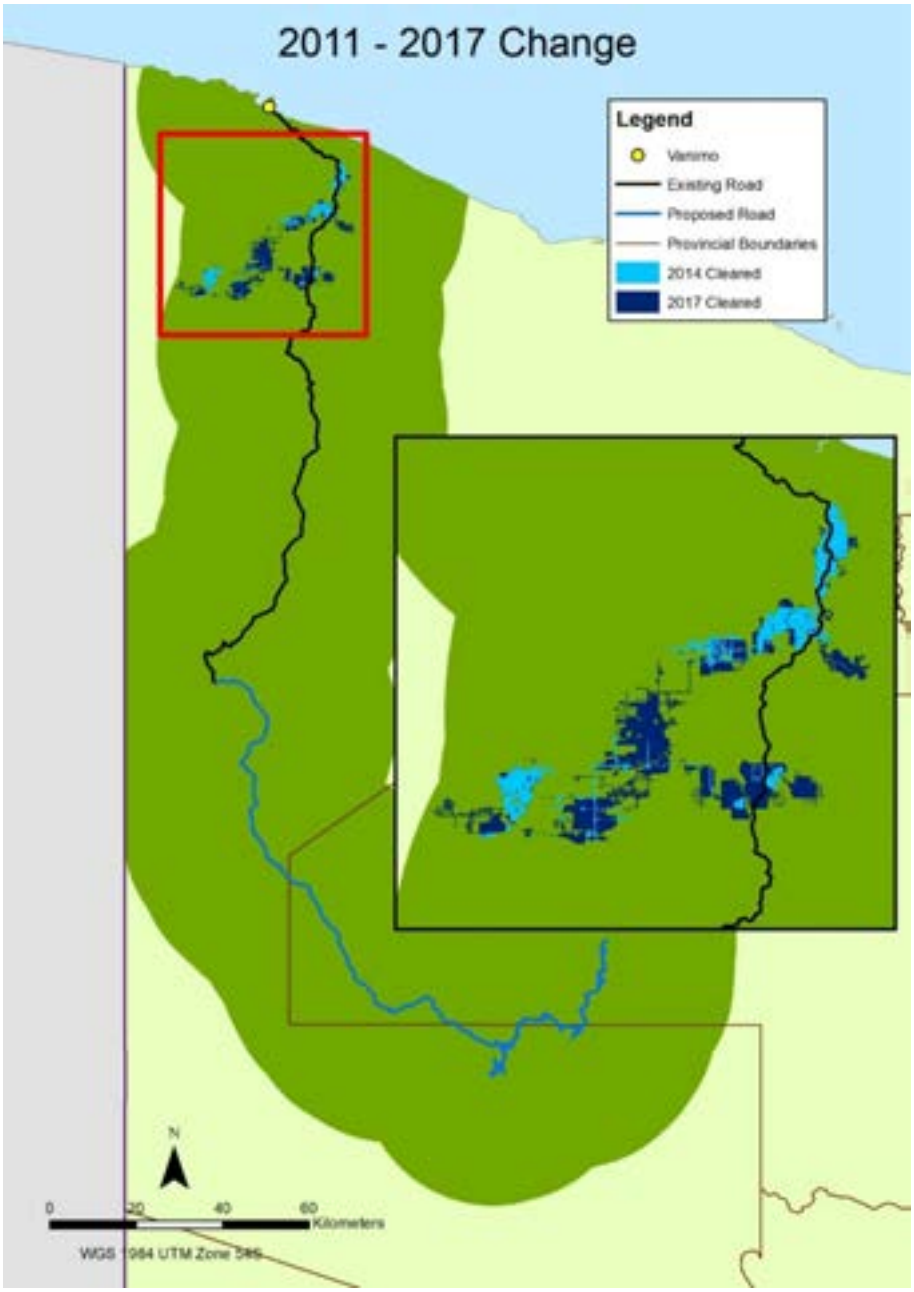

Figure 17: Assessment of total area of cleared area as of 2017.

3.5.5. Summary and accuracy assessment

The analysis showed that most of the clearing occurred near the main road, and north of the Bewani mountain range that runs perpendicular to the existing road approximately 220 km south of Vanimo. The total area cleared as of 2017 was 166.87 km^2. As expected, pixels closer to the main road were more likely to be cleared (Figure 18).

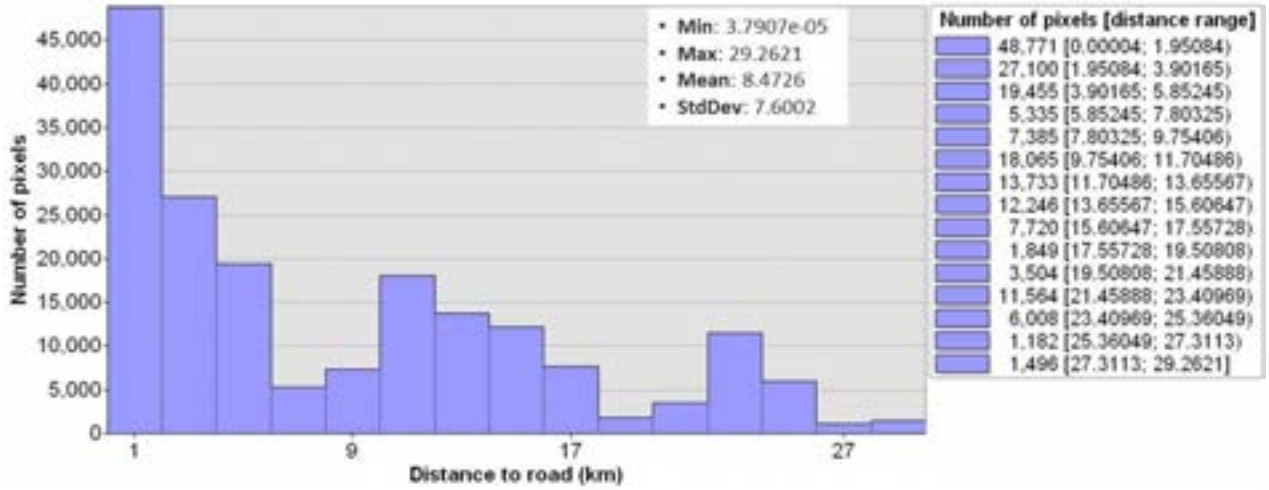

Figure 18: Frequency of cleared pixels at a range of distances from the existing road.

The remote sensing accuracy assessment showed a high overall accuracy of 95.2% and a Kappa coefficient of 0.79 (Table 6) which is considered quite accurate for a remote sensing analysis. For remote sensing, an overall accuracy of about 85% and individual class accuracy of perhaps 70% (i.e. 3 out of 10 pixels are classified incorrectly) is generally acceptable, though there are no standard rules.

Table 6: Confusion matrix

	Classification results (points)		
Ground reference data (points) (pixels)	**Cleared**	**Forest**	**Total**
Cleared	423	24	447
Forest	0	53	53
Total	423	77	500
Producer accuracy (%)	100	68.83	
User accuracy (%)	94.63	100	
Overall accuracy (%)	95.2		
Kappa coefficient	0.79		

While the mapping methods applied represent the leading practice remote sensing methods used for forest change detection in the tropics, it is unlikely that further mapping and even ground truth

are likely to produce much higher quality mapping outputs, as the limitations are primarily driven by lack of available imagery due to cloud cover.

3.6. Results - GIS mapping of logging

3.6.1. Assessment for 2002 to 2015 using PNG observatory data

The digitized PNG observatory data showed that most of the logged area occurred north of the Bewani mountain range and was very extensive in 2002 (Figure 19).

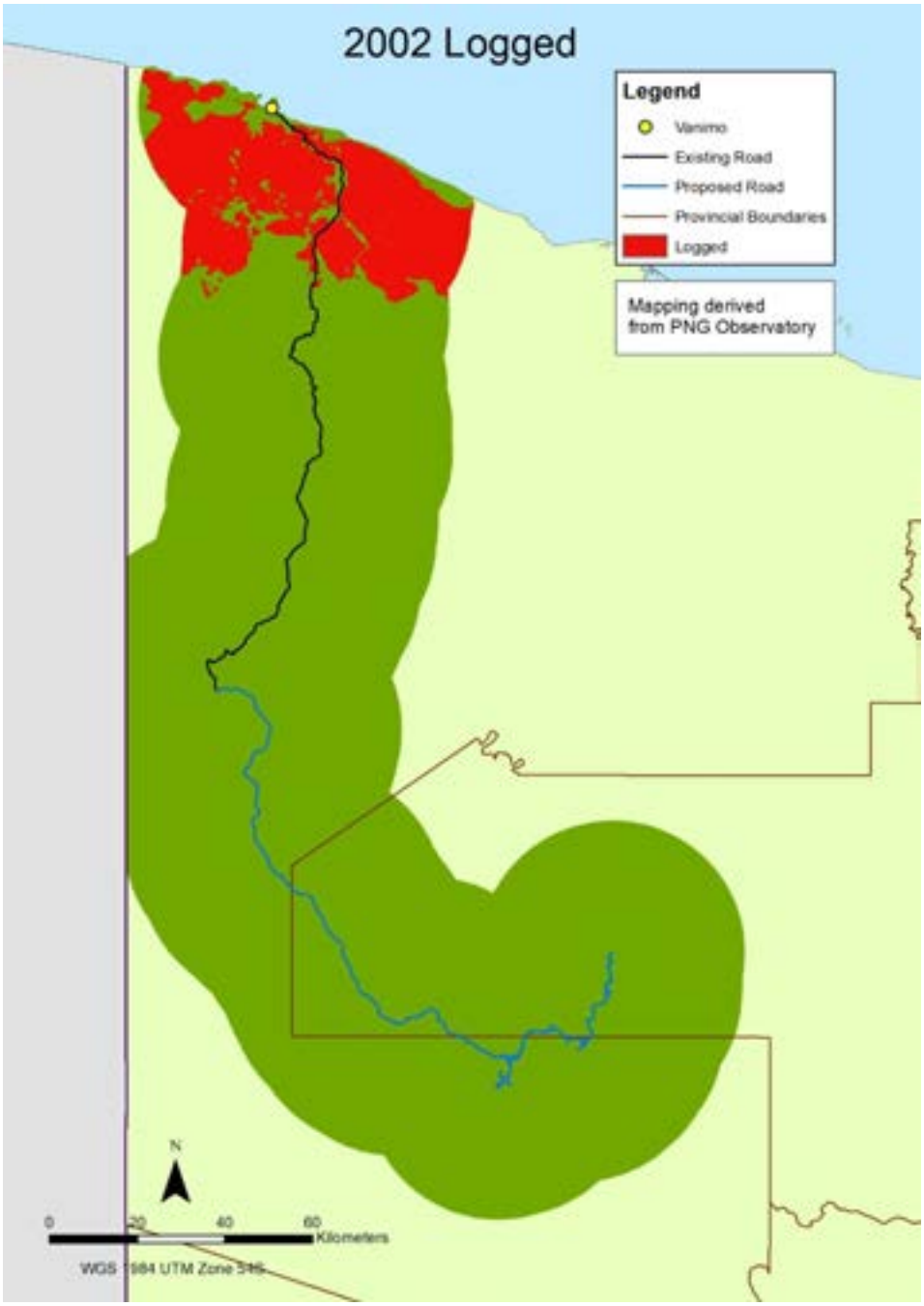

Figure 19: Logged area derived from PNG observatory data in 2002

By 2015 the logged area extended south of the Bewani mountain range (Figure 20). It appears as though the logged areas were closer to the existing road.

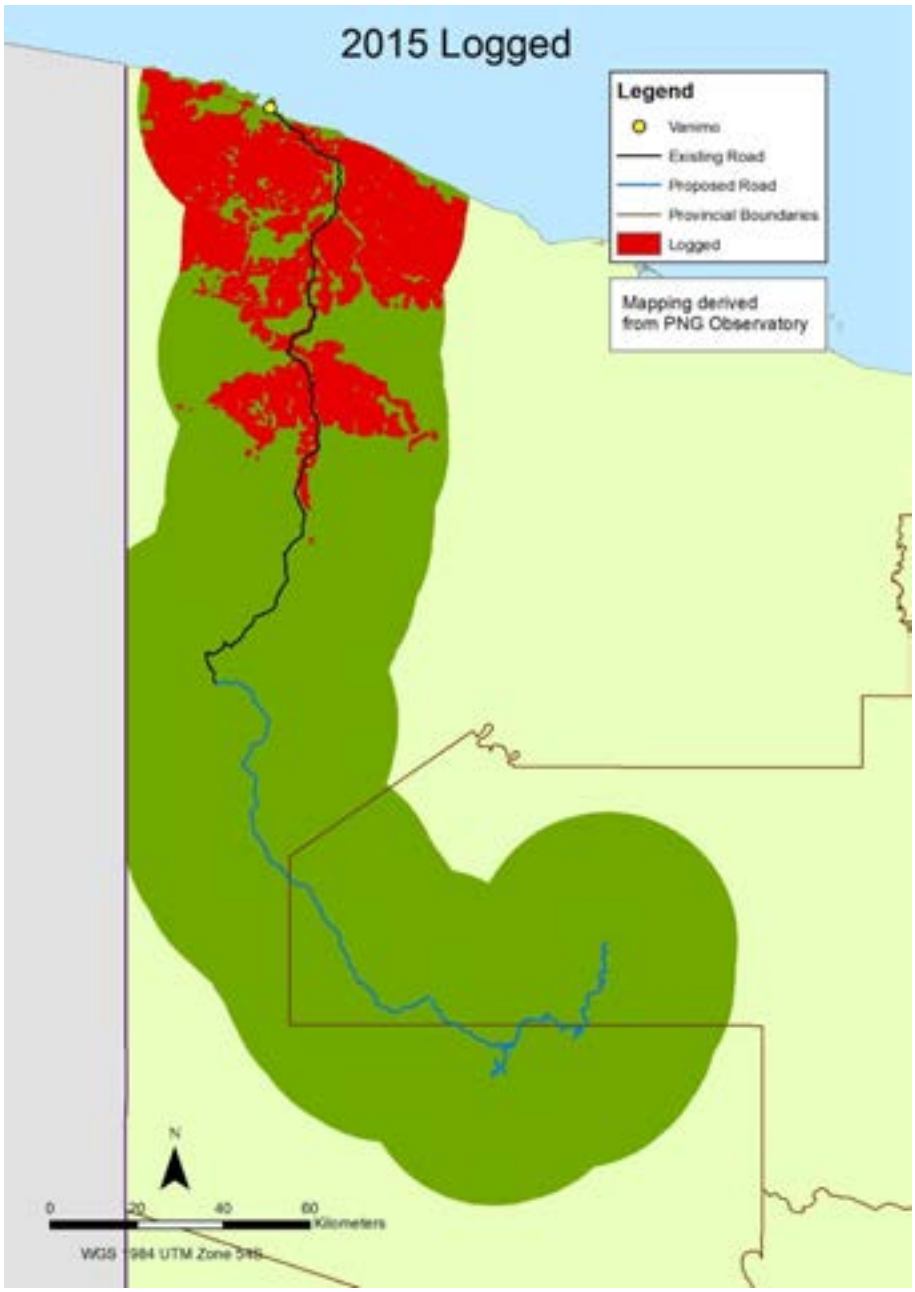

Figure 20: Logged area derived from PNG observatory data in 2015

The total area logged increased from by almost a third from 2002 to 2015 (Table 7). In addition, the frequency of logged pixels decreased with distance from the road (Figure 21).

Table 7: Total area logged area based on extracted PNG observatory data

Year	Area km^2
2002	1990.58
2015	3009.08

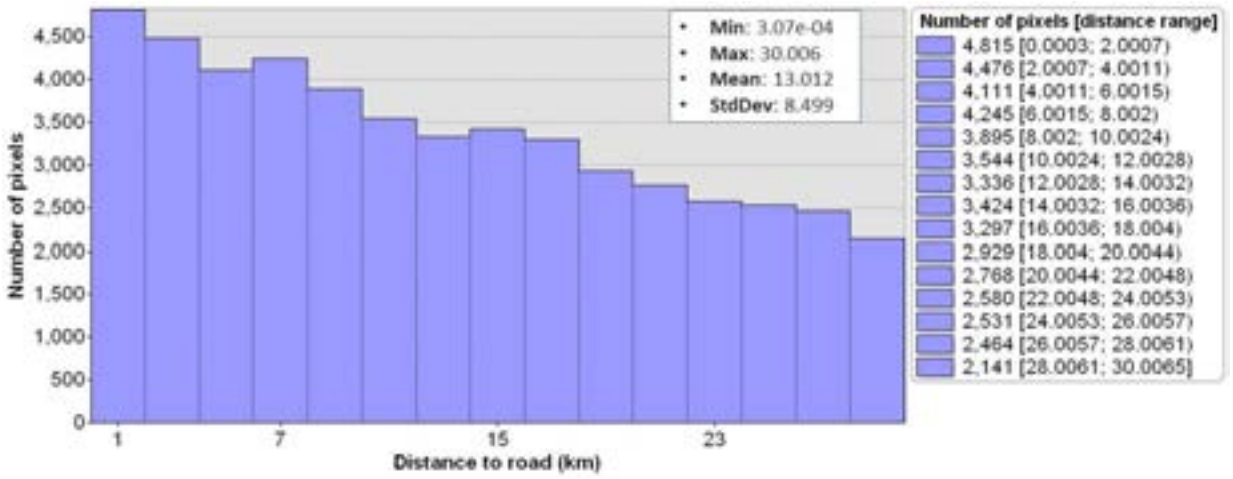

Figure 21: Frequency of logged pixels at a range of distances from the existing road.

3.6.2. Accuracy assessment of PNG observatory data

A comparison between the PNG observatory and independent manual image interpretation of logging south of Bewani mountain range using the Landsat data derived for this study (in 2014 and 2017) identified very similar logged area extents (Figure 22). While the assessment was relatively coarse and qualitative it does indicate that the PNG observatory data may be valid at the regional scale for our study. Commonly large extent data (i.e. country scale) data may not be valid when used at smaller extents.

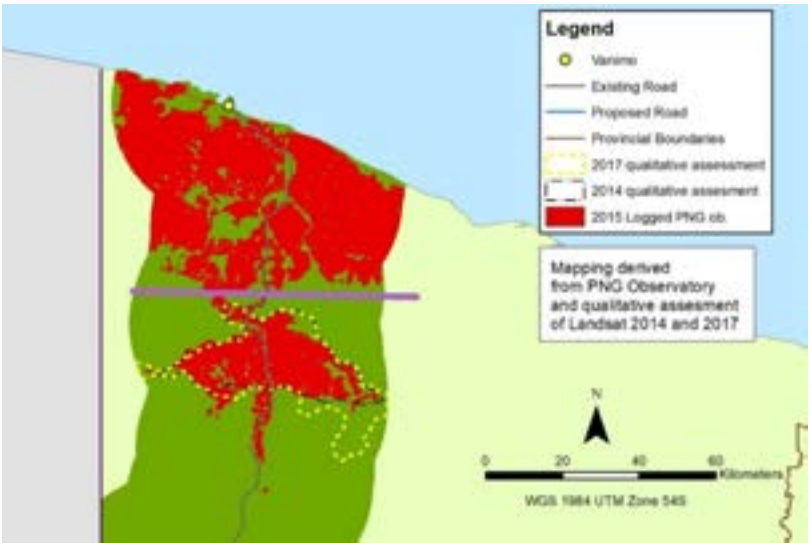

Figure 22: Comparison between extent derived from a qualitative assessment of the SAR and Landsat 2014 and 2017 remote sensing data and the 2015 PNG observatory data. Note that the qualitative assessment was only conducted south of Bewani mountain range identified approximately by the purple line.

3.7. Results – Rates of change

The logged area had a greater increase in total area over time and thus higher rate of change than cleared land cover over the period in which spatial data was available (Figure 23,Table 8). However, relative (i.e. percentage) rates of change per year were higher for the logged forest.

Table 8: Land cover change statistics for logged and cleared areas.

Year	Area (km^2)	Landcover	Difference in area (km^2)	Rate of change per year (km^2)	Percentage change	Data source
2002	1990	Logging	-	-	-	PNG observatory data
2015	3009	Logging	1019.5	78.3	151%	
2011	0	Cleared	-	-	-	Remote sensing analysis
2014	58.9	Cleared	59.9	20.6	-	
2017	166.9	Cleared	108.0	36.0	283%	

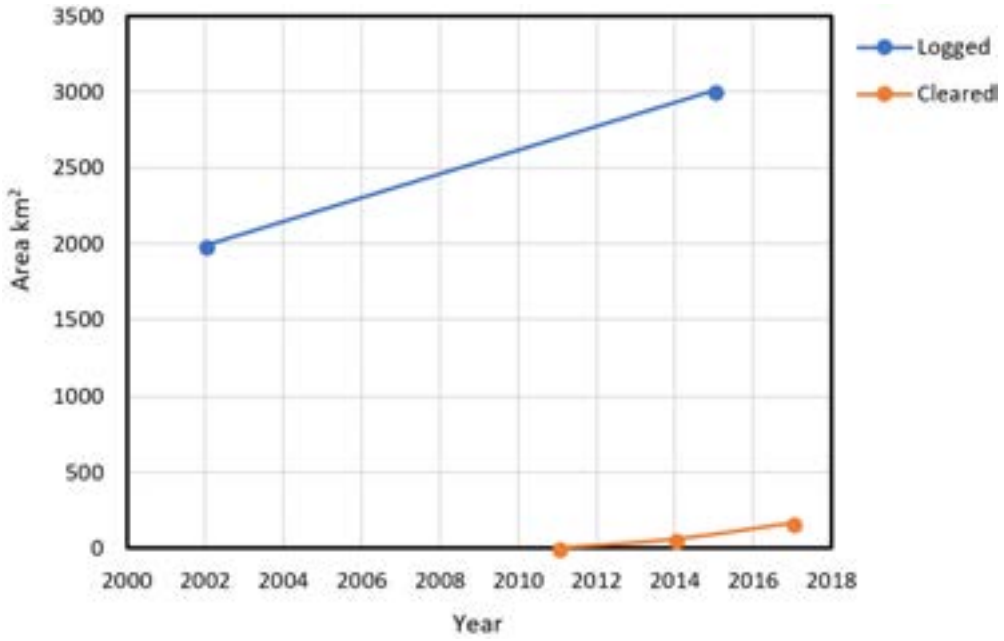

Figure 23: Change in area for logged and cleared land covers over time.

3.8. Final summary

Both the assessment of broad-scale clearing (using the remote sensing) and logging (using the existing GIS data from the PNG observatory) identified an increase in area of cleared and logged over time. In addition, both forms of conversion from forests appear to take place more frequently closer to the road and appeared to occur closer to Vanimo. Finally, over time land conversion appeared to shift further south.

The phenomena of roads being linked to anthropogenic impacts such as land conversion for forestry or agriculture, as observed qualitatively in the above analysis, has been highlighted in the literature across the globe, with roads having a major role in opening up forested tropical regions to exploitation such as logging and colonization (Asner et al., 2013; Koh and Wilcove, 2009; Laurance et al., 2009; Laurance and Arrea, 2017; Shearman et al., 2012). In the next section the relationship between a range of environmental drivers including the presence of roads will be tested quantitatively.

4.0 Land capability, land change modelling and assessment of the impacts of the proposed road

4.1. Background

In this final section we utilised a spatially explicit land change model to characterise regional land capability based on transition probabilities, then modelled future land change associated with logging and clearing for agroforestry. We used the spatial data derived for the previous step (see Section 0) – both the remote sensing derived broad-scale clearance and the logged area data derived from the PNG observatory. For this analysis we utilised the Land Change Modeller module within TerrSet: Geospatial Monitoring and Modelling Software (Eastman, 2015). The Land Change Modeller is a suite of tools for the assessment and prediction of land cover change derived by analysing land cover change and empirically modelling its relationship to explanatory variables in order to project future land cover changes (Eastman, 2016).

Land-change models have been used to characterise the drivers of changes in land cover and land use and project these changes into the future (Committee on Needs and Research Requirements for Land Change Modeling, 2014). There is a wide variety of modelling approaches that can be used for land change modelling ranging from statistical approaches, machine learning and agent-based approaches (Committee on Needs and Research Requirements for Land Change Modeling, 2014). The Terrset software includes both statistical and machine learning approaches which are commonly used for land change modelling (e.g. Geneletti 2013; Reddy et al. 2017). An earlier version of the Terrset Land Change modeller has even been utilised for modelling land use change across PNG (Alei and Alkam, 2016), however, due to its coarse resolution the results and parameterisation are not suitable for assessing and interpreting the impact of the road corridor.

Using Terrset's land change modeller we assessed:

a. regional land capability of future forestry and/or agroforestry (i.e. cleared and logging areas) based on transition probabilities.
b. future forestry and/or agroforestry with and without the road corridor.

In order to project future land use a first step is to understand the current transition potential of a specific pixel within a landscape. Transition potential expresses the likelihood that land will transition in the future to a specific land cover class (Eastman, 2016), such as from forest to agroforestry. Which can be considered analogous to the suitability/capability of a specific location for a specific land use. For the transition modelling we used the Multi-Layer Perceptron artificial neural network procedure which utilises supervised learning within a dynamic learning artificial neural network to assess transition probabilities (Eastman, 2016). For this analysis we assessed clearing and logging separately as they overlapped spatially. This step also allowed for an assessment of the relative contribution of different land change drivers such as distance to road, elevation and soils. In addition, we compared our results with two existing agricultural suitability maps for the region.

Based on the transition potential future change we then projected land change 30 years into the future using Markov Chain approach. A Markovian process is where the state of a system is determined by its previous state and then its transition probability from one state to another is modelled using the earlier and later landcover maps (i.e. 2002 to 2015 for the logging scenario) (Eastman, 2016). This process calculates exactly how much land cover and the location of land cover transitioning from the most recent land cover date. As well as the standard model evaluation methods we also assessed uncertainties associated with the inclusion or exclusion of a range of land change drivers.

4.2. Methods

4.2.1. Overview

We used the remote sensing and GIS data developed in the previous step as inputs into the land change model. We also tested the impact of including or excluding the proposed road for assessing future land change. The modelling involved three steps:

1) Assess transition potential using Multi-Layer Perceptron neural network.
2) Determine the amount of change in the future using Markov Chain modelling.
3) Evaluate alternative model input variables qualitatively and quantitively.

4.2.2. Model input data

We tested a range of variables commonly used in land change models and suitability models (Alei and Alkam, 2016; Kopatlie and Cornelio, 2013). However, as our focus was on regional variations, large scale drivers such as climate which do not vary at regional scales or data not available at the required precision was not included. The variables included elevation, slope, soil etc and the data sources and processing are summarised in Figure 24 and Table 9.

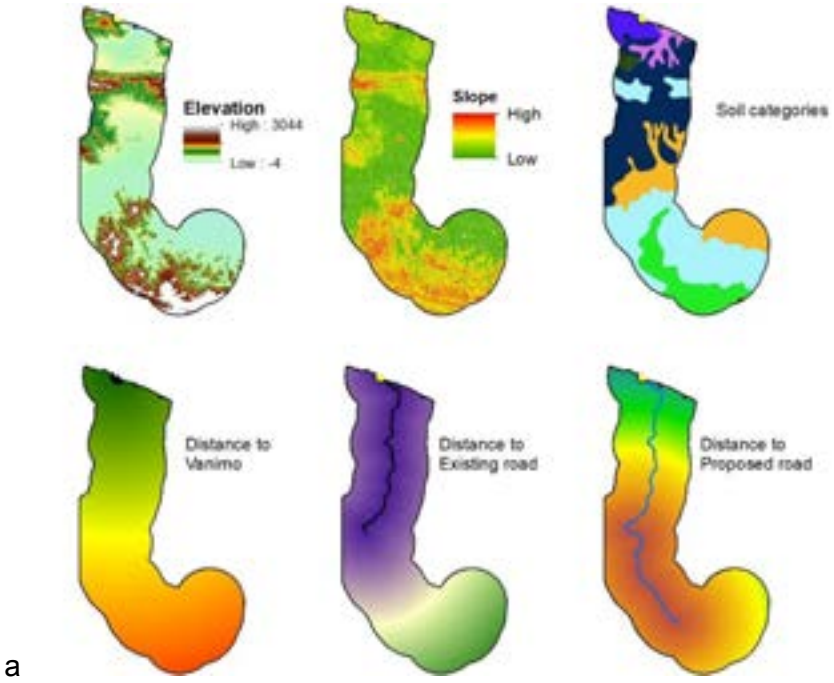

a

Figure 24: Variables tested for assessing land cover change

Table 9: Variables tested in land change model

Input Variables	Included in Cleared model	Included in Logged model	Data sources and processing
Distance to existing road	x	x	Polyline road file provided by Coffey. Euclidean distance road.
Distance to proposed road	x	x	Polyline road file provided by Coffey. Only publicly accessible components of the road modelled. We did not include the parts of the road which service the mine but are not publicly accessible. Euclidean distance from road.
Elevation	x	x	Shuttle Radar Topography Mission (SRTM) Void Filled 3 second arc (https://lta.cr.usgs.gov/SRTMVF). Mosaic of the following tiles 05_e142_3arc; s05_e141_3arc; s04_e141_3arc; s04_e140_3arc; s03_e141_3arc; s06_e142_3arc; and s06_e141_3arc. Additional void filling operations using ArcGIS 10.5 (ESRI, 2018) to interpolate no data pixels were conducted.
Slope	x	x	Derived from elevation data
Soil			Digitized from Papua New Guinea. Bleeker, P. (1983). Soils of Papua New Guinea, Australian National University Press, Canberra
Distance to Vanimo	x	x	Vanimo identified
Distance from cleared land 2014	x		Euclidian distance from cleared land dynamically modelled over time, based on difference between 2014 and 2017.
Distance from logged land 2002		x	Euclidian distance from logged land dynamically modelled over time, based on difference between 2002 and 2015.

4.2.3. Transition analysis and Multi-Layer Perceptron neural network paramaterisation

For the transition analysis we assessed change between:

1) Cleared land from 2014 to 2017
2) Logged land from 2002 to 2015

The Multi-Layer Perceptron neural network procedure was used to assess land transition probabilities based on the input variables described in the previous section. The Multi-Layer Perceptron starts training on sample pixels from the two change input layers that have and have not experienced transitions. There are multiple parameters which can be altered for this procedure, however, most do not need to be modified (Eastman, 2016). The final paramaterisation of the multi-layer perceptron are described in Table 10. These were determined after testing a number of different options.

Table 10: Parameterisation of the multi-layer perceptron (MLP) neural network

Parameter	Value
Input layer neurons	4 or 5
Hidden layer neurons	3
Output layer neurons	2
Requested samples per class	10000
Final learning rate	0.0001
Momentum factor	0.5
Sigmoid constant	1
Acceptable RMS	0.01
Iterations	10000

4.2.4. Land change modelling parameterisation

After testing multiple different drivers, we found that four drivers produced the best results both quantitatively and qualitatively. These input drivers were 1) Distance to existing road; 2) Elevation; 3) Slope; and Distance from previous land cover change (e.g. cleared or logging) (Table 11). In addition, we assessed the importance of distance to Vanimo in a sensitivity analysis, to assess how the inclusion or exclusion of an important variable may change the modelling results. In total we describe 8 model runs. These model runs included the assessment of the proposed road.

Table 11: Land change modelling scenarios and input variables and sensitivity analysis. *Note that distance from previous land conversion (i.e. cleared or logged) compared

Scenario	Input variables	Sensitivity analysis
Cleared land	Distance to existing road Elevation Slope Distance from cleared land 2014*	Distance to Vanimo
Cleared land including proposed road	Distance to existing road Elevation Slope Distance from cleared land 2014* Distance to proposed road	Distance to Vanimo
Logged area	Distance to existing road Elevation Slope Distance from logged land 2002*	Distance to Vanimo
Logged area including proposed area	Distance to existing road Elevation Slope Distance from logged land 2002* Distance to proposed road	Distance to Vanimo

The soil layer was tested in this step; however, the results were qualitatively unsatisfactory, producing outputs with large spatial contrasts in projected land cover change driven by artefacts associated with soil type boundaries. In addition, we were concerned with using country scale soil layer at the regional scale as there appears to be large variation between soil maps e.g. Figure 25. Furthermore, Doyle (2015) suggest that “soils dataset, and hence interpretive map layers, within PNGRIS is a highly extrapolated and modelled GIS dataset [are] generated from a number of sparse and often spatially inaccurate and/or sporadic on-ground observations and datasets”. The soil dataset was therefore not used as an input to the land change modelling.

a) **b)**

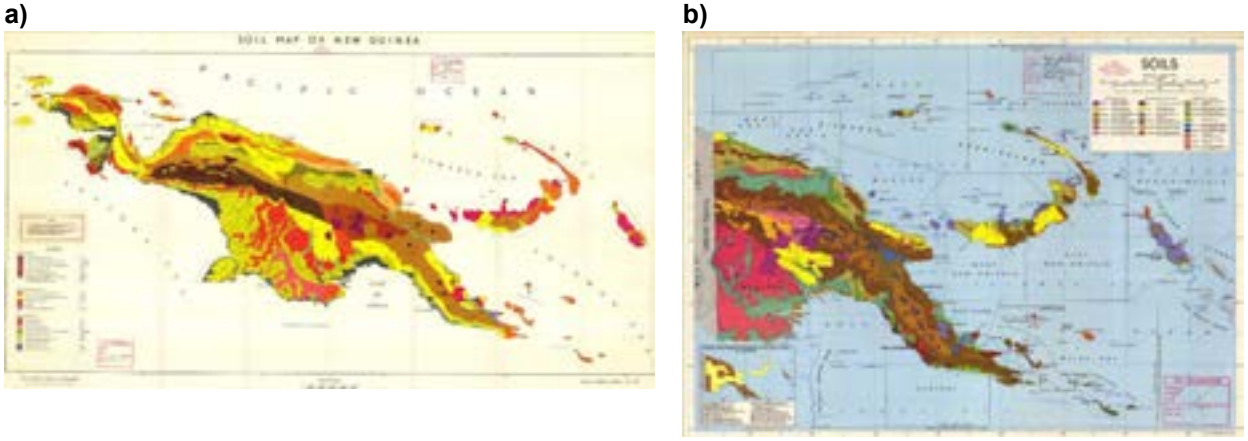

Figure 25: Two soil maps for PNG with contrasting distributions: a) CSIRO 1965 and b) Bleeker 1983.

4.3. Results

4.3.1. Land change transition modelling

The overall accuracy of the final model of land cover transition from forest to clearing using the remote sensing data was based on 4 input variables Distance to Road, Distance to existing cleared, Elevation and slope was high with an accuracy of 83.80 % and a skill measure of 0.6760 (Table 12) (for more details see “Appendix B: Land Change Modeler MLP Model Results for transition between forest and cleared”). Most variables apart from distance to existing clearing showed high accuracy and skill. The most influential variable was distance to road and then elevation.

Table 12: Final forest to clearing transition probability model and assessment of forcing a single independent variable constant on accuracy, skill and assessment of influence

Model	Accuracy (%)	Skill measure	Influence order
With all variables	83.80	0.6760	N/A
Var. 1 Distance to Road constant	50.32	0.0063	1 (most influential)
Var. 2 Distance to existing cleared constant	83.80	0.6760	4 (least influential)
Var. 3 Elevation constant	83.42	0.6684	3
Var. 4 Slope constant	80.45	0.6090	2

The maps of land change transition show that areas located near the road have a higher transition potential than other locations (Figure 26a). However, the Bewani mountain range had a low transition potential most likely as these areas have steep slopes and higher elevation.

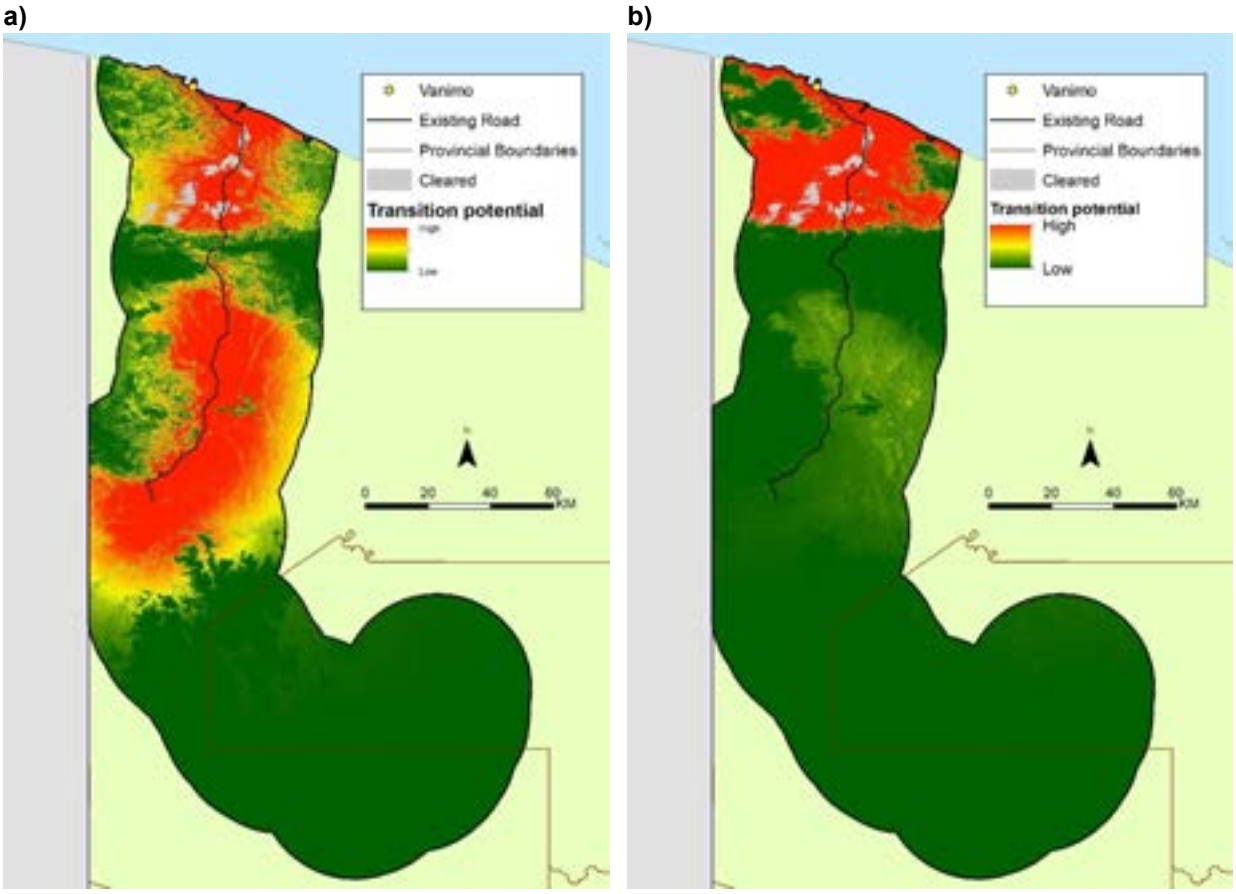

Figure 26: Transition probabilities for clearing. a) final model and b) sensitivity analysis scenario with distance to Vanimo included as a driver

For the sensitivity analysis we included distance to Vanimo as an input driver as it had similar accuracies (for more details see “Appendix C: Land Change Modeler MLP Model Results for transition between forest and cleared sensitivity analysis with distance to Vanimo”) as the final

model. However, for the sensitivity analysis model the mapped transition potentials were much higher near Vanimo (Figure 26b) although the road appeared to still be a key driver for transition.

The modelling of logging transitions with the PNG observatory GIS data had similarly high accuracies as the clearing model at 87.47% and a skill measure of 0.7495. Again, the distance to road appeared to be the most influential variable the least influence variable being distance to existing logging (for more details see “Appendix D: Land Change Modeler MLP Model Results for transition between forest and logging”).

Table 13: Final Logging transition probability model and assessment of forcing a single independent variable constant on accuracy, skill and assessment of influence.

Model	Accuracy (%)	Skill measure	Influence order
With all variables	87.47	0.7495	N/A
Var. 1 Distance to Road constant	49.57	-0.0087	1 (most influential)
Var. 2 Distance to existing logging constant	87.47	0.7495	4 (least influential)
Var. 3 Elevation constant	80.49	0.6098	2
Var. 4 Slope constant	86.35	0.7270	3

Similar to the transition potential maps for clearing the logging transition potential maps showed higher potential near the existing road, but not across the Bewani mountain range (Figure 27a). Again, by adding Vanimo as a driver in the sensitivity analysis high transition potential pixels are concentrated toward the north of the study area Figure 27b) (for more details see “Appendix E: Land Change Modeler MLP Model Results for transition between forest and logging sensitivity analysis with distance to Vanimo”).

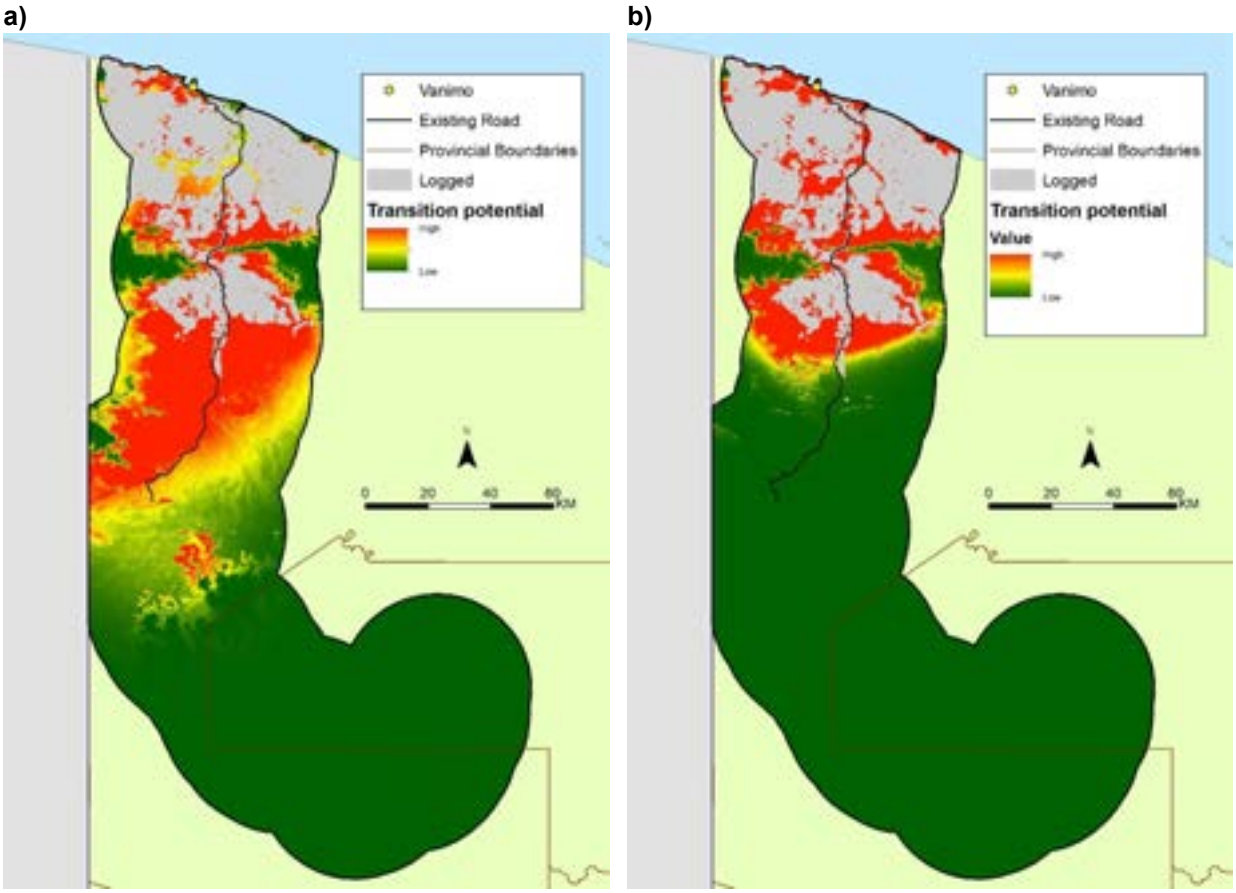

Figure 27: Transition probabilities for logging. a) final model and b) sensitivity analysis scenario with distance to Vanimo included as a driver

In summary, both transition models had high accuracy and in both cases distance to the road was identified as a key driver of land change.

4.3.2. Existing suitability modelling, FIM and link with land change modelling

The transition model provides a surrogate for suitability/capability mapping for the region. It found that areas with high elevation and steep slopes have low transition potential, which is analogous to low suitability. A number of suitability type maps exist for the whole or part of the region and are shown in Figure 28. However, compared to both the existing land cover mapping (cleared and logging) and to our transition modelling there doesn't appear to be a strong resemblance, except perhaps for areas around the Bewani range where most of the suitability maps show low suitability due to the negative influence of steep slopes.

In section 2 we used the FIM layer (McAlpine and Quigley, 1998) to describe the current distribution of timber trees, in the study area. We did not use this data in the modelling as datasets such as FIM can be accurate globally at large scales such as for calculating total area of different land covers and comparing relative differences, but it is unlikely to be accurate in a spatially explicit way at the local scales. Furthermore, it is likely that the producers of the map would never have envisaged their product being used as an input into modelling. This is supported by the FIM report which suggests that it "is not at a scale suitable for use at the actual operational logging

level (eg. in the production of annual logging plans for a concession). This would require a topographic and forest mapping at scale of 1:25,000 or finer".

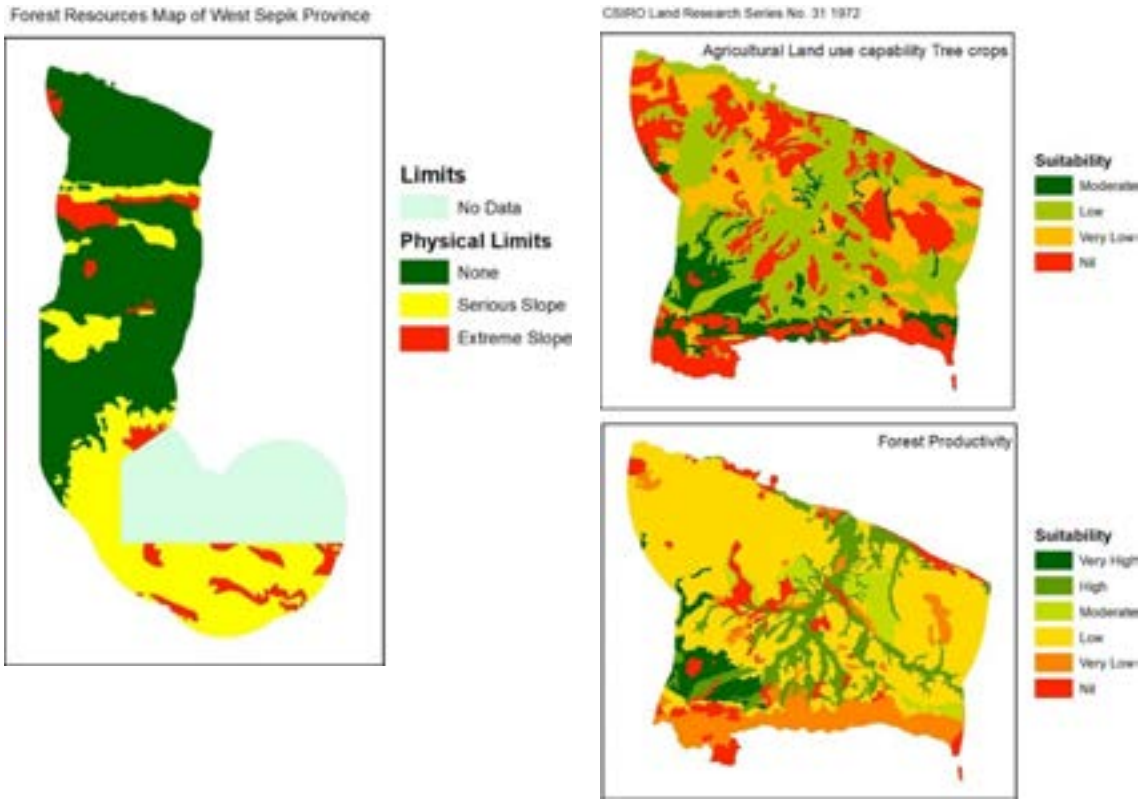

Figure 28: Existing suitability maps for the region. Left: Forest Resources map of West Sepik Province. Right: CSIRO Land Research Series No 31 1972. These diagrams illustrate how different models and maps provide vastly different spatial representations of suitability for forestry.

Finally, another reason for not including the FIM or the suitability map in the modelling is because as our modelling assessed how biophysical drivers affect the probability of transition to logging or clearing which is a surrogate for suitability. Thus, these datasets have been developed using a similar process using the same input variables, whereby biophysical drivers such as elevation and slope are used to make a prediction about the suitability of a certain location for timber or agricultural production. These maps therefore provide alternative models of suitability to what we developed but are not sensible as an input into the land change model.

4.3.3. Land change projections

In this section we project future land change for both cleared and logged areas for a period of 30 years. We conduct the assessment with and without the influence of the proposed road using both a hard and soft classification. "The hard prediction model is based on a competitive land allocation model similar to a multi-objective decision process. The soft prediction yields a map of vulnerability to change for the selected set of transitions…. The hard prediction yields only a single realization while the soft prediction is a comprehensive assessment of change potential."(Eastman, 2016). The hard predictive mapping creates outputs with the same categories as the inputs thus provides more easily understandable results. The soft classification

is useful for assessing the vulnerability to change or the degree to which a pixel has the right conditions to precipitate change and thus useful for evaluating the hard classification results.

The amount of projected land cover is based on rates of change calculated from the input imagery (i.e. the rates identified in Figure 23, Table 8). Pixels projected to change in the future are those that are the most suitable in the study area.

Modelling of clearing for only the existing road shows that projected future clearing will occur mainly around the road (Figure 29a). However, there are locations such as in East Sepik which are considered highly suitable but not near the road which were modelled as cleared. The modelling with the proposed road included suggests that clearing will extend further South near the proposed road (Figure 29b). There are also less pixels cleared pixels near existing road as the proposed road makes locations further south relatively more suitable.

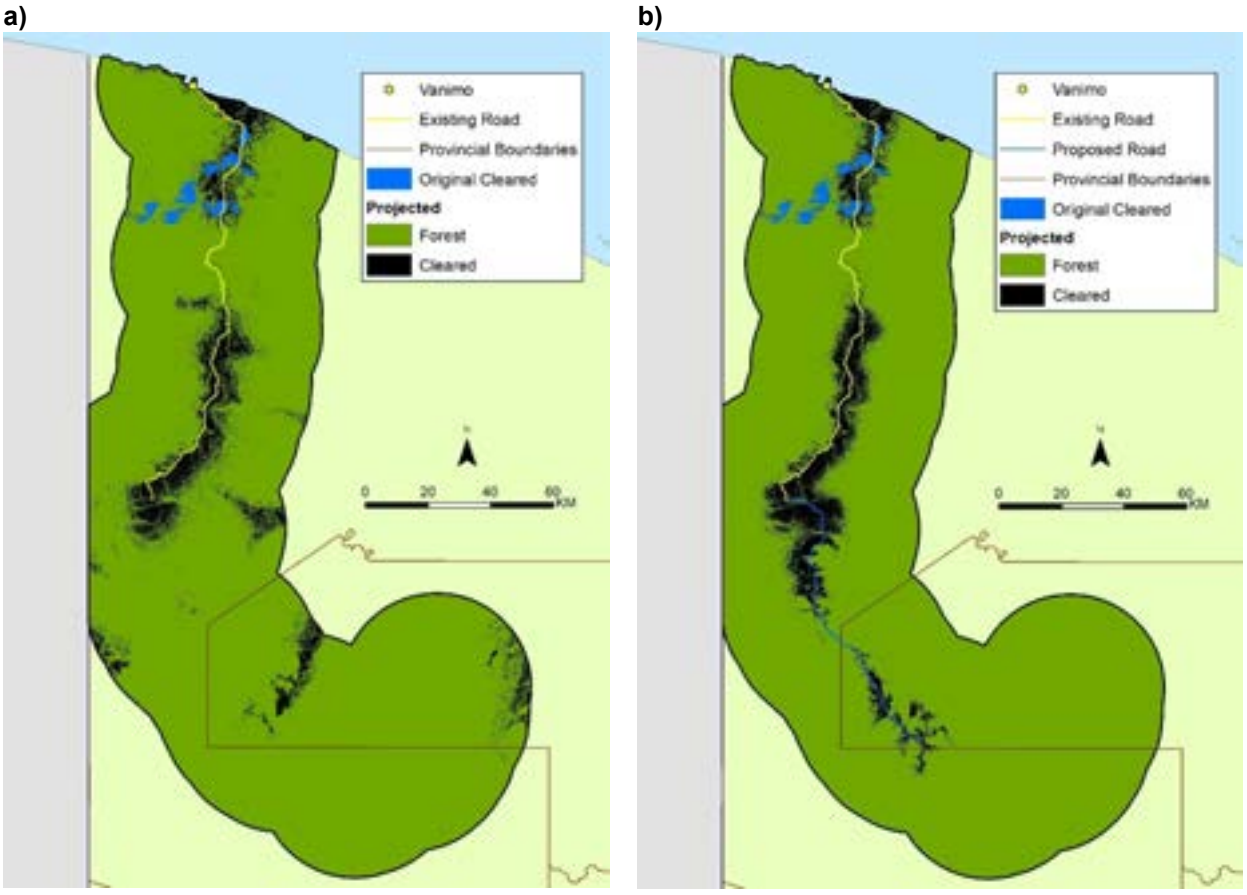

Figure 29: Hard projections for land clearing. a) existing road and b) proposed road.

Similar patterns are shown in the soft classification projections (Figure 30), though there is a lot of heterogeneity in the projection probabilities, meaning that certain areas have conditions to that are more likely to precipitate change.

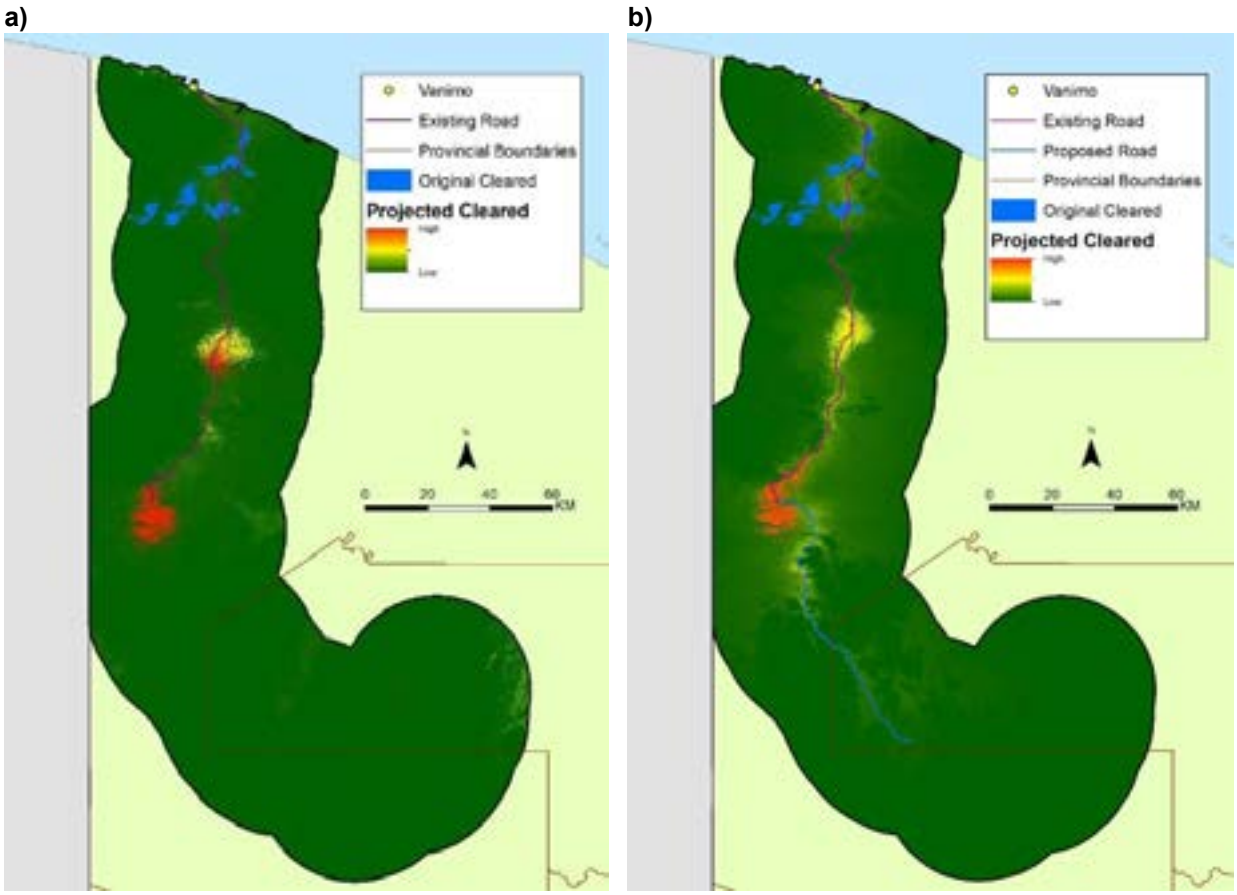

Figure 30: Soft projections for logging. a) existing road and b) proposed road.

As expected the future project logging also occurs near the road and is projected to occur near the future proposed road (Figure 31). Similar patterns are also shown in the soft classification (Figure 32).

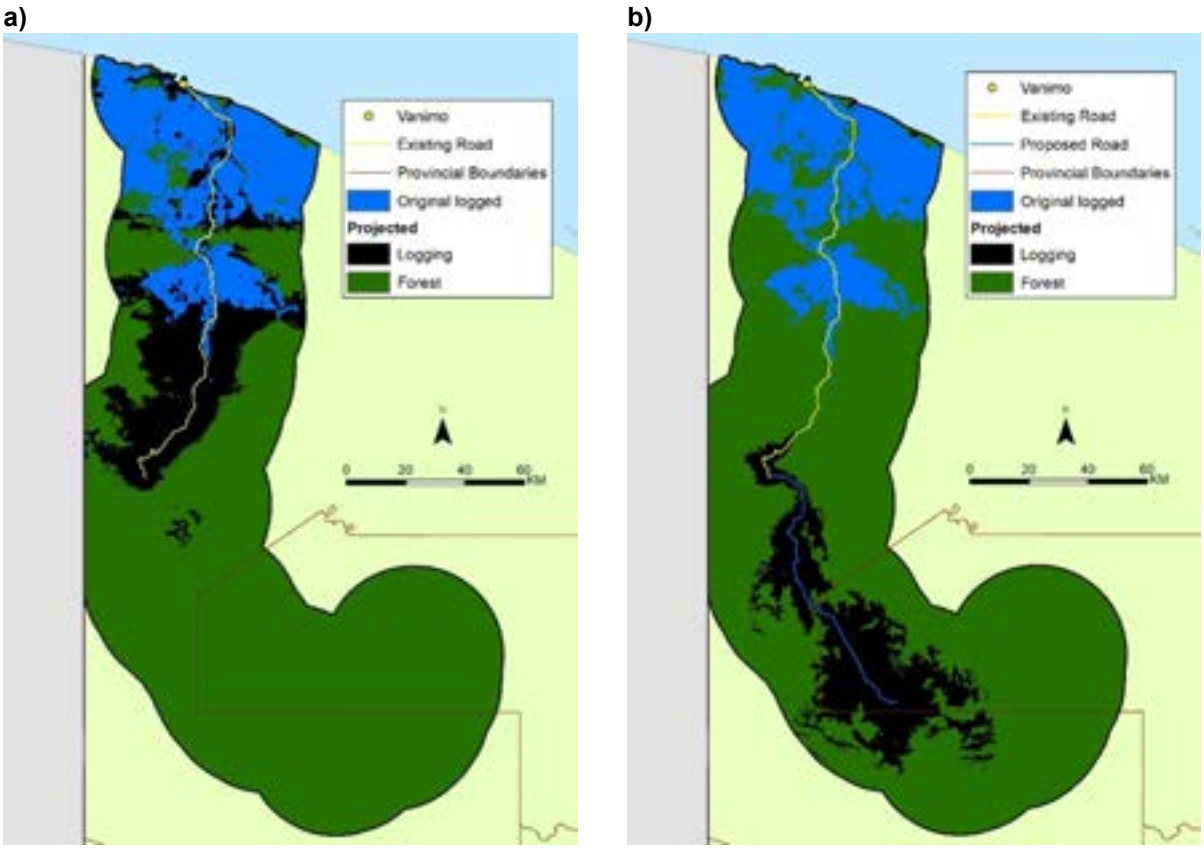

Figure 31: Hard projections for logging. a) existing road only and b) proposed road.

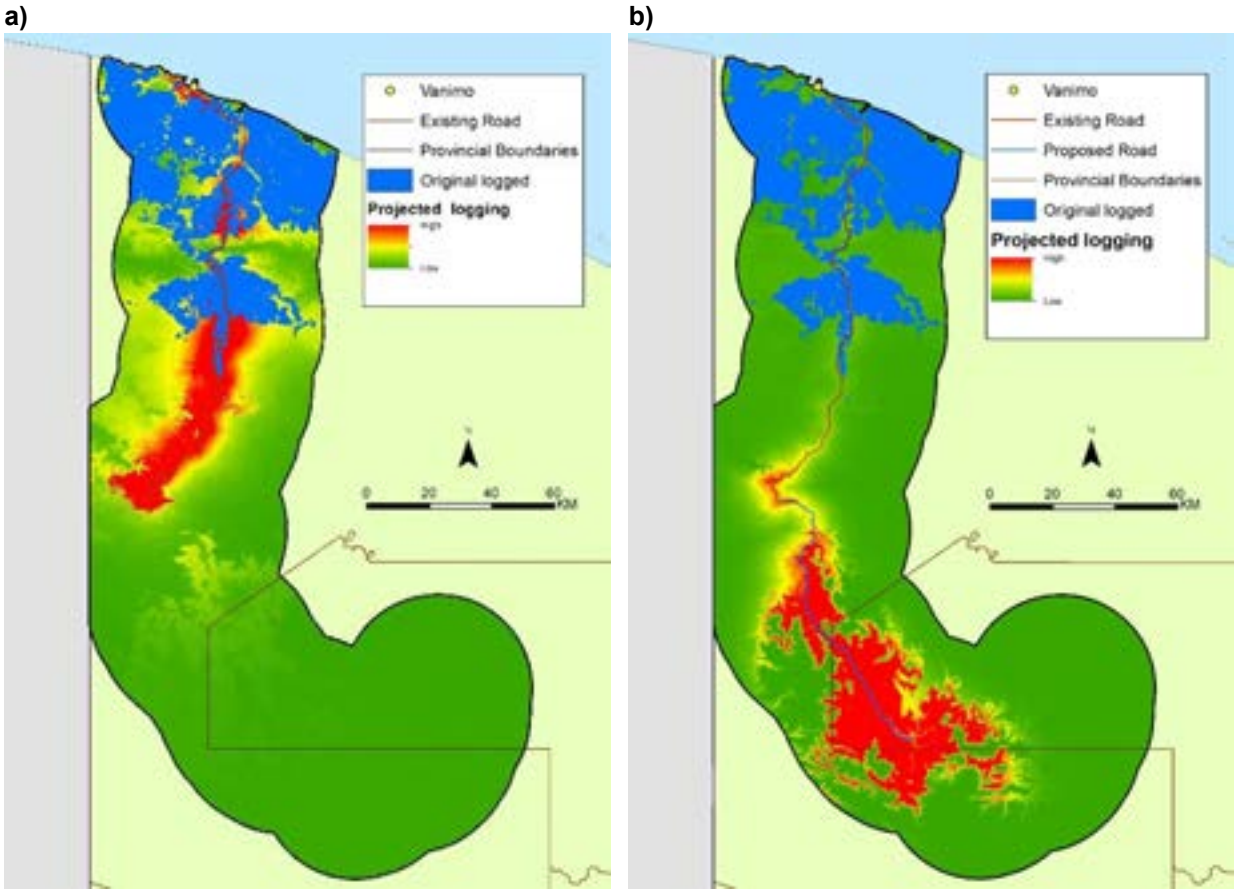

Figure 32: Soft projections for logging. a) existing road and b) proposed road.

Figure 33 describes represents both the cleared and logged layers projections overlayed. In reality both cleared and logged land uses would interact and thus the total area impact area would also change as a result. However, these impacts are difficult to model with the current dataset that do not overlap.

a)

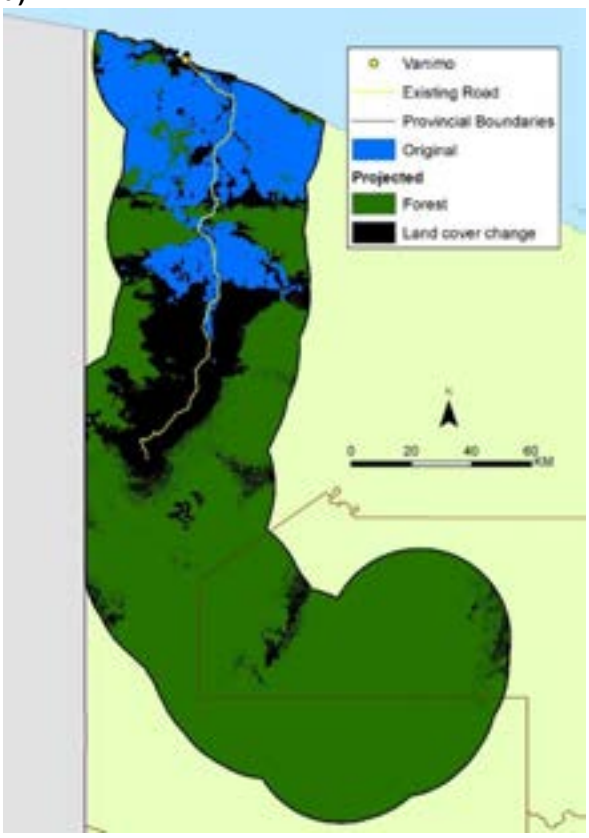

b)

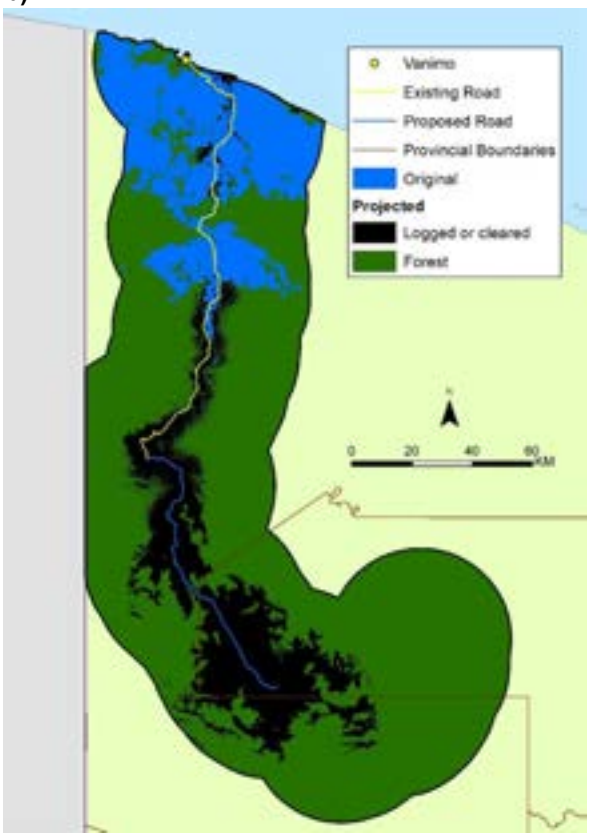

Figure 33: Combined logging and cleared projected land cover change scenarios for both with and without the proposed road.

4.4. Summary

The modelling of transition probabilities and projection of future land cover support what is commonly found across the world - roads drive land use change and degradation. However, the intensity and distribution of these changes needs to be interpreted with caution; which is the case for all complex modelling outputs. The sensitivity analysis suggests that proximity to Vanimo may also be a driver for both logging and clearing. Depending on the accepted model the intensity of land use change associated with the proposed road will also change. But regardless of the input variables included, roads are always identified as influencing land use change for either logging or clearing. The difference between the two models (with and without Vanimo) is that when Vanimo is included as a variable land use change associated with the road is not as great in the south of the study area.

The final model chosen for the analysis did not include Vanimo as an environmental driver. When Vanimo was used as an input driver into the model, roads became the second least influential driver (though still influential) out of the five variables tested, instead of the most influential when distance to Vanimo was not included. Both variables appear to represent a similar spatial driver of land change as they replace each other in the position of most influential variable. Based on the principle of parsimony, in which **the simplest model should be accepted** (i.e. the model with

least number of variables) and the fact that roads are a known driver for land use change we suggest it is sensible to accept the final model (i.e. not including distance to Vanimo). Furthermore, in our analysis it is difficult to differentiate between distance to Vanimo and distance to road as they are highly correlated spatially. For example, pixels with long distances from Vanimo tend to co-occur spatially with pixels that have long distances from roads.

In terms of the influence of each of the driver variables on the modelling outcomes, the most influential variable in the final model was distance to roads for both cleared and logging (Table 13). A number of sensitivity analyses were carried out to assess the influence of the different model drivers (see appendix B to E) of which two are shown in Table 14. In all the assessments roads comes out as the most important driver of land use change. Table 14 shows that if roads are excluded in the model, the accuracy and skill measure of the model would drop to a level where predictions made by the model are considered unusable as indicated by the skill measure being close to 0. Both accuracy and skill measure are indicators of how well the multi-layer perceptron and the variables included are at characterising transition potential. However, Table 14 should not be assessed in isolation as a range of sensitivity analyses are required to assess the contribution of each of the variables. For example, some input variables may not make a important contribution when assessed in isolation but interact with other variables and therefore will make a contribution to the overall accuracy of the model.

Table 14: Sensitivity of Model to forcing a single independent variable to be constant and influence on transition probabilities i.e. impact on Accuracy and Skill measures on overall model performance. A large drop in Accuracy or Skill measures indicate that not including a variable will negatively affect the accuracy of the model.

	Transition between forest and cleared			Transition between forest and logging		
Model	**Accuracy (%)**	**Skill measure**	**Influence order**	**Accuracy (%)**	**Skill measure**	**Influence order**
With all variables	83.8	0.676	N/A	87.47	0.7495	N/A
Distance to Road	50.32	0.0063	1 (most influential)	49.57	-0.0087	1 (most influential)
Distance to existing LC change (i.e. cleared or logged)	83.8	0.676	4 (least influential)	87.47	0.7495	4 (least influential)
Elevation	83.42	0.6684	3	80.49	0.6098	2
Slope	80.45	0.609	2	86.35	0.727	3

For all the scenarios the rates of change modelled for each year are based on the rate of change identified in the transition analysis and therefore is constant each year. A key to interpreting the outputs is focusing on relative spatial differences (i.e. where is change more likely to occur) and also differences between the scenarios with and without the proposed road. The modelling does not allow for an increase in demand (i.e. increase in rate of change) that result from reduced harvesting costs as a result timber resources being more accessible due to the proposed road.

In reality, the rate of change is difficult to model as it is driven by global drivers such as commodity prices (Figure 34), beyond the spatial drivers used as inputs into the model. For example, a large drop in forest area cleared and/or degraded was quantified by Shearman et al., (2009) due to the Asian financial crisis reducing timber export volumes (Figure 34). Such an

assessment is beyond the scope of our modelling and is rarely including in land change analysis.

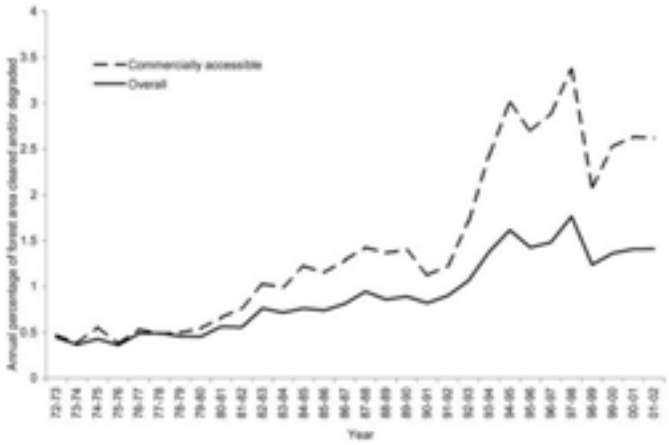

Figure 34: Annual forest change in forest area cleared/and or degraded in commercially accessible forest and overall forest area (Diagram from Shearman et al., (2009)).

5.0 Conclusions and limitations

Our analysis supports the accepted theory that roads are a major contributor to land use change. The analysis of the remote sensing and GIS data showed greater conversion of forests closer to the existing road. This was further supported by the land change model which identified distance from roads as the most influential variable to affect forest conversion in our final model. Based on our analysis it is expected that the proposed access road is likely to increase forest conversion for logging or agroforestry. However, areas closer to Vanimo are most likely to be affected first regardless of the model used and whether the proposed road is included or not. But there is considerable uncertainty associated with predicting the rate and extent at which land use change would occur further south.

As with all quantitative analyses there are a number of limitations and the outcomes need to be interpreted with caution. Access to ground truth would allow for better validation and training of the remote sensing products and potentially allow for the creation of a bespoke logging mapping product further increasing the precision and accuracy of both remote sensing and GIS maps and the land change model. A greater number of timesteps of land use change would allow for the land use model to be validated in a more sophisticated manner. Finally, further analysis through integrating GIS layers such as special agricultural areas, logging coupes and conservation areas could be used to further refine the analysis if they were made available.

However, future land use change projections such as those associated with logging or agroforestry will always be subject to drivers that aren't physical such as changes in commodity prices (Shearman et al., 2012). Thus, further analysis may provide a false sense of precision and therefore be unnecessary. More specifically, for the region the Idam-Siawi Integrated Agro-forestry development near Green River and two proposed industrial parks at Vanimo and Green River are also likely to make a contribution to future land use change but would be difficult to model; these projects are not associated with the Sepik Development Project.

The methods used in this study represent leading practice in applied academic research and have rarely (if ever) been used for assessing potential influence of a mine on offsite land use change at a regional scale for a proposed mine. These results provide a sophisticated means for planning for a mining development.

References

Alei, F., Alkam, F., 2016. Draft Report on Future Deforestation Modeling and Land Suitability Assessment for Oil palm Agricultural Mapping Assessment in Papua New Guinea Giancarlo Raschio.

Asner, G.P., 2009. Automated mapping of tropical deforestation and forest degradation: CLASlite. J. Appl. Remote Sens. 3, 033543. https://doi.org/10.1117/1.3223675

Asner, G.P., Keller, M., Lentini, M., Merry, F., Souza, C., 2013. Selective Logging and Its Relation to Deforestation. Amaz. Glob. Chang. https://doi.org/10.1029/2008GM000722

Brooks, T.M., Mittermeier, R.A., da Fonseca, G.A.., Gerlach, J., Hoffmann, M., Lamoreux, J.F., Mittermeier, C.G., Pilgrim, J.D., Rodrigues, A.S.., 2006. Global biodiversity conservation priorities. Science 313, 58–61. https://doi.org/10.1126/science.1127609

Bryan, J., Shearman, P., Ash, J., Kirkpatrick, J.B., 2010. Estimating rainforest biomass stocks and carbon loss from deforestation and degradation in Papua New Guinea 1972-2002: Best estimates, uncertainties and research needs. J. Environ. Manage. 91, 995–1001. https://doi.org/10.1016/j.jenvman.2009.12.006

Bryan, J.E., Shearman, P., 2015. The State of the Forests of Papua New Guinea 2014: Measuring change over the period 2002-2014, University of Papua New Guinea.

Cane, I., Schleger, A., Ali, S., Kemp, D., McIntyre, N., McKenna, P., Lechner, A.M., Dalaibuyan, B., Lahiri-Dutt, K., Bulovic, N., 2015. Responsible Mining in Mongolia : Enhancing Positive Engagement. Sustainable Minerals Institute, Brisbane.

Committee on Needs and Research Requirements for Land Change Modeling, 2014. Advancing Land Change Modeling. https://doi.org/10.17226/18385

Da Silva, R.P., Dos Santos, J., Tribuzy, E.S., Chambers, J.Q., Nakamura, S., Higuchi, N., 2002. Diameter increment and growth patterns for individual tree growing in Central Amazon, Brazil. For. Ecol. Manage. 166, 295–301. https://doi.org/10.1016/S0378-1127(01)00678-8

Doyle, R.B., 2015. GIS Based Land Capability Assessments of Prime Agricultural Lands (PAL) in Central Province of PNG. https://doi.org/10.13140/RG.2.1.3392.6888

Eastman, J.R., 2016. TerrSet Geospatial Monitoring and Modeling System Manual 391.

Eastman, J.R., 2015. TerrSet: Geospatial Monitoring and Modeling Software, Clark Labs. https://doi.org/10.1017/CBO9781107415324.004

ESRI, 2018. ArcGIS Desktop: Release 10.5. Environmental Systems Research Institute, Redlands, California.

Filer, C., 2010. The impacts of rural industry on the native forests of Papua New Guinea. Pacific Econ. Bull. 25, 135–153.

Filer, C., Keenan, R.J., Allen, B.J., Mcalpine, J.R., 2009. Deforestation and forest degradation in Papua New Guinea. Ann. For. Sci. 66, 813–813. https://doi.org/10.1051/forest/2009067

Geneletti, D., 2013. Assessing the impact of alternative land-use zoning policies on future

ecosystem services. Environ. Impact Assess. Rev. 40, 25–35. https://doi.org/10.1016/j.eiar.2012.12.003

Haas, J., Ban, Y., 2017. Sentinel-1A SAR and sentinel-2A MSI data fusion for urban ecosystem service mapping. Remote Sens. Appl. Soc. Environ. 8, 41–53. https://doi.org/10.1016/j.rsase.2017.07.006

ITS Global, 2006. The Economic Importance of the Forestry Industry to Papua New Guinea.

Jackson, S.M., Fredericksen, T.S., Malcolm, J.R., 2002. Area disturbed and residual stand damage following logging in a Bolivian tropical forest. For. Ecol. Manage. 166, 271–283. https://doi.org/10.1016/S0378-1127(01)00681-8

Jarabo-Amores, P., Rosa-Zurera, M., De La Mata-Moya, D., Vicen-Bueno, R., Maldonado-Bascón, S., 2011. Spatial-range mean-shift filtering and segmentation applied to SAR images. IEEE Trans. Instrum. Meas. 60, 584–597. https://doi.org/10.1109/TIM.2010.2052478

Johnson, S., 2006. Good Practice Guidance for Mining and Biodiversity, Good Practice Guidance for Mining and Biodiversity.

Katsigris, E., Bull, G.Q., White, A., Barr, C., Barney, K., Bun, Y., Kahrl, F., King, T., Lankin, A., Lebedev, A., Shearman, P., Sheingauz, A., Su, Y., Weyerhaeuser, H., 2004. The China Forest Products Trade: Overview of Asia-Pacific Supplying Countries, Impacts and Implications. Int. For. Rev. 6, 237–253. https://doi.org/10.1505/ifor.6.3.237.59980

Koh, L.P., Wilcove, D.S., 2009. Oil palm: disinformation enables deforestation. Trends Ecol. Evol. https://doi.org/10.1016/j.tree.2008.09.006

Kopatlie, J., Cornelio, D.L., 2013. GIS analysis of land suitability for commercial tree species in Papua New Guinea 35–40.

Lang, F., Yang, J., Li, D., Shi, L., Wei, J., 2014. Mean-shift-based speckle filtering of polarimetric SAR data. IEEE Trans. Geosci. Remote Sens. 52, 4440–4454. https://doi.org/10.1109/TGRS.2013.2282036

Laurance, W.F., 2011. Special agricultural and business leases imperil forests in Papua New Guinea. Pacific Conserv. Biol. 17, 297–298.

Laurance, W.F., Arrea, I.B., 2017. Roads to riches or ruin? Science (80-.). 358, 442–444. https://doi.org/10.1126/science.aao0312

Laurance, W.F., Clements, G.R., Sloan, S., O'Connell, C.S., Mueller, N.D., Goosem, M., Venter, O., Edwards, D.P., Phalan, B., Balmford, A., Van Der Ree, R., Arrea, I.B., 2014. A global strategy for road building. Nature 513, 229–232. https://doi.org/10.1038/nature13717

Laurance, W.F., Goosem, M., Laurance, S.G.W., 2009. Impacts of roads and linear clearings on tropical forests. Trends Ecol. Evol. https://doi.org/10.1016/j.tree.2009.06.009

Laurance, W.F., Kakul, T., Tom, M., Wahya, R., Laurance, S.G., 2012. Defeating the "resource curse": Key priorities for conserving Papua New Guinea's native forests. Biol. Conserv. https://doi.org/10.1016/j.biocon.2011.10.037

Laurance, W.F., Peletier-Jellema, A., Geenen, B., Koster, H., Verweij, P., Van Dijck, P., Lovejoy, T.E., Schleicher, J., Van Kuijk, M., 2015. Reducing the global environmental impacts of rapid infrastructure expansion. Curr. Biol. 25, R259–R262. https://doi.org/10.1016/j.cub.2015.02.050

Lechner, A.M., Devi, B., Schleger, A., Brown, G., McKenna, P., Ali, S., Rachmat, S., Syukril, M., Rogers, P., 2017a. A Socio-Ecological Approach to GIS Least-Cost Modelling for Regional Mining Infrastructure Planning: A Case Study from South-East Sulawesi, Indonesia. Resources 6, 7. https://doi.org/10.3390/resources6010007

Lechner, A.M., McIntyre, N., Raymond, C.M., Witt, K., Scott, M., Rifkin, W., Scott, M., Schaefer, C.E., 2017b. Challenges of integrated modelling in mining regions to address social, environmental and economic impacts. Environ. Model. Softw. 93, 268–281. https://doi.org/10.1016/j.envsoft.2017.03.020

Lee, J., Grunes, M.R., Grandi, G. De, Member, S., 1999. Polarimetric SAR Speckle Filtering and Its Implication for Classification 37, 2363–2373.

Marsden, S.J., Pilgrim, J.D., 2003. Diversity and abundance of fruiting trees in primary forest, selectively logged forest, and gardens on New Britain, Papua New Guinea. Trop. Biodivers. 8, 15–29.

McAlpine, J., Quigley, J., 1998. Forest resources of Papua New Guinea: summary statistics from the Forest Inventory Mapping (FIM) system.

Myers, N., Mittermeier, R.A., Mittermeier, C.G., da Fonseca, G.A.B., Kent, J., 2000. Biodiversity hotspots for conservation priorities. Nature 403, 853–858. https://doi.org/10.1038/35002501

Nepstad, D.C., Veríssimo, A., Alencar, A., Nobre, C., Lima, E., Lefebvre, P., Schlesinger, P., Potter, C., Moutinho, P., Mendoza, E., Cochrane, M., Brooks, V., 1999. Large-scale impoverishment of amazonian forests by logging and fire. Nature 398, 505–508. https://doi.org/10.1038/19066

PNGFA, 2016. West Sepik Forest Plan. Papua New Guinea Government.

Reddy, C.S., Singh, S., Dadhwal, V.K., Jha, C.S., Rao, N.R., Diwakar, P.G., 2017. Predictive modelling of the spatial pattern of past and future forest cover changes in India. J. Earth Syst. Sci. 126. https://doi.org/10.1007/s12040-016-0786-7

Rogers, H., 2011. Implications of the proposed Frieda Copper Mine for Forestry and Oil Palm development. Unpublished report for Xstrata Frieda River Limited.

Rogers, H.M., 2010. Impacts of portable-sawmill logging on stand structure and regeneration in the lowland forests of West New Britain, Papua New Guinea. Aust. For. 73, 12–23. https://doi.org/10.1080/00049158.2010.10676305

Shearman, P., Bryan, J., 2011. A bioregional analysis of the distribution of rainforest cover, deforestation and degradation in Papua New Guinea. Austral Ecol. 36, 9–24. https://doi.org/10.1111/j.1442-9993.2010.02111.x

Shearman, P., Bryan, J., Laurance, W.F., 2012. Are we approaching “peak timber” in the tropics? Biol. Conserv. 151, 17–21. https://doi.org/10.1016/j.biocon.2011.10.036

Shearman, P., Bryan, J.E., Ash, J., Hunnam, P., Mackey, B.G., Lokes, B., 2008. The State

of the Forests of Papua New Guinea. Mapping the extent and coindition of forest cover and measuring the drivers of forest change in the period 1972-2002, University of Papua New Guinea.

Shearman, P.L., Ash, J., MacKey, B., Bryan, J.E., Lokes, B., 2009. Forest conversion and degradation in Papua New Guinea 1972-2002. Biotropica 41, 379–390. https://doi.org/10.1111/j.1744-7429.2009.00495.x

Son, N.T., Chen, C., Chen, C., Minh, V., 2017. Assessment of Sentinel-1A data for rice crop classification using random forests and support vector machines. Geocarto Int. 6049, 1–15. https://doi.org/10.1080/10106049.2017.1289555

Tangoy Vivafounder Holdings Limited, 2017. Idam Saiwi Integrated Agro-forestry development project: First Phase of Block One – Environmental Impact Statement.

Tarawa, H., 2018. Districts soon to have agro-forestry industry. Natl.

Testolin, R., Saulei, S., Farcomeni, A., Grussu, G., Yosi, C., Sanctis, M. de, Attorre, F., 2016. Investigating the effect of selective logging on tree biodiversity and structure of the tropical forests of Papua New Guinea. iForest. https://doi.org/10.3832/ifor1732-008

Towney, G., 2011. Frieda River Feasibility Study Power Generation and Transmission: Biomass Removal Study – Appendix I-12. Unpublished report for Xstrata Copper Fried River Project.

Wang, Y.-H., Han, C.-Z., 2010. PolSAR Image Segmentation by Mean Shift Clustering in the Tensor Space. Acta Autom. Sin. 36, 798–806. https://doi.org/https://doi.org/10.1016/S1874-1029(09)60037-9

Young, N.E., Anderson, R.S., Chignell, S.M., Vorster, A.G., Lawrence, R., Evangelista, P.H., 2017. A survival guide to Landsat preprocessing. Ecology 98, 920–932. https://doi.org/10.1002/ecy.1730

Appendix

5.1. Appendix A - Support material for Section 2

South West Wapei - West Sepik

Summary of Major Species in Order of Sawlog Volume Representartion

Species Name		Volume Per Hectare		Percent (%)		Volume by Species	
Scientific	Common/Trade	PulpLog	50 cm +	Composition		Pulp	Sawlog
		(20 - 49 cm)		Pulp	Sawlog		
Intsia bijuga	Kwila	1.037	10.306	5.69	25.45	102,050.13	1,014,203.15
Pometia pinnata	Taun	4.11	6.696	22.54	16.54	404,460.99	658,946.66
Elmerrillia papuana	Wau Beech	0.118	1.151	0.65	2.84	11,612.26	113,268.76
Dysoxylum	Dysox	0.378	1.083	2.07	2.67	37,198.60	106,576.95
Celtis	Celtis	1.27	1.009	6.97	2.49	124,979.43	99,294.68
Terminalia (red-brown)	Terminalia	0.228	0.994	1.25	2.45	22,437.25	97,818.55
Homalium foetidum	Malas	0.455	0.935	2.50	2.31	44,776.10	92,012.42
Planchonella	Planchonella	0.336	0.873	1.84	2.16	33,065.42	85,911.06
Dillenia papuana	Dillenia	0.036	0.8	0.20	1.98	3,542.72	78,727.20
Canarium	Canarium	0.759	0.692	4.16	1.71	74,692.43	68,099.03
Duabanga moluccana	Duabanga	0.11	0.672	0.60	1.66	10,824.99	66,130.85
Dracontomelon dao	Walnut	0.219	0.669	1.20	1.65	21,551.57	65,835.62
Octomeles sumatrana	Erima	0.083	0.597	0.46	1.47	8,167.95	58,750.17
Terminalia (yellow)	Yellow Terminalia	0.161	0.552	0.88	1.36	15,843.85	54,321.77
Anisppptera thurifera	PNG Mersawa	0.058	0.511	0.32	1.26	5,707.72	50,287.00
Litsea	Litsea	0.247	0.493	1.35	1.22	24,307.02	48,515.64
Artocarpus	Kapiak	0.08	0.489	0.44	1.21	7,872.72	48,122.00
Alstonia excl. scholaris	Alstonia	0.129	0.483	0.71	1.19	12,694.76	47,531.55
Myristica	Nutmeg	0.926	0.433	5.08	1.07	91,126.73	42,611.10
Others		7.494	11.052	41.10	27.30	737,477.05	1,087,616.27
Total		**18.234**	**40.49**	**100**	**100**	**1,794,389.71**	**3,984,580.410**

(i) Volume Per Hectare (m3/ha)

Pulp - 18.234 m3/ha

Sawlog = 40.490 m3/ha (Gross)

= 28.343 m3/ha (Net - less 30%)

(ii) Area Statement (Ha)

Total Area = 116,793

Net = 98,409

Survey Date: 23/11/1994

DETAILS OF AMANAB BLOCK 7 TIMBER RESOURCE - SANDAUN PROVINCE

Total Area : 90,932.84 Ha's						Area (Ha) Details		
Potential: 77,2932.91Ha (less 15%)						Total (Original)	166,500.00	
Survey Date : 18/10/99						Imonda	41,567.16	
1.0 Stocking Per Hectare						Walsa	34,000.00	
	Diameter Class		20 - 49 cm	50 cm +	Total	Sub-Total	75,567.16	
						Amanab 7	90,932.84	Gross
			69.062	18.538	87.6		77,292.91	Net (less 15%)
2.0 Basal Area Per Hectare (m2)								
	Diameter Class		20 - 49 cm	50 cm +	Total			
			6.4	6.274	12.673			
3.0 Gross Volume Per Hectare (m3)								
	Diameter Class		20 - 49 cm	50 cm +	Total			
			38.198	44.626	82.824			

4.0 Major Sawlog Species In Order Of Volume Representation

	Volume Per Hectare (m^3/ha)				Total Volume (m^3)				
	Pulp Log (20-49cm)		Sawlog (50 cm+)		Pulp Log		Sawlog		Percent (%)
Species	Gross	Net	Gross	Net	Gross	Net	Gross	Net	
Intsia	0.684	0.4788	9.785	6.8495	52,868.353	37,007.845	756,311.124	529,417.787	21.93
Pometia pinnata	4.312	3.0184	4.436	3.1052	333,287.045	233,300.920	342,871.349	240,009.944	9.94
Terminalia (red-brown)	2.341	1.6387	2.902	2.0314	180,942.702	126,659.892	224,304.025	157,012.817	6.50
Campnosperma brevipetiolata	0.568	0.3976	2.137	1.4959	43,902.373	30,731.661	165,174.949	115,622.464	4.79
Cryptocarya	3.593	2.5151	2.066	1.4462	277,713.426	194,399.398	159,687.152	111,781.006	4.63
Vatica rassak	3.338	2.3366	1.662	1.1634	258,003.734	180,602.614	128,460.816	89,922.571	3.72
Artocarpus	0.422	0.2954	1.566	1.0962	32,617.608	22,832.326	121,040.697	84,728.488	3.51
Canarium	2.079	1.4553	1.377	0.9639	160,691.960	112,484.372	106,432.337	74,502.636	3.08
Dillenia papuana	0.246	0.1722	1.188	0.8316	19,014.056	13,309.839	91,823.977	64,276.784	2.66
Dracontomelon dao	0.494	0.3458	1.056	0.7392	38,182.698	26,727.888	81,621.313	57,134.919	2.37
Celtis	0.696	0.4872	0.947	0.6629	53,795.865	37,657.106	73,196.386	51,237.470	2.12
Dysoxylum	1.080	0.756	0.907	0.6349	83,476.343	58,433.440	70,104.669	49,073.269	2.03
Homalium foetidum	0.269	0.1883	0.825	0.5775	20,791.793	14,554.255	63,766.651	44,636.656	1.85
Maniltoa	1.191	0.8337	0.817	0.5719	92,055.856	64,439.099	63,148.307	44,203.815	1.83
Syzygium	1.221	0.8547	0.810	0.567	94,374.643	66,062.250	62,607.257	43,825.080	1.82
Maranthes corymbosa	0.183	0.1281	0.764	0.5348	14,144.603	9,901.222	59,051.783	41,336.248	1.71
Myristica	1.887	1.3209	0.740	0.518	145,851.721	102,096.205	57,196.753	40,037.727	1.66
Palaquium warburgianum	0.307	0.2149	0.689	0.4823	23,728.923	16,610.246	53,254.815	37,278.370	1.54
Kingiodendron	0.555	0.3885	0.646	0.4522	42,897.565	30,028.296	49,931.220	34,951.854	1.45
Parastemon versteeghii	0.336	0.2352	0.569	0.3983	25,970.418	18,179.292	43,979.666	30,785.766	1.28
Buchanania	0.257	0.1799	0.561	0.3927	19,864.278	13,904.995	43,361.323	30,352.926	1.26
Planchonella	0.564	0.3948	0.552	0.3864	43,593.201	30,515.241	42,665.686	29,865.980	1.24
Others	11.575	8.1025	7.624	5.3368	894,665.433	626,265.803	589,281.146	412,496.802	17.08
Total	38.198	26.7386	44.626	31.2382	2,952,434.576	2,066,704.203	3,449,273.402	2,414,491.381	100.00

1.0 PROVINCE : WEST SEPIK

1.1) Survey Name : Amanab-Green (Amanab Block 1)

Area : 84,000 Ha's *Survey Date : 02/04/92*

A) Stocking Per Hectare

Diameter Class	20 - 49 cm	50 cm +	Total
	48.690	12.342	61.032

B) Basal Area Per Hectare (m^2)

Diameter Class	20 - 49 cm	50 cm +	Total
	4.911	3.613	8.524

C) Gross Volume Per Hectare (m^3)

Diameter Class	20 - 49 cm	50 cm +	Total
	30.957	28.004	58.961

D) Major Sawlog Species In Order Of Volume Representation

	Diameter Class		Percent (%)
Species	**20 - 49 cm**	**50 cm +**	
Intsia	1.575	7.033	25.11
Syzygium	3.728	3.150	11.25
Pometia pinnata	2.496	2.607	9.31
Canarium	2.435	0.977	3.49
Anisoptera thurifera	0.360	0.940	3.36
Dysoxylum	1.042	0.865	3.09
Calophyllum	0.600	0.723	2.58
Planchonella	0.483	0.685	2.44
Terminalia excl. brassii	0.588	0.628	2.24
Cryptocarya	1.132	0.593	2.12
Celtis	0.833	0.544	1.94
Polyalthia	2.060	0.478	1.71
Litsea	0.983	0.477	1.70
Myristica	1.754	0.453	1.62

Elaeocarpus	0.597	0.426	1.52
Elmerrillia papuana	0.333	0.419	1.50
Lithocarpus	0.710	0.393	1.40
Homalium foetidum	0.332	0.388	1.39
Xanthophyllum papuanum	0.753	0.375	1.34
Maniltoa	0.340	0.302	1.08
Hopea iriana or papuana	0.892	0.286	1.02

1.2) Survey Name : Amanab-Imonda (Amanab Block 3)

Area : 62,000 Ha's *Survey Date : 21/07/93*

A) Stocking Per Hectare

Diameter Class	20 - 49 cm	50 cm +	Total
	19.784	21.143	40.927

B) Basal Area Per Hectare (m^2)

Diameter Class	20 - 49 cm	50 cm +	Total
	2.248	6.002	8.250

C) Gross Volume Per Hectare (m^3)

Diameter Class	20 - 49 cm	50 cm +	Total
	13.415	45.332	58.747

D) Major Sawlog Species In Order Of Volume Representation

	Diameter Class		Percent (%)
Species	**20 - 49 cm**	**50 cm +**	
Intsia	0.763	8.706	19.20
Pometia pinnata	2.209	5.130	11.32
Maniltoa	0.788	1.718	3.79
Syzygium	0.404	1.452	3.20
Terminalia (yellow)	0.075	1.348	2.97
Anisoptera thurifera	0.429	1.332	2.94
Canarium	0.471	1.295	2.86
Planchonia papuana	0.096	1.254	2.77
Nauclea	0.285	1.222	2.70
Campnosperma brevipetiolata	0.146	1.029	2.27
Terminalia (red-brown)	0.295	1.010	2.23
Palaquium warburgianum	0.278	1.001	2.21
Dillenia papuana	0.065	0.929	2.05
Calophyllum	0.090	0.925	2.04
Elaeocarpus	0.070	0.925	2.04
Myristica	0.824	0.918	2.02
Maranthes corymbosa	0.299	0.844	1.86

Celtis philippensis or latifolia	0.000	0.647	1.43
Dysoxylum	0.298	0.640	1.41
Hopea iriana or papuana	0.288	0.608	1.34
Homalium foetidum	0.296	0.603	1.33
Neonaualea	0.119	0.599	1.32
Celtis	0.519	0.505	1.11
Sterculia	0.073	0.477	1.05
Planchonella	0.141	0.454	1.00

1.3) Survey Name : Amanab BK4&3 (Amanab Block 4)

Area : 58,000 Ha's *Survey Date : 21/07/93*

A) Stocking Per Hectare

Diameter Class	20 - 49 cm	50 cm +	Total
	36.646	11.889	48.535

B) Basal Area Per Hectare (m^2)

Diameter Class	20 - 49 cm	50 cm +	Total
	3.966	3.699	7.665

C) Gross Volume Per Hectare (m^3)

Diameter Class	20 - 49 cm	50 cm +	Total
	24.473	27.179	51.652

D) Major Sawlog Species In Order Of Volume Representation

	Diameter Class		Percent (%)
Species	**20 - 49 cm**	**50 cm +**	
Intsia	1.790	8.070	29.69
Pometia pinnata	3.911	1.815	6.68
Terminalia (red-brown)	1.170	1.687	6.21
Artocarpus	0.485	1.016	3.74
Campnosperma brevipetiolata	0.633	0.812	2.99
Syzygium	0.973	0.725	2.67
Canarium	0.633	0.708	2.60
Maniltoa	1.068	0.645	2.37
Terminalia (yellow)	0.324	0.584	2.15
Terminalia excl. brassii	0.230	0.555	2.04
Celtis	0.816	0.510	1.88
Buchanania	0.218	0.510	1.88
Myristica	1.181	0.434	1.60
Octomeles sumatrana	0.245	0.423	1.56
Anthocephalus chinensis	0.629	0.374	1.38
Dracontomelon dao	0.398	0.374	1.37

Parartocarpus venenosus	0.127	0.370	1.36
Planchonella	0.417	0.361	1.33
Dysoxylum	0.547	0.350	1.29
Calophyllum	0.175	0.342	1.26
Eucalyptopsis papuana	0.214	0.331	1.22
Dillenia papuana	0.148	0.306	1.13

1.4) Survey Name : Amanab Block 5 *Total Area: 134,008 Ha's*

Forest Potential: 126,963 Ha's

Survey Date: 18/10/98

A) Stocking Per Hectare

Diameter Class	**20 - 49 cm**	**50 cm +**	**Total**
	76.679	15.420	92.099

B) Basal Area Per Hectare (m^2)

Diameter Class	**20 - 49 cm**	**50 cm +**	**Total**
	6.012	4.420	10.432

C) Gross Volume Per Hectare (m^3)

Diameter Class	**20 - 49 cm**	**50 cm +**	**Total**
	34.954	33.549	68.503

D) Major Sawlog Species In Order Of Volume Representation

	Diameter Class		**Percent (%)**
Species	**20 - 49 cm**	**50 cm +**	
Intsia	2.173	12.711	37.89
Pometia pinnata	5.277	2.932	8.74
Anisoptera thurifera	0.798	1.862	5.55
Elmerrillia papuana	0.235	1.853	5.52
Dillenia papuana	0.226	0.955	2.85
Vatica rassak	4.190	0.791	2.36
Calophyllum	0.464	0.711	2.12
Maranthes corymbosa	0.257	0.602	1.79

Syzygium	1.647	0.583	1.74
Garcinia latissima	0.449	0.565	1.68
Artocarpus	0.303	0.543	1.62
Campnosperma brevipetiolata	0.403	0.543	1.62
Canarium	1.719	0.534	1.59
Horsfieldia	0.444	0.507	1.51
Homalium foetidum	0.440	0.406	1.21
Celtis philip. or latif.	0.897	0.385	1.15
Dysoxylum	1.058	0.370	1.10
Heritiera	0.177	0.344	1.02

1.5) Survey Name : Amanab Block 6 *Area : 156,026 Ha's*

Survey Date : 18/10/99

A) Stocking Per Hectare

Diameter Class	**20 - 49 cm**	**50 cm +**	**Total**
	69.062	18.538	87.600

B) Basal Area Per Hectare (m^2)

Diameter Class	**20 - 49 cm**	**50 cm +**	**Total**
	6.400	6.274	12.673

C) Gross Volume Per Hectare (m^3)

Diameter Class	**20 - 49 cm**	**50 cm +**	**Total**
	38.198	44.626	82.824

D) Major Sawlog Species In Order Of Volume Representation

	Diameter Class		**Percent (%)**
Species	**20 - 49 cm**	**50 cm +**	
Intsia	0.684	9.785	21.93
Pometia pinnata	4.312	4.436	9.94
Terminalia (red-brown)	2.341	2.902	6.50
Campnosperma brevipetiolata	0.568	2.137	4.79
Cryptocarya	3.593	2.066	4.63
Vatica rassak	3.338	1.662	3.72

Artocarpus	0.422	1.566	3.51
Canarium	2.079	1.377	3.08
Dillenia papuana	0.246	1.188	2.66
Dracontomelon dao	0.494	1.056	2.37
Celtis	0.696	0.947	2.12
Dysoxylum	1.080	0.907	2.03
Homalium foetidum	0.269	0.825	1.85
Maniltoa	1.191	0.817	1.83
Syzygium	1.221	0.810	1.82
Maranthes corymbosa	0.183	0.764	1.71
Myristica	1.887	0.740	1.66
Palaquium warburgianum	0.307	0.689	1.54
Kingiodendron	0.555	0.646	1.45
Parastemon versteeghii	0.336	0.569	1.28
Buchanania	0.257	0.561	1.26
Planchonella	0.564	0.552	1.24

1.6) Survey Name : Palai 1 (Maimai Wanwan)

Area : 43,800 Ha's Survey Date : 16/11/95

A) Stocking Per Hectare

Diameter Class	20 - 49 cm	50 cm +	Total
	8.230	14.103	22.333

B) Basal Area Per Hectare (m^2)

Diameter Class	20 - 49 cm	50 cm +	Total
	0.848	4.215	5.063

C) Gross Volume Per Hectare (m^3)

Diameter Class	20 - 49 cm	50 cm +	Total
	5.242	32.270	37.512

D) Major Sawlog Species In order Of Volume Representation

	Diameter Class		Percent (%)
Species	**20 - 49 cm**	**50 cm +**	
Pometia pinnata	1.421	5.911	18.32
Terminalia (red-brown)	0.114	2.927	9.07
Intsia	0.062	2.818	8.73
Celtis	0.448	2.026	6.28
Duabanga moluccana	0.064	1.245	3.86
Canarium	0.240	1.236	3.83
Homalium foetidum	0.082	0.873	2.71
Dysoxylum	0.114	0.869	2.69
Dracontomelon dao	0.068	0.865	2.68
Teijsmanniodendron	0.263	0.821	2.54
Alstonia scholaris	0.099	0.718	2.22
Syzygium	0.198	0.680	2.11
Pterocymbium beccarii	0.020	0.605	1.88
Toona sureni	0.015	0.587	1.82
Buchanania	0.000	0.564	1.75
Octomeles sumatrana	0.016	0.523	1.62
Planchonella	0.043	0.504	1.56
Artocarpus	0.041	0.467	1.45
Litsea	0.035	0.456	1.41
Ficus	0.224	0.430	1.33
Sterculia	0.072	0.415	1.29
Pimeleodendron amboinicum	0.316	0.390	1.21
Pterocarpus indicus	0.009	0.342	1.06

1.7) Survey Name : Palai 2 (Maimai Wanwan)

Area : 34,500 Ha's Survey Date : 16/11/95

A) Stocking Per Hectare

Diameter Class	**20 - 49 cm**	**50 cm +**	**Total**

	9.224	15.235	24.460

B) Basal Area Per Hectare (m2)

Diameter Class	20 - 49 cm	50 cm +	Total
	0.885	4.551	5.436

C) Gross Volume Per Hectare (m3)

Diameter Class	20 - 49 cm	50 cm +	Total
	5.431	36.179	41.610

D) Major Sawlog Species In Order Of Volume Representation

	Diameter Class		Percent (%)
Species	**20 - 49 cm**	**50 cm +**	
Pometia pinnata	1.709	7.473	20.66
Celtis	0.398	1.929	5.33
Spondias cytherea	0.135	1.773	4.90
Toona sureni	0.000	1.754	4.85
Terminalia (red-brown)	0.136	1.698	4.69
Artocarpus	0.206	1.580	4.37
Octomeles sumatrana	0.065	1.547	4.28
Duabanga moluccana	0.000	1.517	4.19
Dysoxylum	0.277	1.352	3.74
Alstonia scholaris	0.127	1.046	2.89
Sterculia	0.153	1.040	2.87
Cryptocarya	0.027	0.988	2.73
Burckella	0.139	0.956	2.64
Syzygium	0.214	0.922	2.55
Ficus	0.099	0.818	2.26
Aglaia	0.000	0.685	1.89
Pterocymbium beccarii	0.101	0.632	1.75
Dracontomelon dao	0.039	0.613	1.69
Planchonia papuana	0.000	0.590	1.63
Elmerrillia papuana	0.009	0.529	1.46
Canarium	0.046	0.506	1.40

Teijsmanniodendron	0.135	0.428	1.18
Homalium foetidum	0.000	0.410	1.13

1.8) Survey Name : Tadji-Romei *Total Area: 81,548 Ha's*

Forest Potential: 49,488 Ha's *Survey Date: 14/06/93*

NB: Only one (1) block.

1.8 (i) Romei Tadji - All Blocks

A) Stocking Per Hectare

Diameter Class	**20 - 49 cm**	**50 cm + Total**	
	30.059	12.755	42.813

B) Basal Area Per Hectare (m^2)

Diameter Class	**20 - 49 cm**	**50 cm + Total**	
	2.938	3.907	6.844

C) Gross Volume Per Hectare (m^3)

Diameter Class	**20 - 49 cm**	**50 cm + Total**	
	16.974	29.815	46.789

D) Major Sawlog Species In Order Of Volume Representation

	Diameter Class		**Percent (%)**
Species	**20 - 49 cm**	**50- cm +**	
Pometia pinnata	2.419	4.921	16.51
Campnosperma brevipetiolata	0.575	1.809	6.07
Syzygium	0.679	1.774	5.95
Terminalia (red-brown)	0.600	1.383	4.64
Planchonella	0.319	0.977	3.28
Cryptocarya	0.860	0.976	3.27
Dillenia papuana	0.110	0.939	3.15
Canarium	0.715	0.874	2.93
Celtis	0.651	0.872	2.92
Dysoxylum	0.498	0.813	2.73
Homalium foetidum	0.389	0.731	2.45
Palaquium warburgianum	0.293	0.727	2.44
Pterocymbium beccarii	0.165	0.667	2.24
Litsea	0.596	0.657	2.20

Elaeocarpus	0.500	0.508	1.70
Endospermum	0.103	0.449	1.51
Spondias cytherea	0.067	0.443	1.49
Ficus	0.265	0.424	1.42
Mastixiodendron	0.175	0.416	1.40
Elmerrillia papuana	0.041	0.393	1.32
Alstonia scholaris	0.124	0.390	1.31
Myristica	0.938	0.378	1.27
Terminalia excl. brassii	0.126	0.377	1.26
Intsia	0.087	0.376	1.26
Dracontomelon dao	0.093	0.334	1.12
Chisocheton	0.078	0.324	1.09
Aglaia	0.199	0.323	1.08
Buchanania	0.092	0.319	1.07
Terminalia (yellow)	0.136	0.309	1.04

A2) Tadji-Romei - Block 1 ***Area :***

B) Stocking Per Hectare

Diameter Class	**20 - 49 cm**	**50 cm +**	**Total**
	32.911	14.235	47.146

C) Basal Area Per Hectare (m2)

Diameter Class	**20 - 49 cm**	**50 cm +**	**Total**
	3.029	4.211	7.240

D) Gross Volume Per Hectare (m3)

Diameter Class	**20 - 49 cm**	**50 cm +**	**Total**
	16.278	31.709	47.987

E) Major Sawlog Species In Order Of Volume Representation

	Diameter Class		**Percent (%)**
Species	**20 - 49 cm**	**50 cm +**	
Pometia pinnata	1.638	3.465	10.93

Syzygium	0.940	2.947	9.29
Campnosperma brevipetiolata	0.773	2.645	8.34
Terminalia (red-brown)	0.648	1.328	4.19
Palaquium warburgianum	0.422	1.271	4.01
Dysoxylum	0.610	1.090	3.44
Cryptocarya	1.015	1.015	3.20
Homalium foetidum	0.375	0.936	2.95
Canarium	0.892	0.933	2.94
Dillenia papuana	0.067	0.933	2.94
Planchonella	0.266	0.861	2.71
Elmerrillia papuana	0.072	0.727	2.29
Celtis	0.467	0.704	2.22
Litsea	0.520	0.690	2.18
Terminalia excl. brassii	0.224	0.663	2.09
Mastixiodendron	0.236	0.570	1.80
Elaeocarpus	0.443	0.562	1.77
Endospermum	0.049	0.531	1.68
Myristica	0.781	0.456	1.44
Sterculia	0.380	0.429	1.35
Intsia	0.049	0.393	1.24
Chisocheton	0.030	0.380	1.20
Maniltoa	0.189	0.351	1.11
Pimeleodendron amboinicum	0.711	0.339	1.07
Ficus	0.224	0.338	1.07
Neonauclea	0.354	0.336	1.06
Aglaia	0.130	0.335	1.06

A3) Tadji-Romei - Block 2 ***Area :***

B) Stocking Per Hectare

Diameter Class	**20 - 49 cm**	**50 cm + Total**	
	26.966	11.150	38.116

C) Basal Area Per Hectare (m2)

Diameter Class	**20 - 49 cm**	**50 cm + Total**	
	2.838	3.578	6.415

D) Gross Volume Per Hectare (m3)

Diameter Class	20 - 49 cm	50 cm +	Total
	17.727	27.761	45.488

E) Major Sawlog Species In Order Of Volume Representation

	Diameter Class		Percent (%)
Species	**20 - 49 cm**	**50 cm +**	
Pometia pinnata	3.265	6.500	23.41
Terminalia (red-brown)	0.547	1.443	5.20
Pterocymbium beccarii	0.223	1.246	4.49
Planchonella	0.376	1.103	3.97
Celtis	0.851	1.054	3.80
Dillenia papuana	0.157	0.946	3.41
Cryptocarya	0.693	0.934	3.36
Campnosperma brevipetiolata	0.360	0.904	3.26
Canarium	0.523	0.810	2.90
Spondias cytherea	0.122	0.767	2.76
Litsea	0.678	0.620	2.23
Alstonia scholaris	0.228	0.595	2.15
Ficus	0.308	0.516	1.86
Dysoxylum	0.377	0.513	1.85
Homalium foetidum	0.404	0.509	1.83
Syzygium	0.395	0.503	1.81
Elaeocarpus	0.562	0.449	1.62
Terminalia (yellow)	0.244	0.413	1.49
Dracontomelon dao	0.110	0.412	1.49
Buchanania	0.170	0.387	1.39
Endospermum	0.161	0.360	1.30
Planchonia papuana	0.111	0.359	1.29
Octomeles sumatrana	0.049	0.358	1.29
Intsia	0.128	0.357	1.29
Aglaia	0.273	0.310	1.12
Myristica	1.109	0.294	1.06
Artocarpus	0.283	0.291	1.05

1.9) Survey Name : Yeftim *Area* *Survey Date : 07/03/94*

NB : Sawlog Assessment Survey

A) Stocking Per Hectare = 11.286

B) Basal Area Per Hectare (m^2) = 3.158

C) Gross Volume Per Hectare (m^3) = 22.161

D) Major Sawlog Species In Order Of Volume Representation

Species	Volume (50 cm+)	Percent (%)
Intsia	6.927	31.26
Pometia pinnata	3.502	15.80
Cryptocarya	1.162	5.24
Vatica rassak	1.055	4.76
Hopea iriana or papuana	0.964	4.35
Elmerrillia papuana	0.725	3.27
Terminalia (red-brown)	0.721	3.25
Planchonella	0.714	3.22
Xanthophyllum papuanum	0.561	2.53
Syzygium	0.515	2.32
Pterocarpus indicus	0.367	1.66
Palaquium warburgianum	0.364	1.64
Canarium	0.356	1.61
Dysoxylum	0.313	1.41
Anisoptera thurifera	0.291	1.31
Duabanga moluccana	0.287	1.30
Mastixiodendron	0.281	1.27
Campnosperma brevipetiolata	0.268	1.21
Pterocymbium beccarii	0.247	1.11
Dracontomelon dao	0.228	1.03
Celtis	0.228	1.03

1.10) Survey Name : Kabore *Area :* *Survey Date : 09/03/94*

NB : Sawlog Assessment Survey

A) Stocking Per Hectare = 6.750

B) Basal Area Per Hectare (m^2) = 1.920

C) Gross Volume Per Hectare (m^3) = 13.404

D) Major Sawlog In Order Of Volume Representation

Species	Volume (50 cm +)	Percent (%)
Flindersia	1.660	12.38
Elmerrillia papuana	1.564	11.67
Syzygium	1.073	8.00
Cryptocarya	0.983	7.34
Elaeocarpus	0.904	6.75
Agathis	0.797	5.94
Aglaia	0.733	5.47
Dysoxylum	0.637	4.75
Octomeles sumatrana	0.581	4.33
Celtis	0.520	3.88
Alstonia scholaris	0.400	2.98
Galbulimima belgraveana	0.297	2.22
Podocarpus	0.297	2.22
Canarium	0.282	2.11
Terminalia (red-brown)	0.264	1.97
Hopea iriana or papuana	0.262	1.95
Duabanga moluccana	0.237	1.77
Litsea	0.237	1.77
Endospermum	0.230	1.72
Cerbera floribunda	0.230	1.72
Intsia	0.197	1.47

Schizomeria	0.192	1.43
Lithocarpus	0.170	1.27
Flacourtia	0.137	1.02

1.11) Survey Name : South-West Wapei

Total Area: *116,793 Ha's*
Forest Potential: *98,409 Ha's*
Survey Date: *23/11/94*

A) Stocking Per Hectare

Diameter Class	**20 - 49 cm**	**50 cm +**	**Total**
	25.058	14.854	39.912

B) Basal Area Per Hectare (m^2)

Diameter Class	**20 - 49 cm**	**50 cm +**	**Total**
	2.753	4.927	7.680

C) Gross Volume Per Hectare (m^3)

Diameter Class	**20 - 49 cm**	**50 cm +**	**Total**
	18.234	40.490	58.724

D) Major Sawlog Species In Order Of Volume Representation

	Diameter Class		**Percent (%)**
Species	**20 - 49 cm**	**50 cm +**	
Intsia	1.037	10.306	25.45
Pometia pinnata	4.110	6.696	16.54
Elmerrillia papuana	0.118	1.151	2.84
Dysoxylum	0.738	1.083	2.68
Celtis	1.270	1.009	2.49
Terminalia (red-brown)	0.228	0.994	2.46
Homalium foetidum	0.455	0.935	2.31
Planchonella	0.336	0.873	2.16
Dillenia papuana	0.036	0.800	1.97
Canarium	0.759	0.692	1.71

Duabanga moluccana	0.110	0.672	1.66
Dracontomelon dao	0.219	0.669	1.65
Octomeles sumatrana	0.083	0.597	1.47
Terminalia (yellow)	0.161	0.552	1.36
Anisoptera thurifera	0.058	0.511	1.26
Litsea	0.247	0.493	1.22
Artocarpus	0.080	0.489	1.21
Alstonia excl. scholaris	0.129	0.453	1.12
Myristica	0.926	0.433	1.07

1.12) Survey Name : East Coast Aitape *Total Area: 86,606 Ha's*
Forest Potential: 45,560 Ha's
Survey Date: 21/12/94

A) Stocking Per Hectare

Diameter Class	**20 - 49 cm**	**50 cm +**	**Total**
	18.980	8.662	27.642

B) Basal Area Per Hectare (m^2)

Diameter Class	**20 - 49 cm**	**50 cm +**	**Total**
	2.029	2.721	4.750

C) Gross Volume Per Hectare (m^3)

Diameter Class	**20 - 49 cm**	**50 cm +**	**Total**
	13.338	21.555	34.893

D) Major Sawlog Species In Order Of Volume Representation

	Diameter Class		**Percent (%)**
Species	**20 - 49 cm**	**50 cm +**	
Pometia pinnata	2.564	3.808	17.67
Campnosperma brevipetiolata	1.093	1.929	8.95
Terminalia brassii	0.497	1.107	5.14
Celtis	0.845	1.058	4.91
Octomeles sumatrana	0.112	0.901	4.18
Homalium foetidum	0.309	0.620	2.88

Terminalia (yellow)	0.321	0.619	2.87
Terminalia (red-brown)	0.168	0.600	2.78
Syzygium	0.410	0.572	2.66
Spondias cytherea	0.114	0.514	2.39
Dysoxylum	0.297	0.471	2.19
Planchonia papuana	0.082	0.467	2.16
Alstonia scholaris	0.191	0.463	2.15
Endospermum	0.081	0.450	2.09
Planchonella	0.245	0.415	1.93
Intsia	0.047	0.398	1.85
Litsea	0.353	0.386	1.79
Dracontomelon dao	0.166	0.382	1.77
Canarium	0.359	0.368	1.71
Nauclea	0.171	0.341	1.58
Cananga odorata	0.094	0.305	1.42
Eucalyptus papuana	0.086	0.293	1.36
Calophyllum	0.043	0.282	1.31
Palaquium warburgianum	0.091	0.267	1.24
Sterculia	0.508	0.266	1.24

1.13) Survey Name : Wes *Total Area:* *99,098 Ha's*

Forest Potential: *47,898 Ha's*

Survey Date: *20/11/97*

A) Stocking Per Hectare

Diameter Class	**20 - 49 cm**	**50 cm +**	**Total**
	57.464	11.530	68.994

B) Basal Area Per Hectare (m^2)

Diameter Class	**20 - 49 cm**	**50 cm +**	**Total**
	5.686	3.249	8.935

C) Gross Volume Per Hectare (m^3)

Diameter Class	**20 - 49 cm**	**50 cm +**	**Total**
	36.899	26.219	63.118

D) Major Sawlog Species In Order Of Volume Representation

	Diameter Class		Percent (%)
Species	**20 - 49 cm**	**50 cm +**	
Pometia pinnata	8.593	5.092	19.42
Homalium foetidum	1.275	1.970	7.51
Intsia	0.685	1.378	5.26
Dillenia papuana	0.386	1.027	3.92
Buchanania	0.327	0.899	3.43
Terminalia excl. brassii	0.925	0.869	3.32
Canarium	0.612	0.866	3.30
Terminalia (yellow)	0.705	0.791	3.02
Dysoxylum	2.086	0.719	2.74
Planchonia papuana	0.127	0.697	2.66
Pterocarpus indicus	0.204	0.659	2.51
Mastixiodendron	0.695	0.630	2.40
Duabanga moluccana	0.170	0.541	2.06
Dracontomelon dao	0.211	0.514	1.96
Planchonella	0.469	0.478	1.82
Celtis	1.664	0.470	1.79
Pterocymbium beccarii	0.132	0.455	1.74
Syzygium	0.989	0.421	1.61
Alstonia scholaris	0.370	0.398	1.52
Octomeles sumatrana	0.109	0.379	1.45
Cryptocarya	0.550	0.365	1.39
Litsea	0.972	0.318	1.21
Celtis nyman. or kajwes	0.389	0.314	1.20
Toona sureni	0.014	0.304	1.16
Spondias cytherea	0.224	0.301	1.15
Palaquium warburgianum	0.225	0.275	1.05

5.2. Appendix B: Land Change Modeler MLP Model Results for transition between forest and cleared

1. General Model Information

1) Input Files

Independent variable 1	Distance to Road
Independent variable 2	Distance to existing cleared
Independent variable 3	Elevation
Independent variable 4	Slope
Training site file	Cleared_Train_Fores_to_Clear

2) Parameters and Performance

Input layer neurons	4
Hidden layer neurons	3
Output layer neurons	2
Requested samples per class	10000
Final learning rate	0.0003
Momentum factor	0.5
Sigmoid constant	1
Acceptable RMS	0.01
Iterations	10000
Training RMS	0.3344
Testing RMS	0.3411

Accuracy rate	83.80%
Skill measure	0.6760

3) Model Skill Breakdown by Transition & Persistence

Class	Skill measure
Transition : Forest to Cleared	0.8562
Persistence : Forest	0.4981

2. Weights Information of Neurons across Layers

1) Weights between Input Layer Neurons and Hidden Layer Neurons

Neuron	h-Neuron 1	h-Neuron 2	h-Neuron 3
i-Neuron 1	0.4440	-9.3813	2.2693
i-Neuron 2	0.4034	3.3525	-4.4633
i-Neuron 3	-1.2630	4.0450	7.2339
i-Neuron 4	-0.6254	-12.9532	16.5535

2) Weights between Hidden Layer Neurons and Output Layer Neurons

Neuron	o-Neuron 1	o-Neuron 2
h-Neuron 1	-2.6555	2.6606
h-Neuron 2	6.3100	-6.3130
h-Neuron 3	-12.2189	12.2158

3. Sensitivity of Model to Forcing Independent Variables to be Constant

1) Forcing a Single Independent Variable to be Constant

Model	Accuracy (%)	Skill measure	Influence order
With all variables	83.80	0.6760	N/A
Var. 1 constant	50.32	0.0063	1 (most influential)
Var. 2 constant	83.80	0.6760	4 (least influential)
Var. 3 constant	83.42	0.6684	3
Var. 4 constant	80.45	0.6090	2

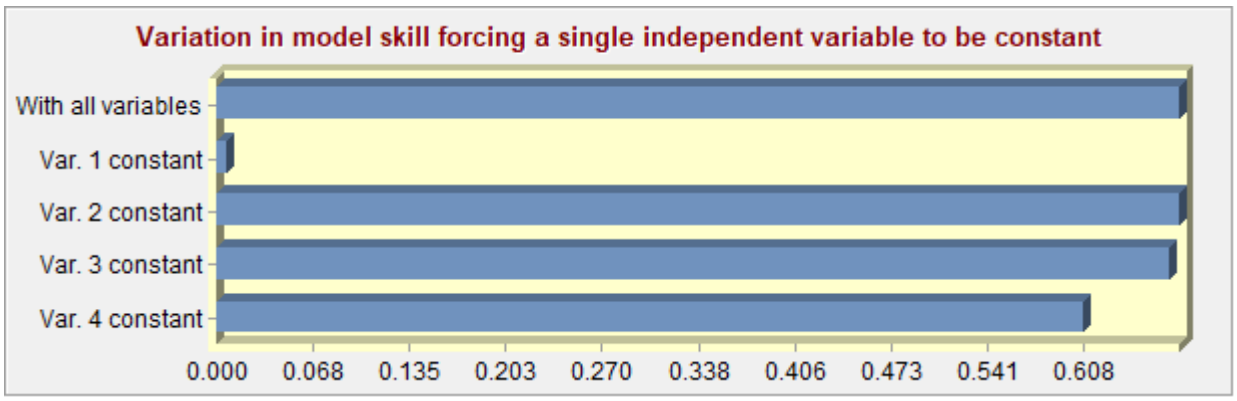

2) Forcing All Independent Variables Except One to be Constant

Model	Accuracy (%)	Skill measure
With all variables	83.80	0.6760
All constant but var. 1	74.06	0.4812
All constant but var. 2	50.32	0.0063
All constant but var. 3	50.32	0.0063
All constant but var. 4	50.32	0.0063

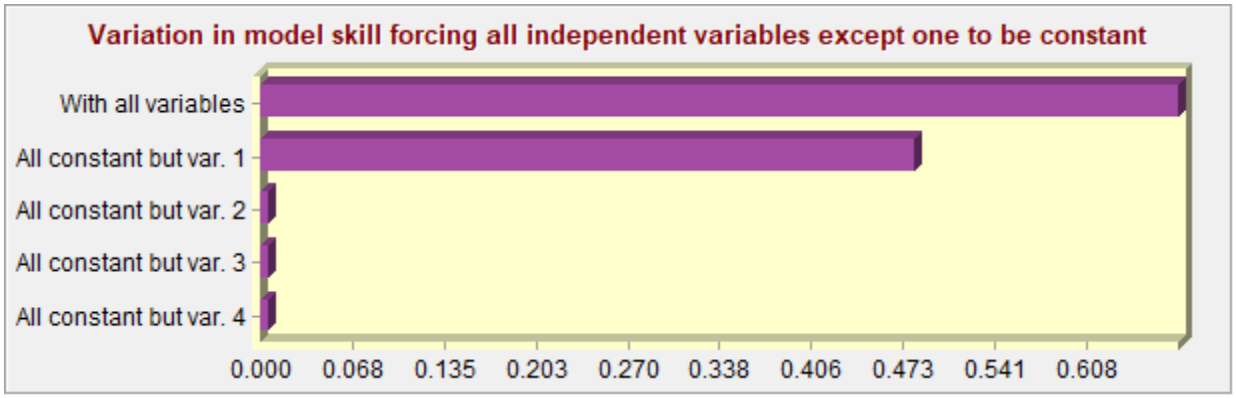

3) Backwards Stepwise Constant Forcing

Model	Variables included	Accuracy (%)	Skill measure
With all variables	All variables	83.80	0.6760
Step 1: var.[2] constant	[1,3,4]	83.80	0.6760
Step 2: var.[2,3] constant	[1,4]	83.42	0.6684
Step 3: var.[2,3,4] constant	[1]	74.06	0.4812

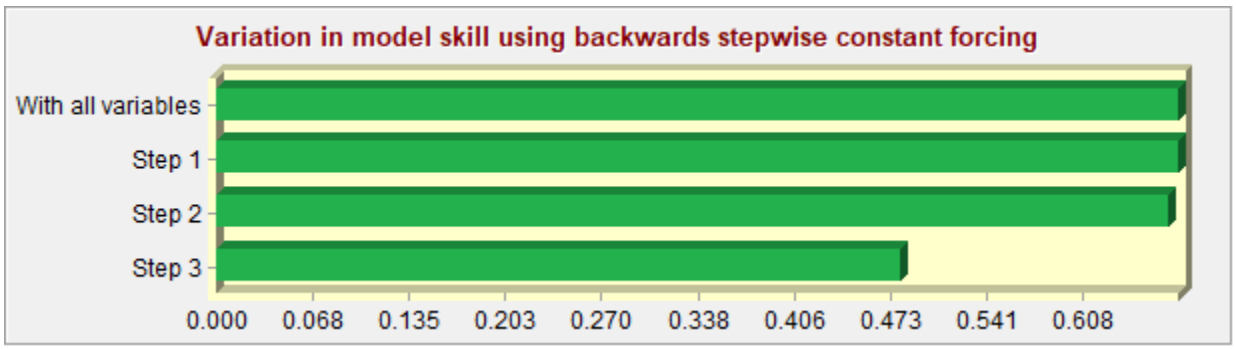

5.3. Appendix C: Land Change Modeler MLP Model Results for transition between forest and cleared sensitivity analysis with distance to Vanimo

1. General Model Information

1) Input Files

Independent variable 1	Distance to Road
Independent variable 2	Distance to existing cleared
Independent variable 3	Elevation
Independent variable 4	Slope
Independent variable 5	Distance to Vanimo
Training site file	Cleared_Train_Fores_to_Clear

2) Parameters and Performance

Input layer neurons	5
Hidden layer neurons	3
Output layer neurons	2
Requested samples per class	10000
Final learning rate	0.0001
Momentum factor	0.5
Sigmoid constant	1
Acceptable RMS	0.01
Iterations	10000
Training RMS	0.2152

Testing RMS	0.2091
Accuracy rate	95.40%
Skill measure	0.9080

3) Model Skill Breakdown by Transition & Persistence

Class	Skill measure
Transition : Forest to Cleared	0.9905
Persistence : Forest	0.8249

2. Weights Information of Neurons across Layers

1) Weights between Input Layer Neurons and Hidden Layer Neurons

Neuron	h-Neuron 1	h-Neuron 2	h-Neuron 3
i-Neuron 1	-1.6174	0.2537	0.5502
i-Neuron 2	-3.8006	2.6877	2.3610
i-Neuron 3	15.4322	-9.9984	-9.3569
i-Neuron 4	11.4261	-7.6175	-6.5349
i-Neuron 5	4.3439	-3.3536	-3.0996

2) Weights between Hidden Layer Neurons and Output Layer Neurons

Neuron	o-Neuron 1	o-Neuron 2
h-Neuron 1	-15.4947	15.4999
h-Neuron 2	8.6846	-8.5513
h-Neuron 3	7.6916	-7.8321

3. Sensitivity of Model to Forcing Independent Variables to be Constant

1) Forcing a Single Independent Variable to be Constant

Model	Accuracy (%)	Skill measure	Influence order
With all variables	95.40	0.9080	N/A
Var. 1 constant	95.34	0.9068	4
Var. 2 constant	95.40	0.9080	5 (least influential)
Var. 3 constant	81.35	0.6270	2
Var. 4 constant	94.54	0.8907	3
Var. 5 constant	39.55	-0.2089	1 (most influential)

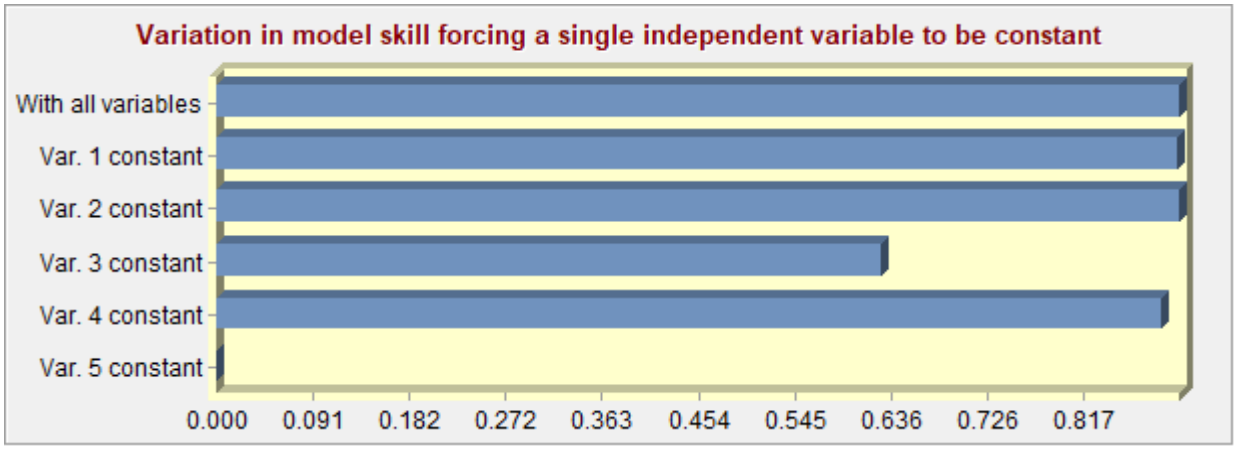

2) Forcing All Independent Variables Except One to be Constant

Model	Accuracy (%)	Skill measure
With all variables	95.40	0.9080
All constant but var. 1	49.85	-0.0031
All constant but var. 2	49.85	-0.0031
All constant but var. 3	42.27	-0.1546

All constant but var. 4	49.85	-0.0031
All constant but var. 5	71.11	0.4221

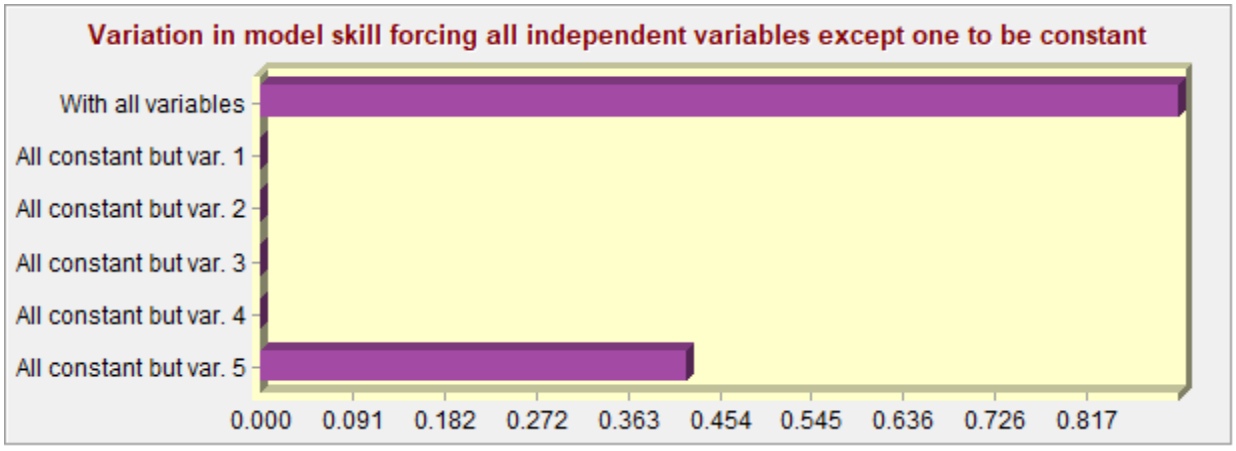

3) Backwards Stepwise Constant Forcing

Model	Variables included	Accuracy (%)	Skill measure
With all variables	All variables	95.40	0.9080
Step 1: var.[2] constant	[1,3,4,5]	95.40	0.9080
Step 2: var.[2,1] constant	[3,4,5]	95.34	0.9068
Step 3: var.[2,1,4] constant	[3,5]	94.89	0.8979
Step 4: var.[2,1,4,3] constant	[5]	71.11	0.4221

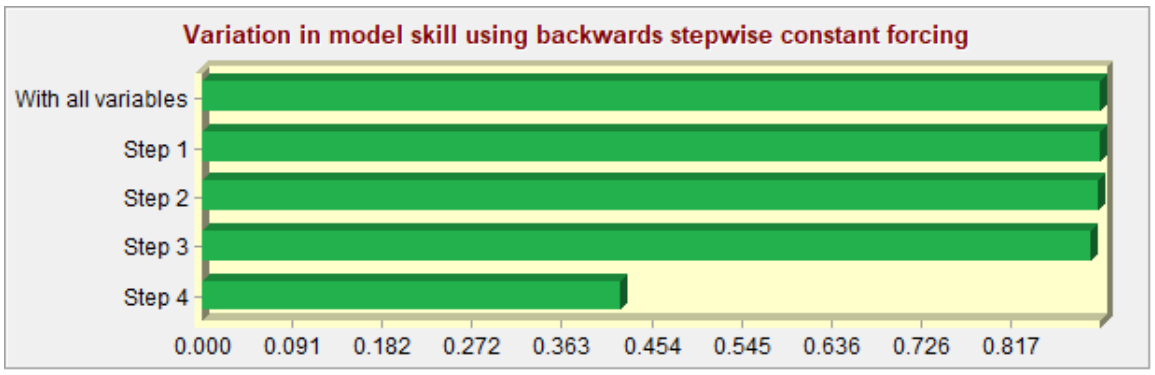

5.4. Appendix D: Land Change Modeler MLP Model Results for transition between forest and logging

1. General Model Information

1) Input Files

Independent variable 1	Distance to Road
Independent variable 2	Distance to existing logged
Independent variable 3	Elevation
Independent variable 4	Slope
Training site file	Logging_Train_Fores_to_Loggi

2) Parameters and Performance

Input layer neurons	4
Hidden layer neurons	3
Output layer neurons	2
Requested samples per class	10000
Final learning rate	0.0003
Momentum factor	0.5
Sigmoid constant	1
Acceptable RMS	0.01
Iterations	10000
Training RMS	0.3132
Testing RMS	0.3128

Accuracy rate	87.47%
Skill measure	0.7495

3) Model Skill Breakdown by Transition & Persistence

Class	Skill measure
Transition : Forest to Logging	0.8707
Persistence : Forest	0.6262

2. Weights Information of Neurons across Layers

1) Weights between Input Layer Neurons and Hidden Layer Neurons

Neuron	h-Neuron 1	h-Neuron 2	h-Neuron 3
i-Neuron 1	0.6572	-3.0681	11.9928
i-Neuron 2	-1.0850	6.2053	-7.6784
i-Neuron 3	31.6474	1.8865	12.6649
i-Neuron 4	7.8283	0.2371	2.5238

2) Weights between Hidden Layer Neurons and Output Layer Neurons

Neuron	o-Neuron 1	o-Neuron 2
h-Neuron 1	12.9541	-12.9535
h-Neuron 2	-8.0455	8.0451
h-Neuron 3	-12.7750	12.7744

3. Sensitivity of Model to Forcing Independent Variables to be Constant

1) Forcing a Single Independent Variable to be Constant

Model	Accuracy (%)	Skill measure	Influence order
With all variables	87.47	0.7495	N/A
Var. 1 constant	49.57	-0.0087	1 (most influential)
Var. 2 constant	87.47	0.7495	4 (least influential)
Var. 3 constant	80.49	0.6098	2
Var. 4 constant	86.35	0.7270	3

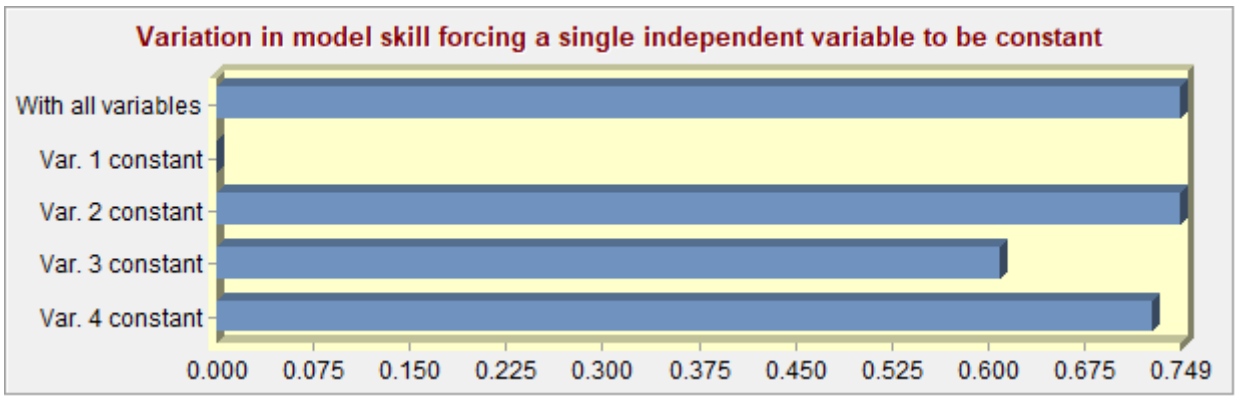

2) Forcing All Independent Variables Except One to be Constant

Model	Accuracy (%)	Skill measure
With all variables	87.47	0.7495
All constant but var. 1	80.55	0.6110
All constant but var. 2	49.57	-0.0087
All constant but var. 3	49.57	-0.0087
All constant but var. 4	49.57	-0.0087

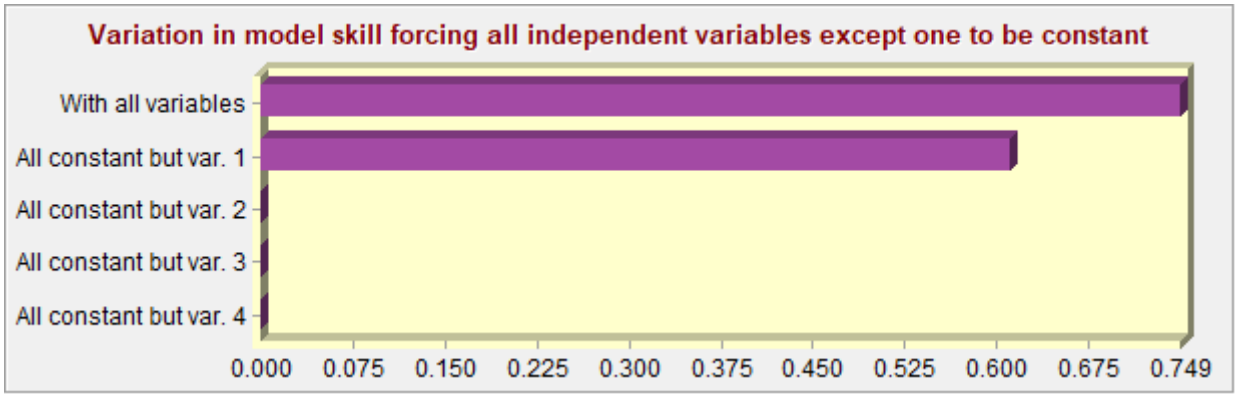

3) Backwards Stepwise Constant Forcing

Model	Variables included	Accuracy (%)	Skill measure
With all variables	All variables	87.47	0.7495
Step 1: var.[2] constant	[1,3,4]	87.47	0.7495
Step 2: var.[2,4] constant	[1,3]	86.35	0.7270
Step 3: var.[2,4,3] constant	[1]	80.55	0.6110

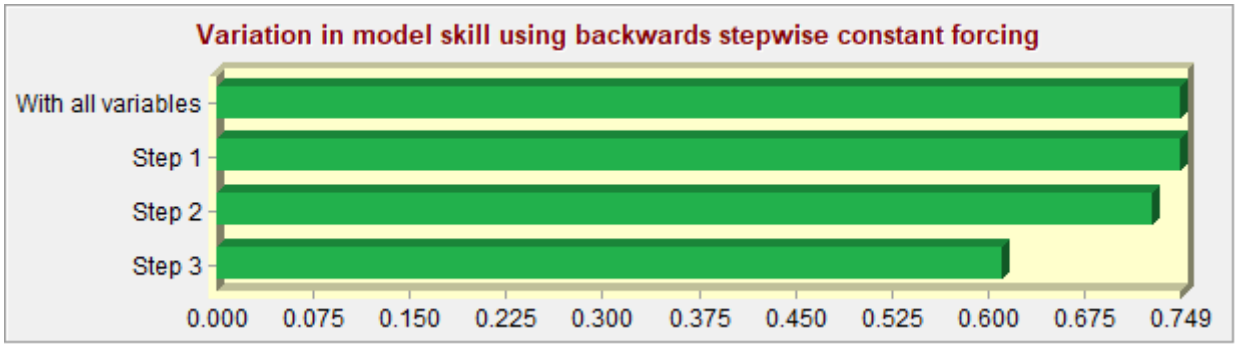

5.5. Appendix E: Land Change Modeler MLP Model Results for transition between forest and logging sensitivity analysis with distance to Vanimo

1. General Model Information

1) Input Files

Independent variable 1	Distance to Road
Independent variable 2	Distance to existing logged
Independent variable 3	Elevation
Independent variable 4	Slope
Independent variable 5	Distance to Vanimo
Training site file	Logging_Train_Fores_to_Loggi

2) Parameters and Performance

Input layer neurons	5
Hidden layer neurons	3
Output layer neurons	2
Requested samples per class	10000
Final learning rate	0.0010
Momentum factor	0.5
Sigmoid constant	1
Acceptable RMS	0.01
Iterations	10000
Training RMS	0.2130

Testing RMS	0.2214
Accuracy rate	93.78%
Skill measure	0.8755

3) Model Skill Breakdown by Transition & Persistence

Class	Skill measure
Transition : Forest to Logging	0.9320
Persistence : Forest	0.8195

2. Weights Information of Neurons across Layers

1) Weights between Input Layer Neurons and Hidden Layer Neurons

Neuron	h-Neuron 1	h-Neuron 2	h-Neuron 3
i-Neuron 1	-12.9854	12.3109	1.3147
i-Neuron 2	19.0665	9.3411	-19.6648
i-Neuron 3	-24.1528	4.4572	-15.9560
i-Neuron 4	-8.3888	-2.5740	-11.3866
i-Neuron 5	-13.6732	-24.7994	34.0503

2) Weights between Hidden Layer Neurons and Output Layer Neurons

Neuron	o-Neuron 1	o-Neuron 2
h-Neuron 1	6.9525	-6.9525
h-Neuron 2	-5.5198	5.5198
h-Neuron 3	-12.8323	12.8323

3. Sensitivity of Model to Forcing Independent Variables to be Constant

1) Forcing a Single Independent Variable to be Constant

Model	Accuracy (%)	Skill measure	Influence order
With all variables	93.78	0.8755	N/A
Var. 1 constant	69.66	0.3933	2
Var. 2 constant	93.78	0.8755	5 (least influential)
Var. 3 constant	92.18	0.8437	3
Var. 4 constant	93.76	0.8751	4
Var. 5 constant	50.20	0.0040	1 (most influential)

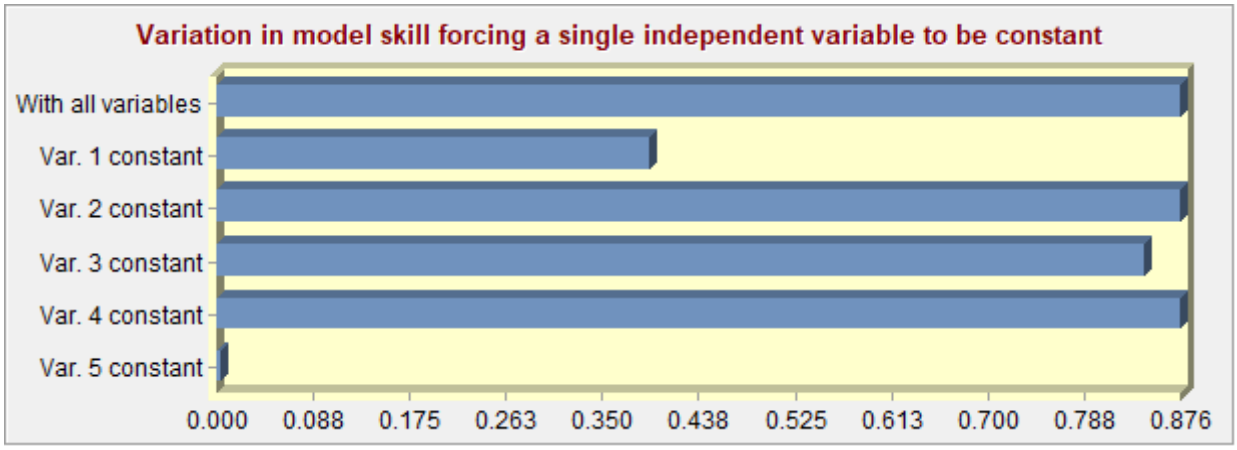

2) Forcing All Independent Variables Except One to be Constant

Model	Accuracy (%)	Skill measure
With all variables	93.78	0.8755
All constant but var. 1	50.20	0.0040
All constant but var. 2	50.20	0.0040

All constant but var. 3	50.20	0.0040
All constant but var. 4	50.20	0.0040
All constant but var. 5	67.03	0.3405

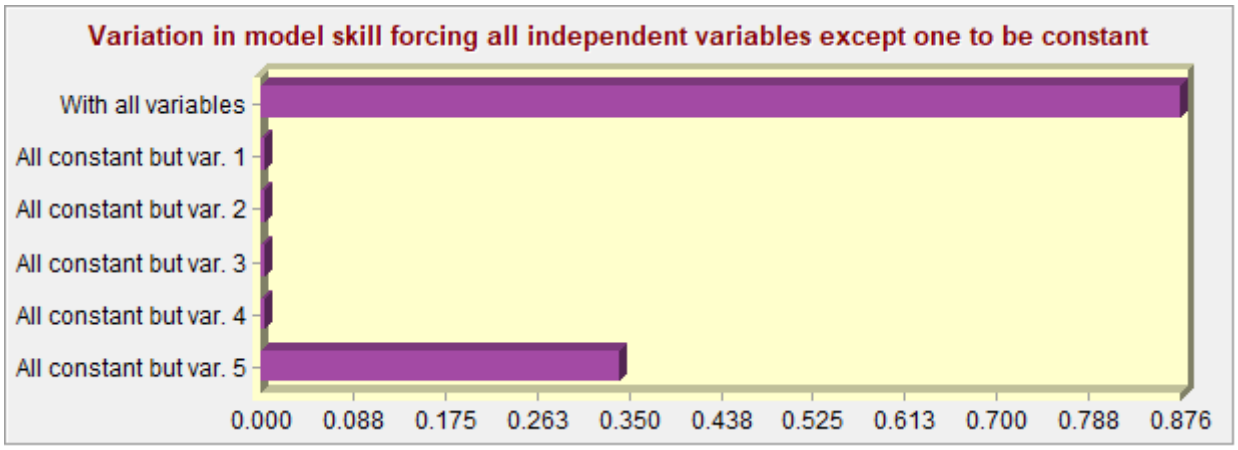

3) Backwards Stepwise Constant Forcing

Model	Variables included	Accuracy (%)	Skill measure
With all variables	All variables	93.78	0.8755
Step 1: var.[2] constant	[1,3,4,5]	93.78	0.8755
Step 2: var.[2,4] constant	[1,3,5]	93.76	0.8751
Step 3: var.[2,4,3] constant	[1,5]	92.21	0.8443
Step 4: var.[2,4,3,1] constant	[5]	67.03	0.3405

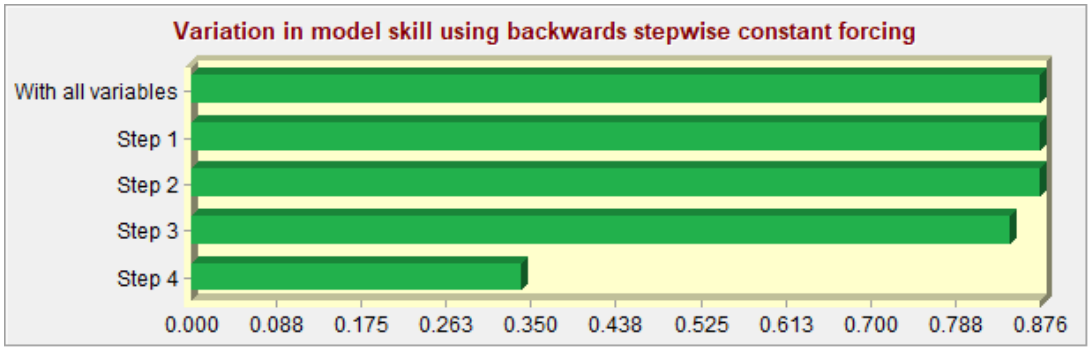
Variation in model skill using backwards stepwise constant forcing
With all variables
Step 1
Step 2
Step 3
Step 4
0.000
0.088
0.175
0.263
0.350
0.438
0.525
0.613
0.700
0.788
0.876